"INFLUENCE OF THE THIRD DIMENSION ON THE ELECTRONIC SPECTRA AND OUT-OF-PLANE TRANSPORT BEHAVIOUR IN BILAYERED HIGH T_c CUPRATES IN NORMAL STATE"

Thesis

Submitted to the

G. B. Pant University of Agriculture and Technology,
Pantnagar – 263145 (Udham Singh Nagar), Uttarakhand, INDIA

By

BHAGYA SINDHU TEWARI

IN PARTIAL FULFILMENT OF THE REQUIREMENTS
FOR THE DEGREE OF

Doctor of Philosophy
(PHYSICS)

January, 2008

DEDICATED TO MY BELOVED PARENTS

for their unconditional love and support

ACKNOWLEDGEMENTS

An advanced degree is often an arduous journey. Fortunately it is not a lonely one; I have received support in many forms from a number of people who ultimately made the experience what it was.

This thesis would not have been completed without the help of many individuals. First of all, I would like to express my profound sense and gratitude to my Advisor Dr. Ajay, Assistant Professor, Department of Physics, for his guidance of my adventure into the vast high-temperature superconductivity field for the enlightening discussions, his constant encouragement, and incomparable optimism despite frequent setbacks with facilities and fundings. His endless successive agreement and discussion always provided me a stimulating atmosphere and kept my interest alive in the research.

I owe a debt of gratitude and deep sense of appreciation to the members of my Advisory Committee Dr. B. R. K. Gupta, Professor, Department of Physics and Dean, College of Basic Sciences and Humanities, Dr. H. M. Agrawal, Professor and Head, Department of Physics and Dr. Manoj Kumar, Associate Professor, Department of Mathematics, Statistics and Computer Science for their valuable suggestions and critical evaluation of this manuscript. Thanks are also due to Dr. J. K. Singh, Dean, College of Post Graduate studies for providing necessary facilities.

I would like to pay warmest regard to Prof. Ram Kishore, Instituto de Pesquisas Espaciais (INPE), São Paulo, Brazil and Prof. Masao Ogata, University of Tokyo, Japan for their valuable suggestions during my calculations. I feel pleasure to express my sentiments towards Mr. S. C. Tewari, Programmer, Computer Centre for his kind help in numerical computation of the entire work. I am also thankful to Dr. Prabha Pant, Assistant Professor, Social Science & Humanities, for her help in editing the manuscripts related to this thesis.

I am highly grateful to Department of Science & Technology, Government of India, New Delhi for providing me funds via grant no. SP/S-2/M-36/2000 as I worked as a JRF in this scheme.

I consider it my privilege to thank all the teaching and non teaching staff of the Physics Department for their day-to-day help throughout the studies.

Aside from research, my life has been tremendously enriched by the numerous interesting friends whom I met in the Pantnagar. Special thanks to Bineet for patiently listening to my (often immature) words, providing to-the-point advice, and sharing his experience, wisdom, and philosophy; to N.S.Tomar, Amarjeet Sir, Sanjeev, Hariom, Alok, Rahul, Iqrar, Manisha, Smita, Anjana, Navdeep for their generosity, love and affection towards me; to my seniors Kailash Pandey, Kuldeep Kholiya, Ravindra Bhatt, Deepika Kandpal, Amarjeet Singh for reaching out and helping me through the time during Ph.D.; to my juniors Jeewan Bhatt, J.P.Singh, Lokesh, Anuj, Mayank Pandey, Ziya, Mangey, Virendra, Gagan, Diwakar, Gokul, Kamla, Girish, Bhawna, Geeta and Raguwesh for sharing the enthusiasm in physics; and to my batchmates especially Manoj Sir, for all the fun discussions and the refreshing perspectives; to Tomar family for their support and grace during my stay at Pantnagar.

Finally, I'd like to express my deepest gratitude to my parents, for their unconditional love and for letting me explore my interests and capability freely; to my colleague Archana, for her companionship in every moments; and to Vinod, Yogesh, Bhagat, RP, Pandey, Dinesh, Palika, Manju who can always bring a smile to my face. They are all lifetime friends, with them one can go to seek shelter from physics.

Pantnagar (Bhagya Sindhu Tewari)

January, 2008

Dr. Ajay
Assistant Professor

Department of Physics
College of Basic Sciences and Humanities
G.B.Pant University of Ag. & Tech.,
Pantnagar-263145,Uttarakhand, India.

CERTIFICATE

This is to certify that the thesis entitled "INFLUENCE OF THE THIRD DIMENSION ON THE ELECTRONIC SPECTRA AND OUT-OF-PLANE TRANSPORT BEHAVIOUR IN BILAYERED HIGH T_c CUPRATES IN NORMAL STATE" submitted in partial fulfilment of requirements for the degree of Doctor of Philosophy with major in Physics and minor in Computer Science of the College of Post Graduate Studies, G.B. Pant University of Agriculture and Technology, Pantnagar, is a record of bona fide research carried out by Mr. Bhagya Sindhu Tewari, Id. No. 29674, under my supervision, and no part of the thesis has been submitted for any other degree or diploma.

The assistance and help received during the course of this investigation have been acknowledged.

(Ajay)
Chairman
Advisory Committee

CERTIFICATE

We, the undersigned, members of the Advisory committee of Mr. Bhagya Sindhu Tewari, Id. No. 29674, a candidate of Doctor of Philosophy with major in Physics and minor in Computer Science, agree that the thesis entitled "INFLUENCE OF THE THIRD DIMENSION ON THE ELECTRONIC SPECTRA AND OUT-OF-PLANE TRANSPORT BEHAVIOUR IN BILAYERED HIGH T_c CUPRATES IN NORMAL STATE" may be submitted in partial fulfilment of the requirements for the degree.

(Ajay)
Chairman

(B.R.K.Gupta)	(H.M.Agrawal)	(Manoj Kumar)
Member	Member	Member

CONTENTS

S.No. Chapters Page No.

INTRODUCTION

Chapter 1

INTRODUCTION

While studying the electrical transport behaviour of highly purified sample of mercury at low temperatures, Onnes (1911) observed that the resistivity of mercury drops suddenly to zero around 4.2^0K (figure (1)). This phenomenon of resistance less flow of current at low temperature called superconductivity and temperature at which this peculiar phenomenon takes place is called the transition temperature (T_c). Soon after the discovery of superconductivity in mercury, the various metals and alloys were found to exhibit the phenomena of superconductivity.

On the other hand, it took almost fifty years to understand the microscopic origin of the phenomena of superconductivity. Frohlic (1950) pointed out that an effective attractive interaction between two electrons in a metal may be induced by the mediation of lattice vibrations at low temperatures. On the basis of Frohlic's idea, Bardeen, Cooper and Schrieffer (1957) developed a microscopic theory of superconductivity based on the idea of pairs of electrons of opposite momentum state and opposite spins mediated by electron-phonon interaction. This theory is known as BCS theory of superconductivity and explains almost all the properties of superconducting state like energy gap around Fermi level, resistance less flow of current due to bound Cooper pair, Meissner effect,

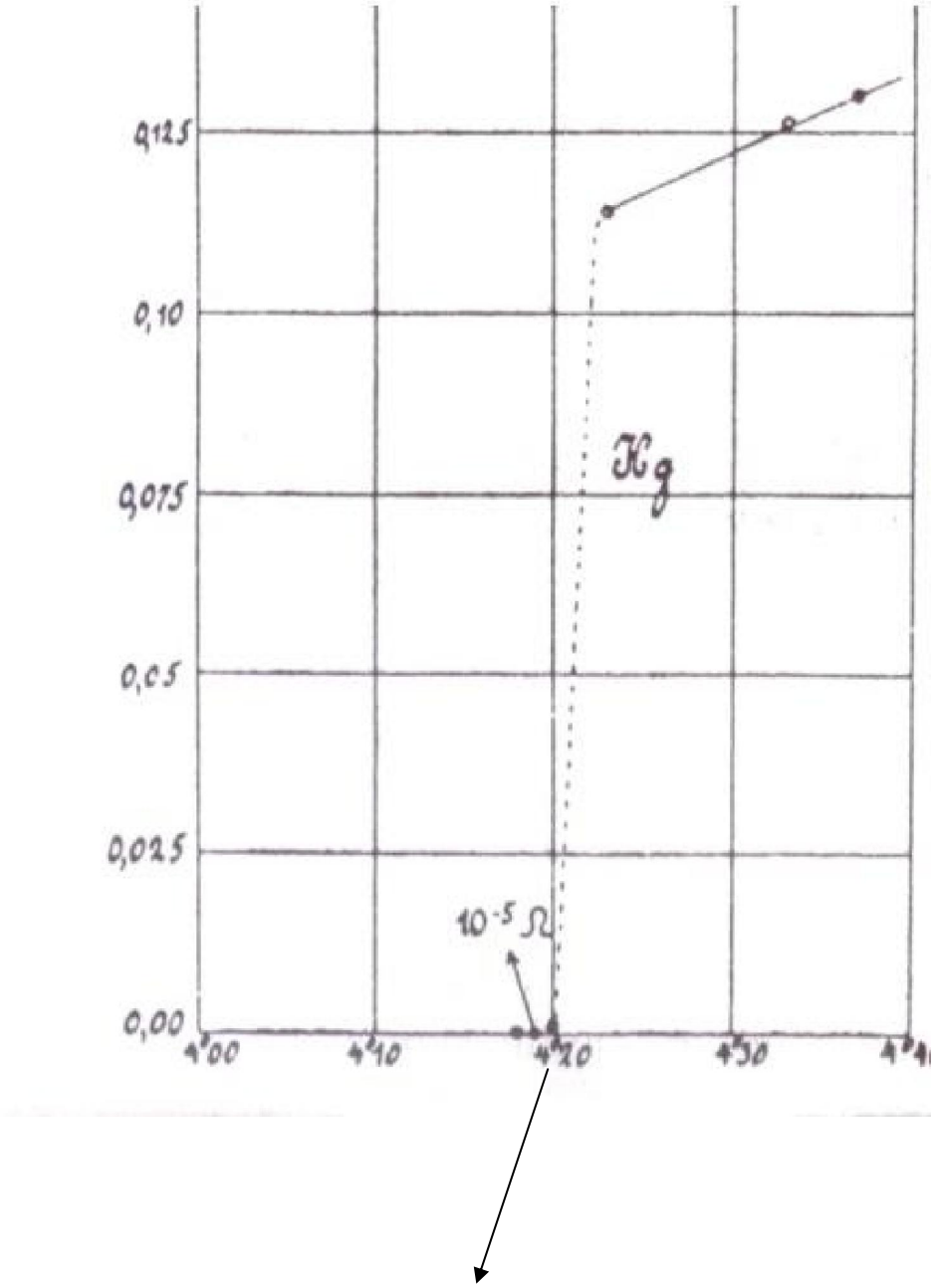

Figure (1). Discovery of superconductivity in mercury (1911)

transition temperature, specific heat jump at superconducting transition, isotope effect, coherence length and penetration depth.

Thereafter, material scientists and technologists looked for other materials to have superconductivity at still higher transition temperature for the practical application of these materials in the electronic industries. The highest recorded transition temperature was about 23^0K (1973) exhibited by Nb_3Ge system till 1986.

1.1 Discovery of high T_c cuprate superconductors

The quest to develop high temperature superconductors saw a breakthrough in 1986, when Bednorz and Muller (1986) discovered copper oxide based ceramic $La_{2-x}Ba_xCuO_4$ superconductor with a T_c as high as 35^0K. Unlike the metallic BCS superconductors, the material studied by Bednorz and Muller were complex oxide with very poor normal state conductivity at room temperature. Afterwards, a number of complex ceremics were discovered and most of them were cuprates having substitution of various elements for La and Ba and varying the stoichiometry under pressure.

In 1987, Chu et al. (1987) synthesized a Yttarium based superconductor ($YBa_2Cu_3O_{6+x}$) having transition temperature close to 90^0K, well above the boiling point of liquid nitrogen. Other ceramic compounds of Yttarium ($Y_{1.2}Ba_{0.8}CuO_x$) having transition temperature around 93^0K was

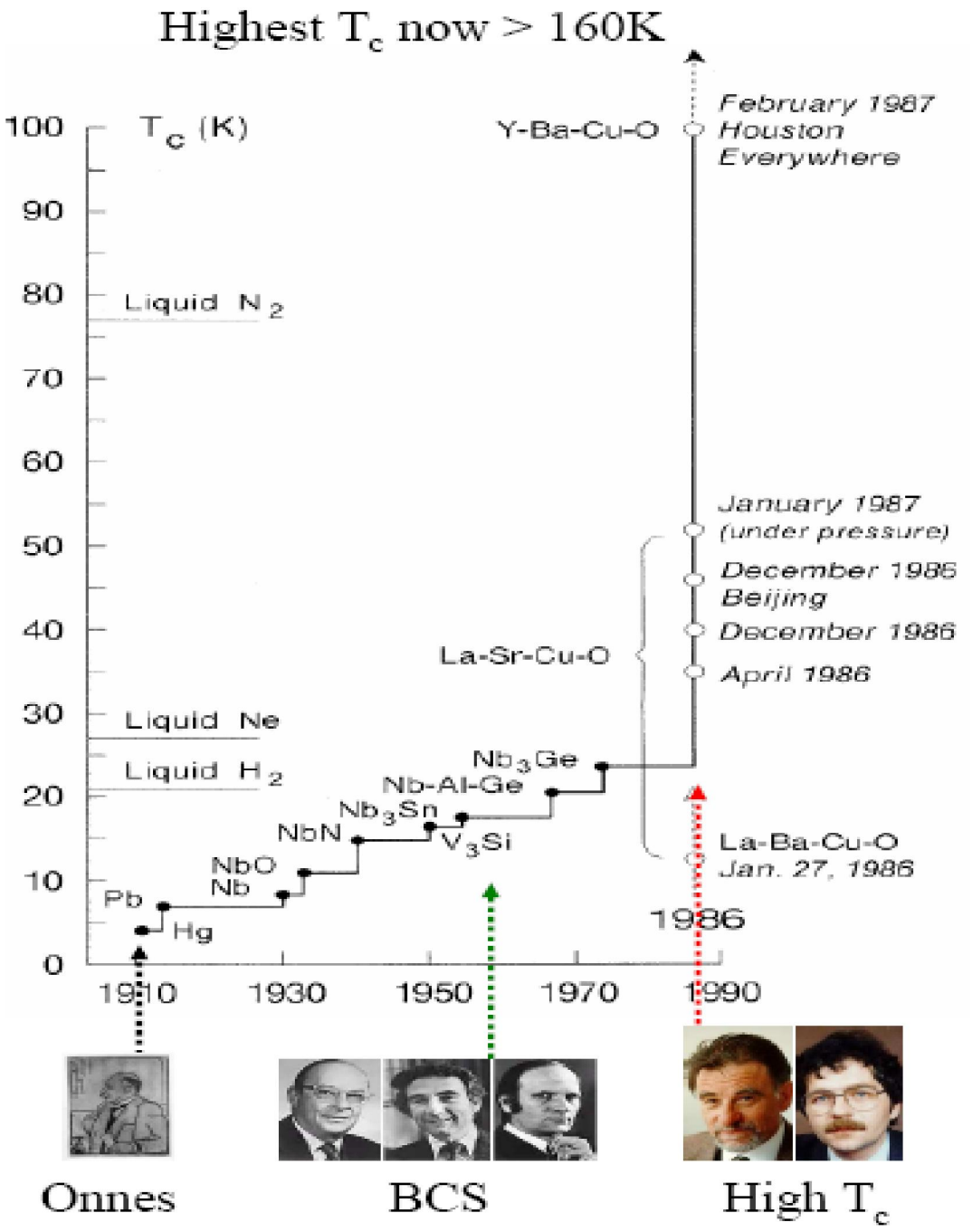

Figure (2). Year-wise advancement of High T_c superconductors

also discovered [Wu et al. (1987)]. Many experiments on cuprates evolves that the structure $RBa_2Cu_3O_{7-x}$, where R=Y, La, Nd, Sm, Eu, Gd, Dy, ho, Er, Tm, is capable of formation of compounds having transition temperature around 90^0K. The improvement in transition temperature of these cuprates was done in a smooth way: $Bi_2Sr_2Ca_2Cu_3O_{10}$ (BSCO or Bi 2223) having $T_c=110^0$K in late January 1988, Thallium based cuprate $Ti_2Ba_2Ca_2CuO_3$ having $T_c= 125^0$K in mid February 1988, in mercury based cuprate $HgBa_2Ca_2Cu_3O_9$ (Hg 1223) having $T_c=134^0$K in May 1993, and recently a mercury based cuprate become superconductor at nearly 165^0K under high pressure. Figure (2) shows year-wise advancement of discovery of high T_c superconductors.

The properties of high temperature cuprate superconductors differ to conventional superconductors in many aspects. In addition to higher transition temperature in cuprates, the isotope effect is also found to be too small or absent. Weber (1987) have done a detailed calculation for phonons and suggested that the BCS theory based on the electron phonon interaction is not adequate to explain the origin of such high transition temperature (T_c) in cuprate materials. Several mechanism of high T_c superconductivity in cuprates have been proposed. Anderson et al. (1987) proposed the resonance valence bond (RVB) theory, followed by bipolarons [Alexandrev (1988)], plasmons [Ginzberg (1964), Little (1969, 1981)], and interlayer tunneling mechanism [Chakrawarty et al. (1993)]. These all theories are based on different arguments and so far there is no

consequence about the single mechanism. A brief description of various theories is well documented in the review article by Dagotto (1994) and Anderson (1997).

1.2 Phase diagram of high T_c cuprate superconductors

Experimental studies of the electronic structure of these cuprate compounds revealed that these materials contain stakes of CuO_2 planes sandwiched between charge reservoir regions. These layered cuprates possess anisotropy in their crystal structure and due to this, electronic properties in the normal and superconducting phase exhibit anisotropic behaviour. The most common way to modify electronic properties is hole doping. The hole doping is achieved by substitution of appropriate elements. For example, La_2CuO_4 cuprates is antiferromagnetic insulator in undoped state and substitution of divalent Sr^{++} for trivalent La^{+++} in the insulating La_2CuO_4 within CuO_2 plane and gives rise to superconducting phase (in $La_{2-x}Sr_xCuO_4$) with a maximum T_c of 40^0 K at a particular doping called optimal doping. On the other hand, in bilayer cuprates (Y-123 and Bi-2212), the holes are generated in CuO_2 plane through introduction of oxygen. All the undoped parent compounds of the high T_c cuprate family are antiferromagnetic Mott insulator oxides with very high Neel's temperature (400^0K to 500^0K) due to strong electronic correlations of the order 5-8 eV at $Cu3d^9$ site. Upon doping (i.e. on introducing holes) upto certain extent they undergo a phase transition from AFM state to a strange normal state or a

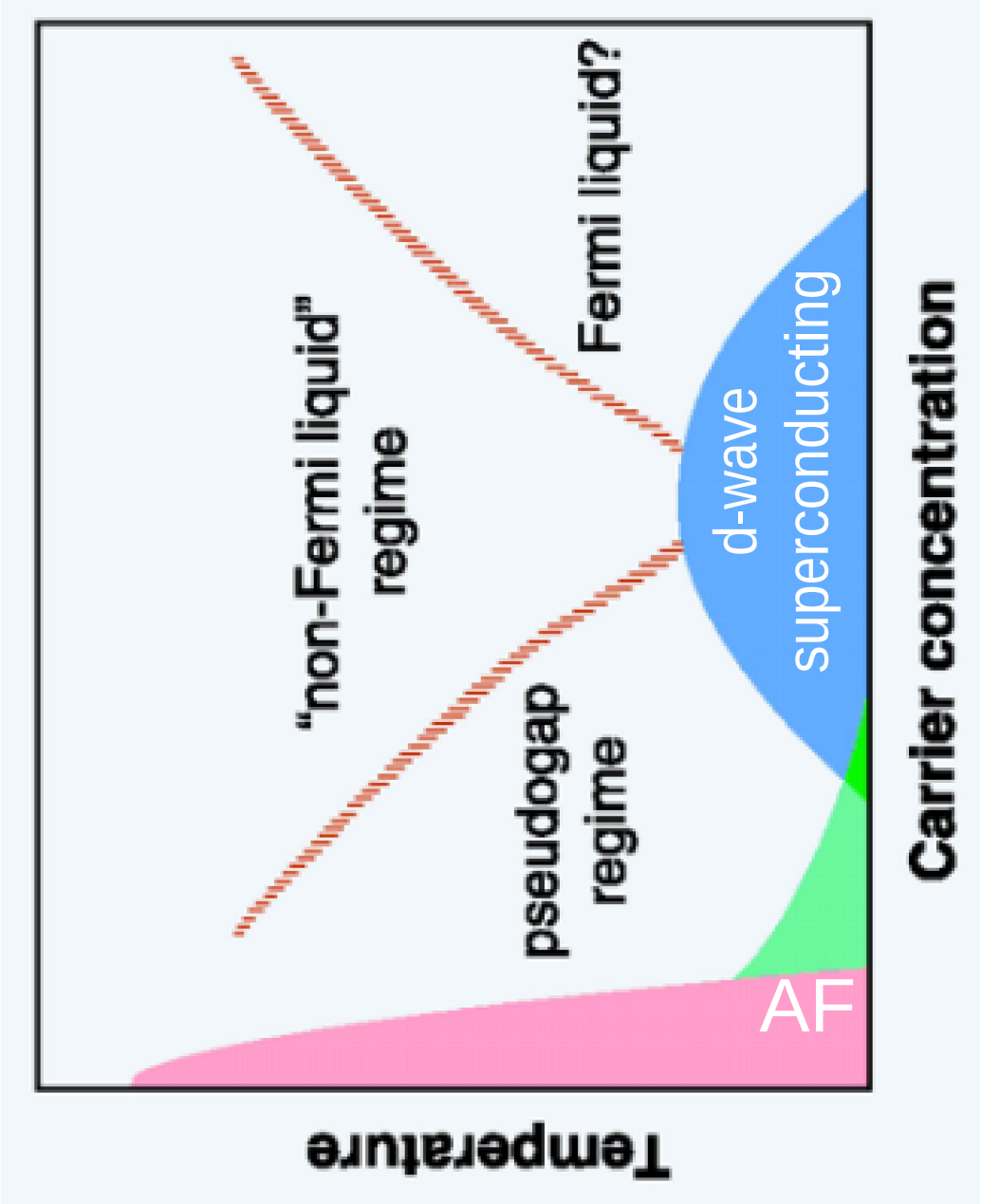

Figure (3). Phase diagram of cuprates

superconducting state depending on the temperature. On increment in carriers (holes) concentration, the insulating state transform into metallic one with a high T_c superconducting dome as shown in phase diagram of high T_c cuprate in figure (3). This range is normally divided into an underdoped (UD), an optimally doped (OP) and an overdoped region. In the heavily overdoped region the superconducting phase transforms to normal metallic state.

The transport, nuclear magnetic resonance (NMR), angle resolved photoemission spectroscopy (ARPES), tunneling and specific heat measurements have confirmed the existence of pseudogap in underdoped region in high Tc cuprates [Timusk and Statt (1999), Norman (2003)]. The common feature of pseudogap is found to depend on temperature and doping range in all high temperature cuprate superconductors. It is also believed that at optimal doping the pseudogap merged superconducting gap having the same d-wave form as that of the superconducting order parameter. So far, there is no microscopic theory to explain the influence of pseudogap on electronic, optical and properties in layered cuprates.

Recently, electronic spectra and transport behaviour in these materials are found to be dependent on doping, temperature and anisotropy in crystal structure.

1.3 Crystal and electronic structure of high T_c cuprates

The crystal structure of high T_c cuprate pervoskites contain the stakes of CuO_2 planes and charge reservoir sandwiched between them. These two dimensional planes are considered essential to the electronic conduction and hence existence of superconductivity in these compounds. The high T_c cuprate materials are classified into single layer material [($Bi_2Sr_2CuO_{6+x}$ (Bi2201), $La_{2-x}Sr_xCuO_4$ (LSCO)], bilayer [($YBa_2Cu_3O_{7-x}$(Y123), $Bi_2Sr_2CaCu_2O_{8+x}$ (Bi2212), $HgBa_2CaCu_2O_{6+x}$ (Hg1212)] and trilayer materials [($Bi_2Sr_2Ca_2Cu_3O_{10+x}$(Bi2223)], on the basis of number of CuO_2 planes in an unit cell. These two dimensional CuO_2 planes (the building blocks of the high T_c cuprates) are responsible for electronic conduction process and existence of the strong electronic correlation effects in layered cuprates. The two dimensional copper oxygen layers are separated either by intervencing Cu-O chains (as in $YBa_2Cu_3O_7$), or by layer containing other metal oxides (Ba-O, Bi-O, and Tl-O) in multilayer material and serves as a charge reservoir region. The lattice parameters (a, b, c) in case of tetragonal phase of single layer ($La_{2-x}Sr_xCuO_4$) are (3.78, 3.78 and 13.18 $\overset{o}{A}$), respectively (figure (4)). The lattice parameters (a, b, c) for bilayer per unit cell system like $YBa_2Cu_3O_{6-x}$ (YBCO) are (3.82, 3.89 and 11.6802 $\overset{o}{A}$) (figure (5)) and for bilayer Bi-2212 are (5.4, 5.4 and 30.7 $\overset{o}{A}$) (figure (6)) (Pickett (1989)). One can see that Bi-2212 system possess the largest c-axis parameter and supposed to have highly anisotropic electronic structure.

The stakes and spacing between the two dimensional CuO_2 planes within the unit cell indicate coupling of charge carriers (holes) between the CuO2 plane. Also in these layered materials there is strong variation in the distance between the neighbouring CuO_2 planes (which is around 11.6 $\overset{o}{A}$ for single CuO_2 layer per unit cell systems and of the order of 3.2 $\overset{o}{A}$ for other multilayer cuprates). These results point that electronic states of nearest CuO_2 planes are overlapped and gives rise to coupling between the electronic states of neighboring CuO_2 planes. The anisotropy in intra and inter layer coupling and electronic correlations play an important role to determine the electronic spectra and transport behaviour of these multilayered cuprates.

Recent studies pointed out that the electronic structure of layered cuprates contains the contribution of third dimension (c-axis) and hopping integral between two neighboring Cu sites along Cu-O bonding direction (t), and long range hopping related to the second nearest Cu neighbor along the diagonal direction (t') and also the hopping to the third nearest neighbor (t''). In bilayer system, there is also coupling between the two adjacent CuO_2 planes which leads to a finite hopping integral ($t_\perp$), and in photoemission measurements indicate a splitting of spectra into bonding and antibonding branches near the Fermi surface due to this interlayer coupling (Chuang et al. (2001), Feng et al. (2001)). Moreover, there is a possibility of coupling of two CuO_2 planes between the adjacent unit cell

along out of plane direction and one need to include the contributions of these long ranged hopping matrix elements and third dimensional coupling to analyze the electronic spectra and transport behaviour of strongly correlated layered high T_c cuprates in normal state.

1.4 Photoemission spectroscopic measurements in high-T_c cuprates

Since the discovery of high T_c superconductivity in cuprates, angle resolved photoemission spectroscopy (ARPES) has provided key experimental insights in revealing the electronic structure of high temperature cuprate superconductors. Several reasons have contributed to this development. First, the great improvement in experimental resolution, both in energy and momentum, aided by a large energy scales presented in cuprates, allow one to see features on the scale of the superconducting gap. More recently, the photon energy of newly developed laser based angle resolved photoemission system is of the order of ~7eV with an energy width of nearly 0.26 meV in comparison to earlier photon energy of 21.2 eV [Zhang et al. (2007)]. The energy and angular resolution are improved now 2-10meV and 0.2^0 respectively (in Scienta hemispherical analyzer) in contrast with previously 20-40 meV energy resolution and $2\text{-}10^0$ angular resolution.

The second reason is the quasi two dimensional electronic structure of the cuprates, which permits one to unambiguously determine the

momentum of the initial state from measured final state momentum, since the component parallel to the surface is conserved in photoemission. Moreover in two dimensions, ARPES directly probes the single particle spectral function, and therefore offers a complete picture of the many body interactions inherent in these strongly correlated cuprates.

There are other reasons to point out as well. For example, the very incoherent nature of the excitation near the Fermi energy in the normal state does not allow the application of traditional techniques, such as de Hass van Alphen effect. Another important reason why ARPES played a major role is the higher anisotropic nature of electronic excitations in cuprates, and implies that momentum resolved probes are desirable to elucidate the electronic structure of these materials.

The principle of photoemission spectroscopy is based on photoelectric effect. When monochromatic light with energy $h\nu$ is shined onto a surface of solid, the intensity as well as the kinetic energy, E_{kin}, of outgoing photoelectron is measured. In the angle resolved mode, an electrostatic detector measures the azimuthal angle (ϕ) and polar angle (θ) of the electrons or holes (relative to normal to the surface). At the same time, the energy of the photon gives the information about the initial energy of the holes (electrons) in the crystal. The component of the momentum parallel to the sample surface can also be determined. The photoemission intensity measured in ARPES can be given by the relation:

$$I(k,\omega) = \mathrm{M}^2 \int_{\delta k} dk' \int d\omega' A(k',\omega') f(\omega') R(\omega,\omega')$$

where, $M = \langle \varphi_f | H' | \varphi_i \rangle$ is a matrix element between the initial and the final state and H' is perturbed part of the Hamiltonian operator. $A(k,\omega)$ is the single particle spectral function, which is the essential results in ARPES study. The spectral function can be calculated from a many body theory of electrons and measures the probability of removing or adding an electron (hole) to the system. $f(\omega) = 1 \Big/ \left\{ \exp\left(\omega \big/ k_B T \right) + 1 \right\}$ is the Fermi function which takes into account that only occupied states are measured. R is the energy resolution function (may be given as a Gaussian form).

In comparison to the single layer material such as $La_{2-x}Sr_xCuO_4$, the ARPES spectra of bilayer cuprates such as $Bi_2Sr_2CaCu_2O_{8+x}$(Bi-2212) showed a splitting of spectral function along the antinodal point of the Brillouin zone. A number of experiments are performed to study the band splitting in Bi-2212 which has two Cu-O planes within a unit cell [Feng et al. (2001), Feng et al. (2002) and Chaung et al. (2001)]. The splitting is found to be large in normal state, with the maximum splitting (~110meV) at $(\pi,0)$ point of the Brillouin zone. It is also pointed out that the normal state of cuprates show a broadening in the spectral function while sharp and prominent spectral features are observed in the superconducting state. The splitting in the electronic states is attributed to the coupling between the Cu-O planes within the unit cell. The absence of band splitting in cuprates

having only one Cu-O layer per unit cell gives credence to the hypothesis that there must be some sort of third dimensional coupling of planner holes in cuprates where there are more than one Cu-O planes per unit cell.

The influence of third dimension on the photoemission spectra of two dimensional materials has also been pointed out recently. Bansil et al. (2005) have analyzed the inter cell coupling on the basis of simulated ARPES lineshapes in Bi-2212 and concluded that the inter cell hopping induces a irreducible broadening to the photoemission spectra which have a characteristic dependence on the momentum $\vec{k}$. Markiewicz et al. (2005) have also analyzed the effect of inter cell coupling and the resulting third dimensional dispersion in the cuprates within the framework of the one-band tight binding (TB) model Hamiltonian. These studies point the role of third dimension of CuO_2 plane on the electronic spectra of these materials and there is a need of theoretical understanding of the spectral and transport properties of these systems in normal state. The precise knowledge of electronic spectra and transport behaviour in layered cuprates in normal state is vital to pinpoint the mechanism responsible for high T_c superconducting as well as anomalous superconducting properties of these systems.

1.5 Anisotropy in transport behaviour in layered high T_c cuprates in normal state

The electronic transport in high T_c cuprate superconductor is found to be anomalous. The strong anisotropy of in plane (ab) and out of plane (c) electronic transport in the cuprate system revealed by ARPES, NMR, resistivity, Hall, Raman and optical conductivity measurements is an unresolved and long standing issue in high T_c cuprates. In these compounds, the temperature dependence of c-axis resistivity ρ_c is semiconducting like in contrast to the planer resistivity ρ_{ab} showing metallic behaviour with temperature in underdoped cuprates. Such a striking difference in temperature dependence of ρ_c and ρ_{ab} presents a challenging problem in the theoretical aspects of layered high T_c cuprates. The resistive ratio $\rho_c(T)/\rho_{ab}(T)$ is found to be large in underdoped state while around optimal doping, the ρ_c transforms from semiconducting behaviour to metallic one and and $\rho_c \propto \rho_{ab}$ at all temperature [Tallen et al. (2001), Watanabe et al. (1997) and Kendziora et al. (1993)].

Several phenomenological models have been proposed to explain the anisotropy in transport behaviour in layered cuprates. Models include effect of strong interlayer scattering [Kumar and Jayannavar (1992)], non-Fermi-liquid ground states[Anderson and Zou (1988)], the general phenomena of confinement[Anderson (1997)], interplane, and inplane charge fluctuations[Leggett (1992)], indirect c-axis coupling through the particle-

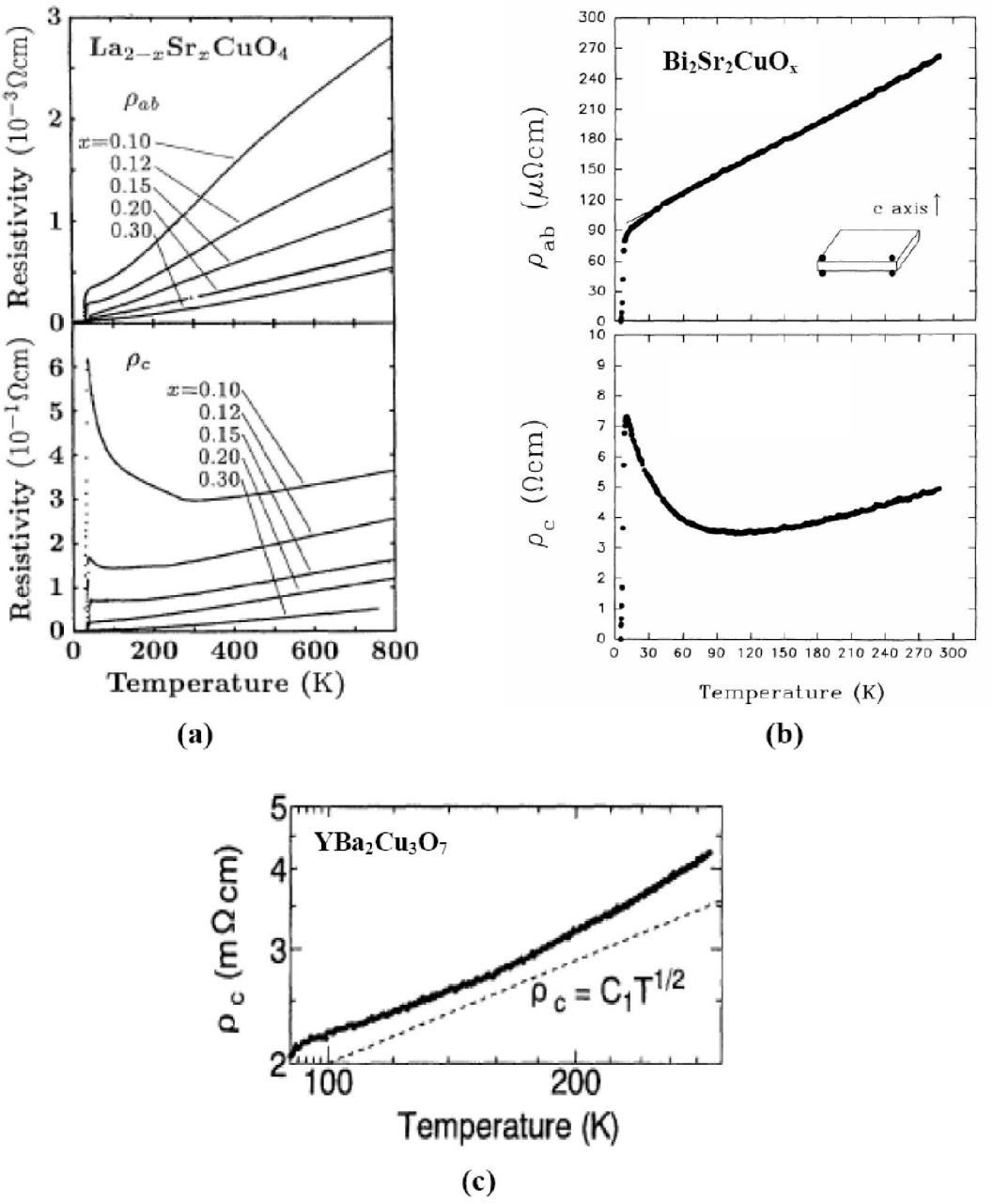

Figure (8) **(a)** Temperature dependence of the in-plane (upper panel) and out-of-plane (lower panel) resistivity for single layer cuprate [$La_{2-x}Sr_xCuO_4$] with various concentrations [**Nakamura and Uchida (1993)**], **(b)** Temperature dependence of the plane resistivity of $Bi_2Sr_2CuO_x$ crystal (upper panel) and temperature dependence of the out of plane resistivity of $Bi_2Sr_2CuO_4$ crystal (lower panel)[**How et al. (1994)**]. The inset shows schematic of the CuO_2 planner structure. **(c)** The out of plane resistivity versus T for $YBa_2Cu_3O_7$ compound [**Terasaki et al. (1995)**],

particle channel [Tesanovic (1988)], as well as coherent motion of polarons [Alexandrov et al. (1996)], orbital structure and correlation effects in cuprates [Lal et al. (1998)], and the effect of electron-phonon and strong inharmonic interactions [Zoli et al. (1997)].

So far there is no general agreement on a single model proposed to explain anomalous transport behaviour in layered cuprates. In the light of above facts it is important to study the electronic transport behaviour by including the third dimensional coupling as suggested by recent ARPES measurements [Bansil et al. (2005) and Markiewicz et al. (2005)].

More general results for the electronic conductivity and interband transitions have been obtained by Kubo (1957) using a decoupling scheme for the two particles real time temperature dependent Green's functions. Further, there are several techniques to calculate the propagator (Green's function) for the model Hamiltonian. Therefore, the present work incorporates correlation function, obtained by extended Hubbard model, in Kubo formalism of electric conductivity and analyze the role of third dimensional (c-axis) inter unit cell resonant tunneling in bilayer cuprates in normal state.

1.6 Model description of high T_c cuprates

Soon after the discovery of high T_c copper oxides, Anderson (1987) analyzed the orbital structure in the conducting CuO_2 planes and formulated a microscopic model for cuprates. He pointed out the possibility

of coupling of orbital states between the CuO_2 planes and argued that the hybridization in the conducting CuO_2 planes mainly takes place in $3d_{x^2-y^2}$(Cu), $2p_x$ and $2p_y$ orbitals (figure (9)). As a result of hybridization, the degeneracy in the p and d orbitals is lifted up in such a way that the states of maximum energy is $3d_{x^2-y^2}$ with a strong onsite Coulomb energy at $Cu3d^9$ site having single localized hole. For one particle per lattice site, the lower Hubbard band is completely filled and the system behaves as an AFM insulator in undoped state. Upon doping a transition from AFM insulating state to superconducting state occurs at low temperatures ($T<T_c$).

1.6.1 Tight binding Hubbard model

Anderson (1987) suggested that the Hubbard model (used to explain metal-insulator transition and magnetism in transition metal oxides, long back 1963 [Habbard (1963)) would be the simplest many electron model which can be used to describe the essential features of the electronic interactions which occurs in materials like cuprate compounds. Also, the holes play an important role in both magnetism and high T_c superconductivity. The dominant interaction is repulsive and carriers (holes) are strongly correlated due to large Coulomb energy (5-8eV) at $Cu3d^9$ site.

The simplest form of Hubbard model contains terms which describe the transfer of electron between orbitals as well as the repulsion between two electron occupancy on the same orbitals, having their spins opposite as per Pauli exclusion principle. Mathematically, the Hubbard model applicable

for cuprates can be expressed by the following Hamiltonian (for hole doped material like cuprates):

$$H = -\sum_{<i,j>,\sigma} t_{ij}\left(d^{+}_{i\sigma}d_{j\sigma} + h.c\right) + U\sum_{i} n_{i\uparrow}n_{i\downarrow}$$

where, $d^{+}_{i\sigma}$ is defined as the creation operator, placing a hole into the d orbital at i^{th} ion site with spin $\sigma((\uparrow)$ or $(\downarrow))$. Its Hermitian conjugate $d_{i\sigma}$ is the annihilation operator at j^{th} ion site with spin σ. $n_{i\sigma} = d^{+}_{i\sigma}d_{j\sigma}$ is the number of holes at the i^{th} site with spin σ, and t is the hopping parameter. U is the onsite Columbic repulsion among holes at Cu-$3d^9$ site.

Several authors have used the Hubbard model and its extension to study the spectral and transport behaviour in multilayer cuprates. The out-of-plane coupling not only connects the Cu-O planes within the unit cell (intra unit cell) but also Cu-O planes of the adjacent unit cells (inter unit cell) for cuprates having two CuO_2 planes per unit cell. In bilayer cuprates (Bi-2212) due to small separation (of the order of 3.2 $\overset{o}{A}$) between two Cu-O planes within the unit cell, the intra unit cell coupling between two Cu-O bilayers results in the band splitting as observed in ARPES measurements. On the other hand, the inter unit cell coupling that connects the two adjacent Cu-O planes in different unit cells is believed to be weaker due to greater separation (of the order of 12 $\overset{o}{A}$ in Bi-2212 cuprates) between Cu-O planes of two adjacent unit cells. Because of very low strength of inter unit cell interaction between Cu-O planes, their effect shows up only in recent

high resolution ARPES measurements of Chuang et al. (2001, 2004) on Bi-2212 system.

In cuprates, most of the studies on out-of-plane coupling is restricted within the unit cell. Further, there is no clear understanding about the coupling between the two layers of adjoining unit cell. Abrikosov (1997, 1999) used the concept of 'resonant tunneling' proposed initially by Bohm (1951) to explain the possible mechanism responsible for the out-of-plane electronic conduction processes in layered cuprates. When electrons (holes) tunnel through a potential barrier, the probability is exponentially small but the tunneling probability can be raised nearly equal to 1 if there is a potential well exactly in the middle of the barrier, and the energy of the carriers (holes) that tunnel the barrier matches with the energy of the one of the bound states in the well. It is also emphasized that the important physics of CuO_2 planes in the superconducting state can also be captured by negative U (attractive) Hubbard model.

Therefore, the second section of the present thesis is devoted to study the role of intra cell coupling and inter cell resonant tunneling on the electronic spectra of multilayered cuprate superconductors (like $Bi_2Sr_2CaCu_2O_{8+\delta}$ (Bi-2212)) by considering tight binding multilayered Hubbard model containing the contributions corresponding to the coupling between the planes in the unit cell as well as the resonant tunneling term between two adjacent unit cells. In the third section of the theoretical formulation, we have also attempted the theoretical analysis of c-axis

electronic conduction in the light of resonant tunneling by considering one CuO_2 plane per unit cell in the framework of Kubo formula. In the preceding section, the review of literature related to above issues is presented.

1.6.2. t-J model and its extensions:

The t-J model containing kinetic energy and AFM exchange energy (J) is also a relevant model to study the electronic properties of doped high temperature cuprates. The t-J model is the strong coupling version of the Hubbard model in the large U limit [Gros et al. (1987), and Su et al. (1993)]. Strong correlation makes the limit $U/t \to \infty$ and the system avoids doubly occupied sites of holes in this limit. The t-J model as obtained from Hubbard model can be described as

$$H = H_t + H_{J\text{-}J_3}$$

$$H = -t\sum_{r\langle ij\rangle\sigma}(c^{+}_{ri\sigma}c_{rj\sigma} + h.c.) + \frac{J}{2}\sum_{r\langle ij\rangle}\left(\overset{\circ}{S}_{ri}.\overset{\circ}{S}_{rj} - \frac{1}{4}n_{ri}n_{rj}\right) - \frac{J_3}{4}\sum_{ri\delta'\neq\delta\sigma}\left(c^{+}_{ri+\delta\sigma}n_{ri-\sigma}c_{ri+\delta'\sigma} + c^{+}_{ri+\delta\sigma}c^{+}_{ri-\sigma}c_{ri+\delta'-\sigma}c_{ri\sigma}\right)$$

Where $c^{+}_{i\sigma}(c_{i\sigma})$ is creation (annihilation) operator of holes with spin $\sigma(\sigma = \uparrow, \downarrow)$ at site i on the two dimensional square lattice. S_i is the spin operator at site i. $n_i = n_{i\uparrow} + n_{i\downarrow}$, where $n_{i\sigma}$ is the number operator $c^{+}_{i\sigma}c_{i\sigma}$. $\langle i,j\rangle$ denotes the nearest neighbour sites i and j. J is the antiferromagnetic exchange energy between the sites of opposite spins in two sublattices (say one of spin $\uparrow$ and one of spin $\downarrow$) and given by $J = \frac{4t^2}{U}$. The last term is three site exchange interaction term (J_3) entered in t-J model naturally.

(a)

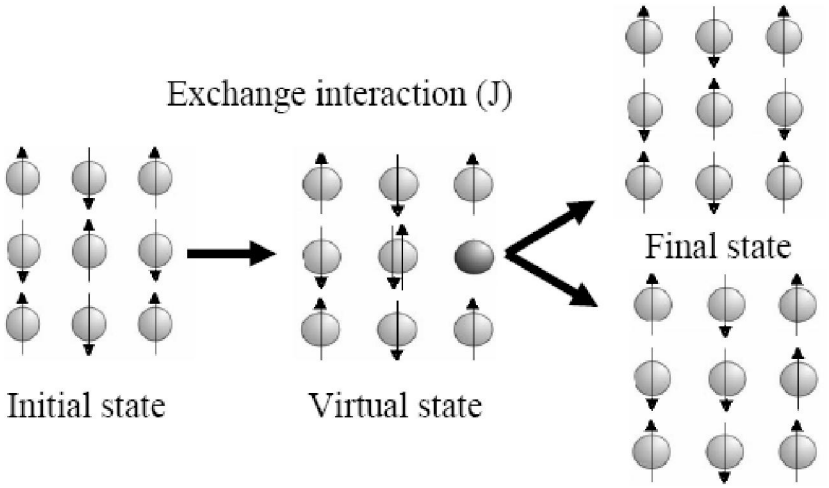

(b)

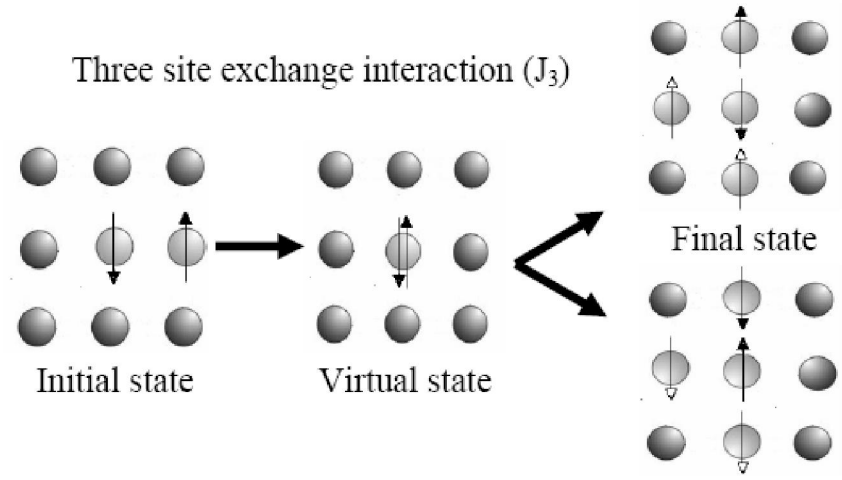

Figure (10). The schematic presentation of the initial, virtual and final states (a) for spin-spin exchange term (J) (b) for the three site exchange interaction term (J_3) on two dimensional antiferromagnetically ordered cuprate square plane.

Generally, the three site exchange interaction term (J_3) which arises naturally in the strong coupling version of Hubbard model i.e. t-J model, has not been given due attention so far in theoretical studies. Though the magnitude of J_3 is of the order δJ, (where δ is the hole density and J is antiferromagnetic exchange interaction). Recently, Li et al. (1993) have pointed out on the basis of numerical analysis that the three site exchange term becomes important in the dilute limit (where δ is greater than 0.05). The three site exchange term comprises the coupling of a site with the two distinct nearest neighbor sites.

The depiction of the virtual processes involved in spin-spin exchange term (J term) and the three site exchange term (J_3) are shown in figure (10). The virtual process occurs when two spins are on the nearest neighbor site on a square planar lattice. The virtual hopping of one spin onto the site occupied by other spin followed by either spin (spin up or spin down) hopping back to the earlier site: resulting the exchange interaction (J). On the other hand the three site exchange interaction (J_3) arises in dilute limit, when the possibility of finding the other three nearest neighbor sites unoccupied is exactly one. There is equal chance of one of the spin hopping onto any of these vacant neighbor sites when one spin has a virtual hopping onto the site occupied by the other spin [Koltenbah et al. (1997)].

Further, the role of coupling between the planes on the electronic spectra of multilayer cuprates is not properly understood upto now from theoretical point of view. Therefore, the first part of the present work have

been devoted to study the spectral properties of cuprate system having two CuO_2 layers in a unit cell (like in the case of $Bi_2Sr_2CaCu_2O_{8+x}$, and $YBa_2Cu_3O_{7-x}$) on the basis of extended $t-t'-t_\perp-J-J_3$ model and also the tight binding Hubbard model for the bilayer system by including momentum dependent interlayer coupling ($t_\perp$) term. This coupling energy between the CuO_2 planes is found highly anisotropic and predicted with the momentum dependence form of $\varepsilon_{\perp k} = -\frac{t_\perp}{4}$ $(\cos k_x a - \cos k_y a)^2$ [Chakravarty et al. (1993)].

A review of work carried out by several researchers through the years and closely connected to the present investigations is given in chapter 2. During the present investigations, we have employed Zubarev's double time Green's function formalism to investigate the model Hamiltonian and Kubo formula to obtain the conductivity expression. A brief description of these is given in chapter 3. The theoretical formulation of our present study is presented in chapter 4. Finally, we have summarized our results in Chapter 5.

REVIEW OF LITERATURE

Chapter 2

REVIEW OF LITERATURE

Recently, the development of photoemission spectroscopic measurement technique has evolved it as one of the most powerful probes to study the electronic spectra of layered cuprate superconductors. There are now highly resolved photoemission spectroscopic measurements of single layer, bilayer as well as trilayer cuprates, available in the superconducting as well as normal states in optimal and overdoped regimes [Zhou et al. (2006), Norman and Pepin (2003)].

These measurements have emphasized some of the most relevant issues related to the electronic structure and hence the spectral and transport properties, such as the remnant Fermi surface, the superconducting gap, the pseudogap in normal state (*d*-wave-like dispersion), the emergence of coherent quasiparticle peak through the superconducting transition, evidence of electronic inhomogeneity, nanoscale phase separation and bilayer splitting, many-body effects in the single-particle spectral function in the context of the role of interlayer coupling on the electronic spectra. The spectral and transport properties of these layered cuprates are anomalous in normal state, which depend on doping level, electron correlations as well as number of CuO_2 planes in a unit cell and coupling between these planes. Previous studies show that the inter unit cell coupling affects the spectral function as well as transport behaviour of

these layered cuprates. Therefore, we have planned to review the work related to spectral properties in the normal state in the first section of this chapter. In the second section, the literature related to transport behaviour of these high T_c cuprate superconductors is reviewed.

2.1 Electronic spectra in normal state

The subject of normal-state properties in the high T_c superconductors has received a great deal of attention. The most of the theoretical and experimental attempts of the spectral properties are based on the electronic structure of CuO_2 plane in the normal state as compared to superconducting state.

In a bilayer cuprates (Bi-2212) the two CuO_2 planes in a unit cell are just crystallographically equivalent and the carrier concentration is uniformly distributed among these two layers. However in trilayer cuprates (like Bi-2223), Stasio et al. (1990) predicted the highly non-homogenous charge distribution among the cuprate planes due to different chemical environment around the CuO_2 planes. The inner CuO_2 layer of trilayer Bi-2223 has no apical oxygen which makes it unidentical crystallographically with outer two layers. Tokura et al. (1989) pointed out the importance of apical oxygen in multilayered cuprates. The role of oxygen vacancies and the apical oxygen above as well as below CuO_2 planar sites becomes more important in the inhomogenous doping processes and electronic structure.

Therefore, the electronic structure and hence spectral properties of these multilayer cuprates is strongly dominated by doping level, electron correlations as well as number of CuO_2 plane in a unit cell and coupling between these planes. Recently, the progress in energy and momentum resolution of ARPES further enables us to directly observe the bilayer splitting due to the interaction between the CuO2 planes in normal state [Feng et al. (2001), Chuang et al. (2001)].

A dramatic change in the photoemission intensity just below superconducting transition temperature near $(\pi,0)$ point of the Brillouin zone was pointed out by Norman et al. (1998). These authors observed that a broad peak in the normal state ($T>T_c$) turns into a sharp low energy photoemission peak followed by a higher binding energy hump. Dessau et al. (1991) have also observed the anomalous transfer of spectral weight from the gap region to the pile up peak in bilayer Bi-2212 system at the superconducting transition. While along $\Gamma(0,0)-M(\pi,\pi)$ direction of Brillouin zone there has been a transfer of spectral weight from higher binding energies to lower one with the appearance of a dip in the spectra.

Chuang et al. (2001) presented the first high energy and momentum resolution angle resolved photoemission (ARPES) data of a cuprate superconductor which shows a clear doubling of the bands in normal state. These authors observed a splitting in bilayer compounds $Bi_2Sr_2CuO_{6+x}$ (Bi-2201). This splitting was found minimum along $(0,0)\rightarrow(\pi,\pi)$ points of the Brilloiuin zone and maximum at $(\pi,0)$ point of the Brillouin zone (figure (1)).

Further, it was concluded that the intracell out of plane coupling between the planes is responsible for such type of splitting.

The angle resolved photoemission spectroscopic studies of the electronic spectra of trilayer cuprates (Bi-2223) have been reported by Feng et al. (2002). They used high quality single crystals with dimensions suitable for ARPES measurements. These authors have observed a large Fermi surface, a d-wave superconducting gap alongwith a large superconducting peak in optimal doped (Bi-2223) trilayer cuprates. It is further pointed out that the superconducting gap magnitude and the relative weight of superconducting peak both increases with superconducting transition temperature for optimally doped trilayer cuprates. Investigations of the ARPES spectra of trilayer cuprate system (Bi-2223) by Feng et al. (2002) have also pointed out intra-trilayer coupling to be weaker in the trilayer cuprates in comparison to interlayer coupling in the bilayer system like Bi-2212. Thus, it becomes essential to consider the interlayer coupling and study the relative effect on the evolution of the electronic spectra and hence mechanism involved in high-temperature cuprates (figure (2)).

Several authors [Ozyuzer et al. (2000), Pan et al. (2000), Kim et al. (2001), Tensanovic et al. (1987)] have emphasized the role of layered structure on the anomalous electronic properties of these multilayer cuprates. Based on bilayer electronic band structure calculations, Chakravarty et al. (1993) have estimated a highly anisotropic intra unit

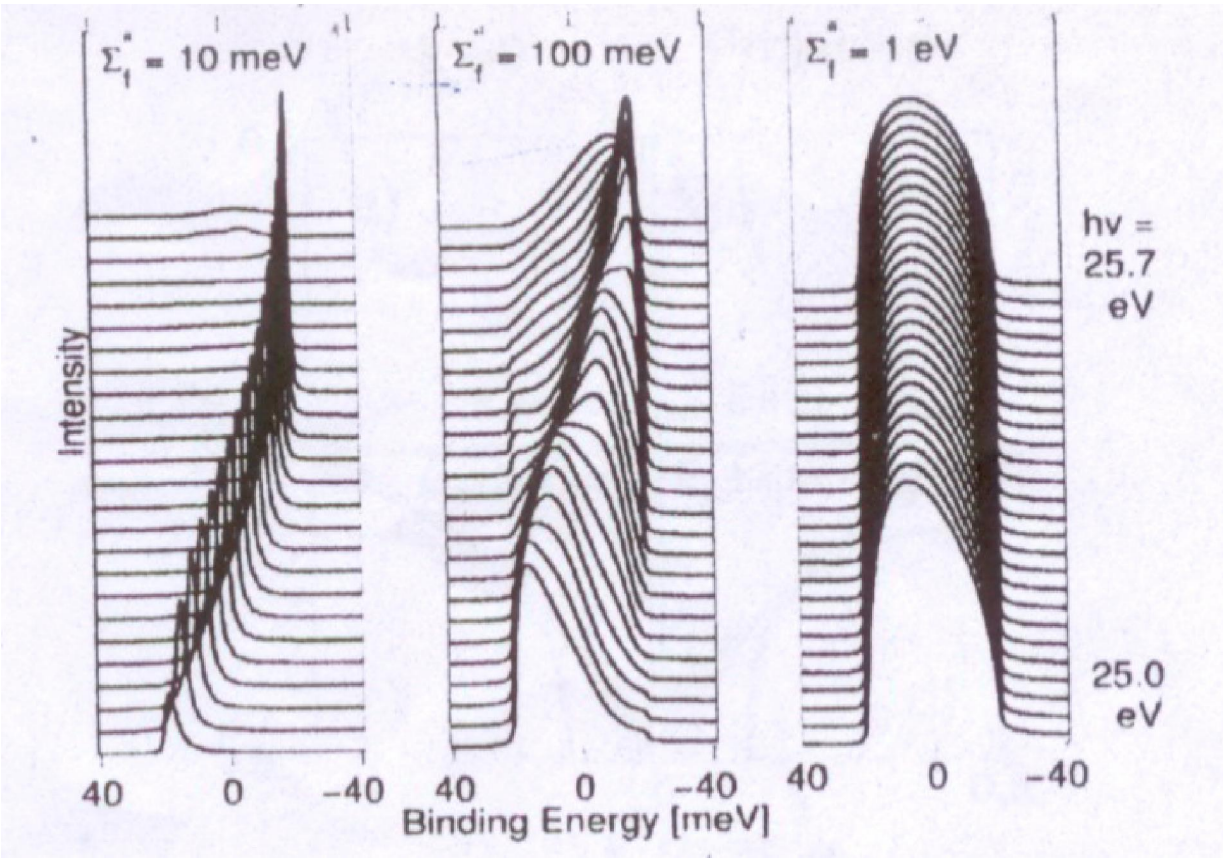

Figure (3) Irreducible broadening in normal state ARPES line shapes in Bi-2212 [Bansil et al., Phys. Rev. B 71 (2005)]

cell coupling having a planar momentum dependence of the form $\varepsilon_{k\perp} = -\frac{t_\perp}{4}\left(\cos k_x a - \cos k_y a\right)^2$ which provides maximum bilayer splitting to be at antinodal $(\pi, 0)$ point of the Brillouin zone and is in tune with the recent ARPES measurements in cuprates. This peculiar in-plane momentum dependence of $\varepsilon_{k\perp}$ results from the hybridization between the bonding O 2p orbitals and Cu 4s orbitals in each CuO2 plane and was confirmed by the angle-resolved photoemission spectroscopy (ARPES) measurements [Feng et al. (2001)].

Kamanski et al. (2003) using ARPES measurements pointed out that overdoped sample of $Bi_2Sr_2CaCu_2O_{8+x}$ at low temperatures shows a coherent metal phase which is characterized by coherent bilayer splitting effects in the electronic spectra. These authors also reported the absence of the coherence and hence bilayer splitting at low doping. The issue of doping dependence of bilayer splitting is still not clearly understood. The studies of Chuang et al. (2004) showed that the bilayer splitting effects are observable even in underdoped regime and have negligible effects due to doping.

Recently, Bansil et al. (2005) have analysed the manifestation of intercell coupling between CuO_2 planes on the ARPES spectra of bilayer Bi-2212 system. These authors concluded that the inter cell hopping, which is responsible for the k_z dispersion of the bands also induces an irreducible broadening to the ARPES lineshapes (figure (3)). This inter unit cell third dimensional coupling is found to have a characteristic dependence on the

inplane momentum. Thus, it plausible to take into account interlayer couplings between two CuO_2 planes within the unit cell and between the unit cells, while studying electronic properties of high temperature cuprates.

Quite recently, super-high resolution based angle resolved photoemission measurement on an optimally doped $Bi_2Sr_2CaCu_2O_8$ high temperature superconductor reveal a dramatic sensitivity of nodal excitation to temperature and superconductivity [Zhang et al. (2007)]. These observations provided evidence that in addition to coupling with low energy excitations like phonons or magnetic resonance mode, there are high-energy excitations involved in electronic coupling.

It is interesting that most of the known high T_c superconductors are cuprates. Several theoretical attempts have been made to explain the possible origin of high transition temperature and other features of oxide superconductors. But there is no consensus over a single mechanism so far. To mention a few, there are resonating valence bond (RVB) theory, antiferromangnetic fluctuations [Auerbach et al. (1988)], bipolarons [Alexandrov (1988)] and interlayer tunneling mechanism [Chakravarty et al. (1993)]. Pickett (1989), Dagotto (1994) and Anderson (1997) have put forward well documented review articles relating to description of various theories in this field.

As far as theoretical attempts are concerned, the Hubbard model and t-J model become good candidates to describe the various experimental results related to electronic structure of cuprates. Most of the theoretical

attempts are based on these models and their extensions with various approximate schemes. Maska (1997) studied t-J model within the mean field level and analyzed a competition between antiferromagnetism and s (or d) wave pairing. These authors have introduced the electronic self-energy in the calculation for the infinite-U Hubbard model to project out the states with doubly occupied sites.

Jaklic et al. (1997) studied the t-J model using the finite-temperature Lanczos method to calculate the single-particle spectral functions A(k, ω) and self-energy $\sum(k,\omega)$. These authors have pointed out a remarkable asymmetry between the electron and hole part of spectra. The photoemission spectra of hole part are found to be overdamped, with Im $\sum$ proportional to ω in a wide energy range, consistent with the marginal Fermi liquid scenario, and also found to be in good agreement with ARPES data in the cuprates.

Leung, Wells and Gooding (1997) used exact diagonalisation method to study $t-t'-t''-J$ model including next nearest neighbouring hopping (t') and second next nearest neighbouring hopping (t''). It was revealed that the extended t-J model is necessary when one compares the calculated spectral functions with the observed ones [Wells et al. (1995)]. It was also pointed out that the extended t-J model shows better agreement with ARPES experiment line shape in comparison to t-J model alone.

The extended t-t'-J model was used to find the variation in the chemical potential shift, density of states and the change in the density of doped holes in high-T_c cuprates [Ajay et al. (1999)]. The fictitious Coulomb interaction (U') was introduced and treated within the Hubbard self-energy approximation. In order to avoid double occupancy, $U' \rightarrow \infty$ limit was taken to calculate the electronic self energy. These authors have explained the doping dependence of the density of states (DOS) and shift in the chemical potential with hole doping (n_H) in the overdoped regime of the $La_{2-x}Sr_xCuO_4$ system.

An analysis of the effects of the Cu d-d inter orbital electron correlations on the electronic conduction along c-axis in high T_c cuprates was studied [Ajay et al. (2002)] within a microscopic model Hamiltonian for the three atom cluster (CuO_2) which incorporates the essential features of the basic unit of high-T_c cuprates. The model Hamiltonian for this three atom cluster includes various in-plane and out of plane orbital energies, their intra and inter-orbital Coulomb interactions relevant for the electrons in the cluster.

Pratap et al. (2001) used a self-consistent perturbative approach for investigating the effects of bilayer coupling on the electronic spectra in bilayer cuprates in normal state. They used $t-t'-J$ model including a layer-to-layer hopping matrix element alongwith an AFM exchange interaction term using a self-consistent perturbative approach and studied the strong

electron correlation effects that exist in the individual CuO_2 layers. These authors have calculated the single particle electronic spectral function A(k, ω) and self-energy for different values of the hole concentration, temperature, and anisotropy for analyzing the appropriate conditions for the splitting of the quasiparticle peak in the normal state spectra. These authors found that splitting in quasiparticle peak becomes favorable for higher values of the hole doping and higher anisotropy ratios. Also, it has been found that self-energy depend on the momentum, and the energy dependence of electronic self-energy varies like ω^{α} ($1< \alpha <2$) and contradicts marginal Fermi liquid (MFL) theory.

Mori et al. (2002) studied a two dimensional multilayer $t-t'-t''-J$ mode using Gutzwiller approximation and analyzed the electron-removal spectral functions at $(\pi,0)$ point of the Brillouin zone in the CuO_2 plane to understand the angle-resolved photoemission spectroscopic (ARPES) spectra. These authors pointed out that the trilayer spectrum is narrower than the bilayer cuprates spectrum but is wider than the monolayer cuprate. Further, it was also pointed out that the magnitude superconducting order parameter differs between outer CuO_2 plane and inner CuO_2 plane in the tri and tetra layer cuprate systems. On the other hand, the bilayer system was found to have same superconducting amplitude in each layer due to crystallographically identical environment.

Prevolsek et al. (2002) used the method of equation of motion for projected fermion operator to calculate the spectral function within the generalized t-J model. It has been analyzed that the method can be used to reproduce the self-consistent Born approximation results in an undoped antiferromagnet. For finite doping with short-range antiferromagnetic order the approximation evolves into a large incoherent contribution in the hole part of the spectral function as well as the hole-pocket-like Fermi surface at low doping. It was also concluded that the electronic density of state at the Fermi level get reduced at low doping.

It is important to note that in most of the above theoretical attempts based on extended t-J model, there are very few studies about the influence of three site exchange term (J_3) on the anomalous electronic properties of cuprates in normal state. The three site interaction term (J_3) arise naturally in t-J model as derived from the Hubbard model under strong coupling limit. Li et al. (1993) have pointed out on the basis of numerical analysis that the three site exchange term becomes important in the dilute limit (where δ is greater than 0.05). The three site exchange term (J_3) comprises the coupling of a site with the two distinct nearest neighbor sites and can play a role to renormalize the electronic spectra in doped normal state of cuprates.

On the other hand, there have also been the theoretical attempts to analyze the electronic properties in layered cuprates on the basis of

Hubbard model and its various extensions using uncontrolled approximation and numerical approaches. But so far the role of electron correlation effects as well as various in-plane and out of plane hopping energy parameters on the spectral properties is not well understood as analytical solution of Hubbard model in two dimensions is not available and there are a series of appropriate analytical and numerical approaches.

Kishore (1987) studied the quasi-particle spectrum of two dimensional Hubbard model using projection operator formalism of the Green's function. The exact results up to second order in the intra atomic Coulomb interaction were obtained in the weak-electron-correlation regime, while two bands are found in quasi particle spectrum for strong electronic correlations. A semiclassical approximation was also developed [Kishore et al. (1990)], which gives the exact results in proper limit. This approximation has been applied in paramagnetic phase of the Hubbard model and pointed out that the electrons near the Fermi energy become localized above a certain value of the ratio between the intra-atomic Coulomb interaction and the bandwidth of the non-interacting electrons. They concluded that this localization of electrons can give rise to a metal- non metal transition in a nearly half-filled band as found in the high T_c superconducting oxides also. Further, it is noted that this semiclassical approximation within the Hubbard model can also be applied for studying the role of electronic correlation and various hopping energies on the electronic spectra in high-T_c cuprates.

Neal et al. (1996) calculated non interacting density of states as a parameter within the Hubbard model in the limit of infinite dimensions. Their calculation indicated the results of broadening in bandwidth and narrowness in the central photoemission peak due to many body correlations. The effect of onsite and nearest neighbour Coulomb repulsion was studied in mean field theory using extended Hubbard model [Pietig et al. (1999)]. On the basis of their calculations, these authors showed a transition to a charge ordered phase with different sublattice occupancies at quarter filling. The drastically improvement in the effective mass was also indicated at a critical value of nearest neighbour interaction and a pseudogap opens in the single particle spectral function for higher values of this interaction.

The dynamical cluster approximation on the two dimensional Hubbard model in the intermediate coupling regime was studied by Maier et al. (2002). A crossover was found from a normal Fermi liquid with a Fermi surface around the Brillouin-zone center at large doping to a non-Fermi liquid for small doping, where the Fermi surface is hole like [around $M=(\pi,\pi)$].

The theoretical approaches to identify the role of the out of plane coupling within extended Hubbard and t-J models have also been a part of great attention in recent years. The out-of-plane coupling not only connects the Cu-O planes within the unit cell (intra unit cell) but also Cu-O planes of the adjacent unit cells (inter unit cell). In bilayer cuprates due to small

separation (of the order of 3.2 $\mathring{A}$) between two Cu-O planes within the unit cell, the intra unit cell coupling between two Cu-O bilayers results in the band splitting as observed in ARPES measurements. On the other hand, the inter unit cell coupling that connects the two adjacent Cu-O planes in different unit cells is believed to be weaker due to greater separation (of the order of 12 $\mathring{A}$ in Bi-2212 cuprates) between Cu-O planes of two adjacent unit cells. Because of very low strength of inter unit cell interaction between Cu-O planes, their effect shows up only in recent high resolution ARPES measurements of Chuang et al. (2001, 2004) on Bi-2212 system.

According to Inoue et al. (1987), the high transition temperature in these compounds could be partly due to interlayer interactions because cuprates having more than one CuO_2 plane in a unit cell have higher values of T_c. Tesanovic (1987) also analysed the role of interlayer coupling in high T_c cuprates. His results indicated that the interlayer coupling plays a role in enhancement of T_c and in stabilizing the superconductivity long range order. Hofmann et al. (1990) studied a theoretical model based on the double layer structure of $YBa_2Cu_3O_7$-x which included intra and interlayer pairings for the electrons (holes) involved so as to provide an explanation for high transition temperature in cuprates.

Recently, Govind et al. (2003) investigated the effect of intrabilayer coupling and out-of-plane Coulomb correlations on spectral properties of bilayer cuprates in their normal state. The electron correlations which exist

in the individual CuO_2 layers are described by t'-t''-U model. The coupling between the two layers of same unit cell is included by hopping matrix element and out-of-plane Coulomb correlation. These authors have calculated the electronic spectral function for various values of intrabilayer hopping and out-of-plane Coulomb correlation at different *k*-points of Brillouin zone in the overdoped regime. It is found through numerical calculations that the intrabilayer coupling provides favorable condition for splitting of quasiparticle peak of spectral function, while out-of-plane Coulomb correlation tries to suppress this effect. These authors have also made calculation of density of states as a function of hole density.

Pathak et al. (2005) extended the t-J model and studied the role of next nearest neighbor (t') and interlayer coupling ($t_\perp$) on the spectral function and density of state of the cuprates by using $t-t'-t_\perp-J$ model. These authors show a bilayer splitting in the presence of interlayer coupling term.

The effect of the coupling between two Cu-O planes in adjacent unit cell is analyzed by Markiewicz et al. (2005). These authors have pointed out the resulting k_Z dispersion in the cuprates within the framework of the one-band tight binding (TB) model Hamiltonian. They have obtained various values of tight binding parameters by fitting to the first principles local density approximation (LDA) based band structures, and also with experimental Fermi surfaces obtained by ARPES experiments in optimally

doped and overdoped single layer cuprates, $La_{2-x}Sr_x CuO_4$ and $Nd_{2-x}Ce_xCuO_4$ and bilayer cuprate Bi-2212.

Pathak et al. (2006) have studied the role of next nearest neighbor (t'), second next nearest neighbour (t''), interlayer coupling ($t_\perp$) and electron correlation on the spectral function and density of state of the cuprates within $t-t'-t''-t_\perp-U$ model. These authors have used Green's function equation of motion approach within semi-classical approximation due to Kishore (1987) for calculating spectral function and density of state. It was pointed out that t' shifts the $A(k,\omega)$ away from the Fermi level with increasing sharpness and provides favorable conditions for the bilayer splitting effects in the electronic spectra of bilayer cuprates. On the other hand the effect of second next nearest neighbour hopping (t'') was found just opposite to that of t' and opposes the bilayer splitting effects. The Coulomb energy U also plays an important role in the shape of spectral function at Fermi level. These authors observed that DOS is suppressed at the Fermi level in underdoped region with two peak structure and in optimal doped region, a finite DOS emerges at the Fermi level with the evolution of third peak structure. In the theoretical calculating, these authors have not analyzed the influence the third dimensional c-axis coupling between CuO_2 planes in adjacent unit cell.

Recently, Plakida et al. (2007) have proposed a microscopic theory for electronic spectrum of the CuO_2 plane within an effective p-d Hubbard model. They derived the Dyson equation for one-electron Green's function in

terms of the Hubbard operator and solved self-consistently for the self energy evaluated in the noncrossing approximation. These authors studied the doping dependence of electron dispersion, spectral function, the Fermi surface and the coupling constant.

2.2 Anomalous out of plane (c-axis) transport in layered cuprates

Measurement of the transport properties of a solid provides important information about the dynamics of charge carriers (quasiparticles). For example, conventional electronic transport depends on the charge mobility, electronic band structure and scattering processes in solids. However, the electrical transport in strongly correlated high T_c cuprate superconductor is trivial task since the transport properties varies with different parameters such as temperature, doping, pressure and shows different type of behaviour in plane and out of plane directions (highly anisotropic).

The through understanding of the electronic transport behaviour in normal state of high T_c cuprates is vital to pin point the mechanism responsible for high T_c superconductivity in these systems. Keeping above view in mind, Allen et al. (1988) indicated the analysis of transport behaviour of high T_c cuprates immediately after the discovery and predicted anisotropic transport behaviour of the oxide superconductors $La_{2-x}Sr_xCuO_4$ and $YBa_2Cu_3O_7$. They adopted local density functional (LDF) theory to calculated electronic energy bands and assuming only electron-phonon scattering. These authors pointed out that LDF theory overestimates the

Fermi velocity and suggested that some other scattering mechanism may dominate.

Therefore, several authors [Anderson et al. (1988), Nagaosa (1996), Anderson (1990)] have emphasized resonance-valence-bond (RVB) approach to explain anisotropic transport properties of the high T_c superconductors. Anderson (1988) proposed that the tunneling and anisotropic behaviour in resistivity can be explained, by a two dimensional resonating-valence-bond state. The physical properties including conductivity along c-axis was studied and compared with experiment in high T_c cuprates for the uniform RVB state by Nagaosa (1996). The author pointed out that interlayer hopping, occurs through the electrons whose spectrum has a (pseudo) gap and the conductivity ($\sigma_c = \rho_c^{-1}$) is reduced and show an insulating behavior as a function of temperature.

Electrical transport along the c-axis of high T_c layered oxide was pictured as a coherent interplaner tunneling between neighboring layer blocked by repeated interplanar incoherent scattering [Kumar and Jayannaver (1992)]. These authors described the temperature dependence of out of plane and in plane resistivity. They have pointed out that the temperature dependence arises from the temperature renormalization of the tunneling matrix element by an ohmic coupling to adiabatic phonons because of the large effective electronic mass along the c-axis in high T_c cuprates.

Littlewood and Verma (1992) derived the marginal Fermi-liquid phenomenology for studying the tunnelling characteristic within an anisotropic metal. They showed that tunnelling matrix element lead to a anisotropic conductance, which was found typically V shaped for c-axis tunnelling, and almost flat for in-plane tunnelling. They concluded that the resistive upturn in ρ_c is caused by incoherence in the hopping mediated by disorder directly related to the observed c-axis tunnelling characteristics. Leggett (1992) found that the c-axis tunnelling is strongly suppressed by charge fluctuations excited in the process of tunnelling, which later observed in many strongly correlated and mesoscopic systems.

Cooper et al. (1993) have reported optical studies of the a-, b-, and c-axis charge dynamics in $YBa_2Cu_3O_{6+x}$. These authors have analyzed the c-axis optical response in fully oxygenated $YBa_2Cu_3O_7$ (T_c~90K), characterized by a weak Drude conductivity and a c-axis polarized Raman continuum. Both optical responses are found consistent with incoherent hopping transport to a dephasing of c-axis transport by uncorrelated dynamical fluctuations in adjacent CuO_2 plane layers. These authors also suggested that the unconventional dephasing process should allow one to probe the dynamics in the ab plane using c-axis measurements. With decreased doping, they found that the CuO_2 bilayers become rapidly decoupled due to the loss of oxygens in the CuO chains. The unusual ab- plane optical response appears to be rather insensitive to interbilayer decoupling,

providing evidence that the normal state dynamics which characterize the CuO_2 planes persist in nearly isolated CuO_2 bilayers.

The model for c-axis resistivity ρ_c on the basis of static and dynamical disorder for cuprates has been presented by Rojo et al. (1993). These authors concluded from their higher order perturbative calculations that this special disorder stabilizes a low temperature metallic state and in the dynamical limit leads to temperature-dependent slope $(\partial\rho_c/\partial T)$ which is negative (positive) for low (high) hole concentrations. These authors have also presented the prediction for calculations which associate a nonlinear planar resistivity.

Wang et al. (1993) showed that the unusual normal state properties of the Copper oxide superconductors can be derived from the one band t-J model with the use of a rigorously imposed constraint of single electron occupancy and Wigner-Jordan representation of the spin-relaxation spectrum.

Liu et al. (1994) presented an analysis of anisotropic data of $YBa_2Cu_3O_{7-\delta}$ and showed that out of plane resistivity changes from nonmetallic to metallic behaviour. They further analyzed that the metallic (ρ_c) arises from a conventional relaxation mechanism within the framework of the band theory, while the nonmetallic ρ_c, is dominated by hopping conduction. This type of distinction is found between relaxation transport and hopping conduction.

How et al. (1994) studied anisotropic resistivity of $Bi_2Sr_2CuO_x$ and found that the ab- plane resistivity varies linearly with temperature down to 10^0K, but deviated slightly from linearity around 40K. The out of plane resistivity show metallic behaviour above 150^0K, but non-metallic below 105^0K. On the basis of these measurements, it is predicted that the anisotropy ratio in in-plane and out-of-plane resistivity (ρ_c / ρ_{ab}) is temperature dependent and becomes at low temperature.

The normal state transport properties of $YBa_2Cu_3O_x$ has also been investigated by Terasaki et al. (1995) along the in-plane and out-of-plane directions. They have pointed out anomaly in the scattering time which is compatible with a conventional Boltzmann transport or the 2D-Fermi-liquid approach involving incoherent interplane hopping. It is concluded that the residual resistivity along c-direction may be ascribed by the empirical relation $\rho_c = c_1 \rho_{ab} + c_2 / \rho_{ab}$.

Ando et al. (1995) have measured the resistivity of two $(La\text{-}Sr)_2CuO_4$ samples, one of them in the fully metallic optimally doped range, in magnetic fields up to 60 T, which completely destroys superconductivity. These results confirmed measurements from other which showed that at sufficiently low temperatures the resistivity of the cuprate along *ab*-plane crosses over to a negative temperature derivative with approximately logarithmic-T dependence, as opposed to the conventional linear T behaviour. The important results predicted by these authors has been that

the *c*-axis and *ab*-plane conductivities become proportional to each other at low temperatures although with an extraordinarily large anisotropy of the order 1000.

Nyhus et al. (1994) reported (within c-axis polarized Raman scattering and optical reflectivity measurements) doping and phonon induced changes in O(4)-Cu(1)-O(4) structure which further influence c-axis charge dynamics in $YBa_2Cu_3O_{6+x}$. They suggested that the decreasing semiconducting behaviour in $\rho_c(T)$ with increased doping may be arise because there is a decreased relative contribution of assisted hopping to the total c-axis conductivity as interbilayer coupling increases. Wang et al. (1996) have pointed out the doping dependence of c-axis resistivity $\rho_c(T)$. They measured anisotropy in resistivity using a generalization of the Montgomery method. Their analysis indicated that for all the samples, the in-plane transport mimic the metallic side of the Ioffe-Regel criterion. On the other hand the out-of-plane transport show the insulating behaviour. It has been concluded that the evolution of $\rho_c(T)$ with low doping level is caused by the reducing of both the impurity- and boson-assisted hopping processes.

Alexandrov et al. (1996) proposed a microscopic theory of the normal state transport in cuprates based on the bipolaron theory [Alexandrov and Mott (1994)] of high-temperature superconductors, which describes qualitatively the temperature and doping dependence of the in-plane (ρ_{ab})

and out-of-plane (ρ_c) resistivity and spin susceptibility (χ_s) in underdoped, optimally doped and overdoped $La_{2-x}Sr_xCuO_4$ systems. They developed a relation $\left(\rho_c(T,x)/\rho_{ab}(T,x) \sim x/T^{1/2}\chi_s(T,x)\right)$ between the anisotropy in resistivity and the spin susceptibility.

The pressure dependence of out-of-plane resistivity has also been investigated in an optimally-doped high-T_c cuprate $La_{2-x}Sr_xCuO_4$ [Nakumara et al. 1996]. By applying pressure, these authors found a drastic decrease in ρ_c. This surprisingly large pressure dependence implies that the thermal contraction along the c- axis is reflected in the $\rho_c(T)$, leading to a metal-like behaviour. It is proposed that the non-metallic conduction along the *c* axis can be described in terms of the tunnelling or quantum hopping between adjacent CuO_2 layers and emphasized the third dimensional coupling.

The interactions between polarons and the anharmonic vibrations of the apical oxygen atoms in the normal state of $YBa_2Cu_3O_{7-\delta}$ superconductors have been studied by Zoli (1997) using a path integral formalism. The influence of temperature on the distribution of double-well potential associated with the anharmonic modes have been taken into account. It has been shown that the *c*-axis electrical resistivity depends linearly on temperature for intermediate values of the electron-phonon coupling, whereas strong anharmonicity induces a nonmetallic behavior as a consequence of trapping of the charge carriers.

Ramsak et al. (1998) caluclated c-axis resistivity within the t-J model assuming the incoherent interlayer hopping. In the optimally doped regime they found an anomalous relaxation rate following $\tau_c^{-1} \propto \omega + \xi_c T$ behaviour and $\rho_c(T) \propto \rho_{ab}(T)$ suggesting a common relaxation mechanism for intra- and interlayer transport. These authors pointed out the appearance of pseudogap in the density of states at low doping responsible for a semimetallic like behaviour of $\rho_c(T)$.

Wu et al. (1998) analyzed the effect of interband transitions on the c-axis conductivity in a plane-chain bilayer model of a cuprate. They have pointed out that the relation between the c-axis resistivity and thermal conductivity is governed by the Wiedemann-Franz law. For a small perpendicular hopping matrix element between chain and plane ($t_\perp$), they obtained a characteristic upturn in the c-axis resistivity as the temperature is lowered. On increasing $t_\perp$, they obtained a more conventional response as intraband transitions start to dominate.

A simplified model of c axis transport in the high-T_c cuprates in normal state has also been presented by Atkinson et al. (1998). They have obtained the expressions for the c-axis optical conductivity, dc resistivity, and the c-axis penetration depth within the framework of a model and pointed out the existence of pseudogap in the optical conductivity arising naturally as a result of the layered band structure of the high T_c materials. They have also discussed the occurrence of the pseudogap in terms of three

parameters: a band gap, a temperature dependent scattering rate, and the strength of the interlayer coupling. They have obtained the analytic expressions for the dc conductivity and the low temperature penetration depth in terms of these three parameters.

Lal et al. (1998) developed a phenomenological model based on hybridization of out-of-plane O $2p_z$ and Cu $3d_{3z^2-r^2}$ orbitals, which are involved in the hopping along c-axis. They have pointed out that below finite temperature (T^*), the c-axis resistivity shows a semiconducting behaviour at low carrier concentration (holes). At temperatures greater than T^*, the $\rho_c(T)$ shows metallic behaviour. On the other hand $\rho_{ab}(T)$ remains metallic for all temperature. In overdoped system $\rho_c(T)$ turns out to be always metallic.

A model to explain *c*-axis transport properties in cuprates has been proposed by Tukalov and Leggett (2001). They suggested inter-plane and in-plane charge fluctuations as an important parameter responsible for incoherent and diffusive hopping between planes. These authors showed that the most of the c-axis transport properties can be qualitatively understood on the basis of the in-plane and inter-plane charge density fluctuation excited spectrum. The non-Drude optical conductivity $\sigma_c(\omega)$ and the temperature dependence of the dc conductivity were explained by the strong fluctuations excited in the process of inter-planer tunnelling.

Ajay et al. (2002) have developed a model to study the effect of the Cu d-d inter orbital electron correlation on the motion of charge carriers

along c-axis in high T_c cuprates. These authors considered a microscopic model Hamiltonian for three atom cluster (CuO_2) which includes various in-plane and out-of-plane energies, their intra and inter orbital Coulomb interactions relevant for the electrons in the cluster. They have concluded that the out-of-plane conduction of charge carriers depends on the Coulomb interactions, the level energies and the hole occupancy of the out-of-plane orbital as well as the temperature in an essential way. These calculations qualitatively indicated how the out-of-plane conduction of holes in bulk high T_c cuprate system depends on intra and inter orbital Coulomb correlations.

Recently, Giura et al. (2003) studied normal state c-axis transport in $Bi_2Sr_2CaCu_2O_8$. These authors presented a series of simultaneous measurement of resistivity tensor components ρ_{ab} and ρ_c on samples with different doping. A model was proposed for the conduction along the c-axis based on the hypothesis that BSCCO (2212) is made of 2D Cu-O planes separated by two different barriers, the temperature (T) range experimentally explored coincides with the temperature region where ρ_c decreases, resulting in an overall semiconducting behaviour. At high doping, ρ_c becomes small at lower temperatures and in the temperature range explored, the full resistivity is dominated by the contribution of the other barriers. Devereaux (2003) presented symmetry analysis of in-plane and out-of-plane transport in a family of high T_c oxide cuprates and pointed out that the nodal transport is largely doping dependent and metallic, while transport near the Brillouin zone axes is governed by a quantum critical

point near doping ~0.22 holes per CuO_2 plaquette. The author has shown that the c-axis conductivity rises for $T<<T_c$ is a consequence of partial conservation of in-plane momentum for out plane transport.

A phenomenology of incoherent transport for layered cuprates has been presented by Levin (2004) mainly based on the exploration of the consequences of a general assumption that the out of plane phase coherence length of the charge carriers is a short fixed distance of the order of interatomic distances. These authors have pointed out that the metallic branch of incoherent crystal can be described by logarithmically increasing conductivity: $\sigma_{ab} \propto \ln(^{a}_{\phi})$ (where $^{a}_{\phi}$ is in plane coherence length).

Ho and Schofield (2005) proposed a model assuming strong coupling between electronic and bosonic modes that propagates along c-direction only. They found a broad maximum in the c-axis resistivity at a temperature near the characteristic energy of the bosonic mode, while no corresponding feature appear in the in-plane transport. At temperatures far from this bosonic energy scale, the c-axis resistivity follows the in-plane electron scattering rate. These authors have also demonstrated a reasonable fit of their theory to the apparent metallic to non-nonmetallic crossover in the c-axis resistivity of the layered structured ruthenate.

Recently, Giura et al. (2007) presented a phenomenological model for the electrical transport in double-layered cuprates based on the existence of two energy barriers along the c-axis. The model has been applied to analyze of the dc resistivity in $Bi_2Sr_2CaCu_2O_{8+\delta}$ single crystals. They have pointed

out that the model provides a comprehensive description of the out-of-plane normal resistivity (ρ_c) at various doping and concluded that once the normal state has been determined, it is possible to obtain the fraction of the carriers that do not participate to the c-axis conductivity below the pseudogap temperature.

Above experimental and theoretical analysis indicates that in order to analyze the out-of-plane transport behaviour of layered high T_c cuprates, it is vital to emphasis on interlayer coupling of CuO_2 planes within the unit cell as well as in adjacent unit cell. A different approach towards the coupling between two CuO_2 planes in adjacent unit cells is proposed by Abrikosov (1997, 1999).

Abrikosov (1997, 1999) explained the out-of-plane (c-axis) electronic conduction in multilayered structures using the concept of resonant tunneling (initially proposed by Bohm (1951)). The idea was based on the tunneling of electrons (holes) through a potential barrier. It was argued that if there is an potential well exactly in the middle of the barrier, the tunneling probability can be raised nearly equal to 1, in comparison to normal exponential small value.

Abrikosov (1997) argued that broken CuO chains in underdoped $YBa_2Cu_3O_{6+x}$(Y-123) and BiO-layers in bilayer Bi-2212 cuprates plays the role of such barrier centers and gives rise to ‘resonant tunneling’ responsible for electronic conduction along the c-axis. The Cu-O chain in Y-123 system lies exactly in the middle of the two bilayers of nearest neighbor unit cell

and provide resonant tunneling in the out of plane direction in a natural way. In the case of bilayer Bi-2212 system, on which a lot of recent ARPES spectroscopic measurements have been carried out, the BiO chains are slightly displaced from the mid position of the two Cu-O planes in different unit cell. Abrikosov has argued that this displacement is too small to influence quantitatively the tunneling probability [Abrikosov (1999)]. Therefore, the resonant tunneling mechanism is able to account for out of plan (c-axis) electronic conduction processes in systems like Y-123 and Bi-2212.

Most of the recent theoretical studies based on extension of tight binding Hubbard model have not taken into account the inter cell coupling. Therefore in the second and third section of theoretical formulation, the extended Hubbard model is taken in the light of inter unit cell resonant tunneling to analyze its effect on spectral properties and out-of-plane transport behaviour.

MATHEMATICAL TECHNIQUE

Chapter 3

Mathematical Technique

In this chapter, we present a brief account of mathematical technique employed to calculate the spectral properties, like electronic spectral function $A(k,\omega)$, and density of states (DOS) as a function of various hopping energies and interlayer coupling term and the other parameter of the model Hamiltonian. To obtain the expressions for spectral function $A(k,\omega)$ and density of states (DOS) we have employed the double time retarded Green's function formalism (Zubarev, 1960). The Green's function is a propagator and a generalization of correlation function. By the knowledge of relevant Green's functions for a quantum many body system the corresponding desired correlation functions can be derived. These correlation functions can be used to get the expressions for various parameters like spectral function $A(k,\omega)$ and density of states (DOS) in normal state of high T_c cuprates. A brief discussion of this formalism is given below.

3.1 Green's function technique

The Green's functions are convenient for the study of the properties of interacting quantized fields. Their applications are suitable in the cases where one has to sum some types of perturbation theory

diagrams, particularly in the quantum theory of fields when combined with the spectral representation.

The Green's functions are the appropriate generalization of the concept of correlation functions and work as a propagator. They are connected with the experimentally observed quantities like $A(k,\omega)$ and density of states etc. and have well known advantages to solve the many body problems when exact solutions are not available.

In statistical mechanics, there are various kinds of Green's functions, for instance; the double-time causal Green's function $G_c(t,t')$, the retarded Green's function $G_r(t,t')$ and the advanced Green's function $G_a(t,t')$. These are defined as :

$$G_c(t,t') = \langle\langle A(t);B(t')\rangle\rangle_c$$
$$= -i\langle TA(t);B(t')\rangle \quad \ldots (1a)$$

$$G_r(t,t') = \langle\langle A(t);B(t')\rangle\rangle_r$$
$$= -i\theta(t-t')\langle[A(t);B(t')]\rangle \quad \ldots (1b)$$

$$G_a(t,t') = \langle\langle A(t);B(t')\rangle\rangle_a$$
$$= i\theta(t'-t)\langle[A(t);B(t')]\rangle \quad \ldots (1c)$$

where, A(t) and B(t') are the Heisenberg representation of operator A and B expressed in terms of product of quantized field functions.

$A(t) = e^{iHt} A(0)e^{-iHt}$, with H being Hamiltonian operator and

$[A,B]_\eta = AB - \eta BA,$

$\eta = +1$ for Bosons and $\eta = -1$ for fermions

The $\theta(t)$ is the unit step function and notation $\langle\cdots\rangle$ denotes the average over grand canonical ensemble at temperature T.

3.2 Green's function equation of motion

In the present thesis, we have mainly used the retarded Green's function. To obtain the equation of motion of Green's function we differentiate equation (1b) with respect to time t and obtain:

$$i\frac{dG_r}{dt} = i\frac{d}{dt}\langle\langle A;\ B\rangle\rangle_r$$

$$= \frac{d}{dt}\theta(t-t')\langle[A(t);B(t')]\rangle + \langle\langle i\frac{dA(t)}{dt};\ B(t')\rangle\rangle \qquad \ldots(2)$$

Taking into account the relation between step function $\theta(t)$ and the δ-function of time t as :

$$\theta(t) = \int_{-\infty}^{t}\delta(t)dt \qquad \ldots (3)$$

and the time evolution equation of the motion of the operator as:

$$i\frac{dA}{dt} = AH - HA\ , \qquad \ldots (4)$$

the equation for Green's function G_r may be written as

$$\frac{dG_r}{dt} = \delta(t-t')\langle[A(t);B(t')]\rangle + \langle\langle[A(t),H];\ B(t')\rangle\rangle \quad \ldots (5)$$

To solve equation (5) we have to solve the commutator [A(t), H] for a given Hamiltonian operator H. Therefore, equation (5) contains some higher order Green's functions. In order to linearize these higher order Green's functions into lower ones to obtain a closed form of equations of motion, we normally employ decoupling approximations based on plausible physical grounds. The Fourier transform of the Green's function with frequency ω yields:

$$\langle\langle A;\ B\rangle\rangle_{\omega} = \frac{1}{2\pi}\int_{-\infty}^{\infty}\langle\langle A(t);B(t')\rangle\rangle e^{-i\omega(t-t')}d(t-t') \qquad \ldots (6)$$

which satisfy the equation of motion :

$$\omega\,\langle\langle A;\ B\rangle\rangle_{\omega} = \frac{1}{2\pi}\langle[A,B]_{\eta}\rangle + \langle\langle[A,H];B\rangle\rangle_{\omega} \qquad \ldots (7)$$

The correlation function ⟨B(t') A(t)⟩ is related to the corresponding Green's function by :

$$\langle B(t')\ A(t)\rangle = i\lim_{\xi\to 0}\int_{-\infty}^{\infty}\frac{\left[\ \langle\langle A,\ B\rangle\rangle_{\omega+i\xi} - \langle\langle A,B\rangle\rangle_{\omega-i\xi}\ \right]}{\left\{e^{\beta\omega}-\eta\right\}}e^{i\omega(t-t')}d\omega \qquad \ldots(8)$$

By the knowledge of the relevant Green's function, we can obtain the desired correlation functions which are important to study normal state electronic spectra of layered high T_c cuprates as well as other interacting electronic system.

The Spectral function A (k, ω) is calculated from the Green's function $G(k,\omega)$ by using the standard spectral relation:

$$A(k,\omega) = -\frac{1}{\pi}\mathrm{Im}G(k,\omega) \quad . \qquad \ldots(9)$$

Where Im stands for the imaginary part of the Green's function $G(k,\omega)$. The spectral function is directly accessible via photoemission measurements (as the spectral intensity is directly proportional to $A(k,\omega)$) and can be analysed numerically. From the expression of spectral function $A(k,\omega)$ one can also calculate the density of states for high T_c cuprates at zero temperature by using the formula:

$$N(\omega) = \frac{a^2}{4\pi^2}\int_{-\frac{\pi}{a}}^{\frac{\pi}{a}}\int_{-\frac{\pi}{a}}^{\frac{\pi}{a}} A(k,\omega)\, dk_x dk_y \quad , \qquad \ldots(10)$$

Finally hole density can be calculated from equation (10) by integrating over the occupied energy states as:

$$n_H = \int_{-\infty}^{\mu} N(\omega) d\omega \qquad \ldots(11)$$

Where, μ is the chemical potential. The other electronic properties can also be analyzed from the relevant Green's function and spectral function.

In the present investigations the spectral function $A(k,\omega)$ involve δ-functions and to analyze the spectral function in the context of line shape of the ARPES photoemission experimental results in cuprates in normal state we need to solve δ - functions involved in the above theoretical calculation, which is just equivalent to broadening of the quasiparticle peak as observed in photoemission spectra. For this purpose we have considered Lorentizian type of broadening by using the relationship:

$$\delta(\omega - \tilde{\varepsilon}_k) \cong \frac{1}{\pi} \operatorname{Lim}_{\Gamma \to 0} \frac{\Gamma}{(\omega - \tilde{\varepsilon}_k)^2 + \Gamma^2} \qquad \ldots(12)$$

The broadening factor Γ is related to width of the spectral functions takes care of quasi-particle scattering rate and can be connected with the photoemission experimental energy resolution limit.

3.3 Kubo formula for conductivity

Kubo (1957) first derived the expression for electrical conductivity in solids using many body formalism. Within Kubo formalism the dissipative part of electrical conductivity tensor is defined as

$$\sigma_{\mu\nu}(\omega) = \frac{i}{V} \lim_{\eta \to 0} \int_0^\infty \langle [j_\mu(t), \chi_\nu] \rangle e^{-i\omega t - \eta t} dt \qquad \ldots.(13)$$

Where V is the volume of the system, j_μ is the μ component of the current operator and χ_ν is the ν component of the polarization operator. In Wannier basis we have

$$\breve{\chi} = e \sum_{i\sigma} R_i \eta_{i\sigma} \qquad \ldots(14)$$

The μ component of electric polarization vector can be given by

$$\chi_\mu = e \sum_{ij\sigma} (\delta_{ij})_\mu c^+_{i\sigma} c_{j\sigma} \qquad \ldots.(15)$$

the μ component of the current operator (j_μ) can be calculated from equation (15) as: $j_\mu = \frac{d}{dt} \chi_\mu$

$$= -ie \sum_{ijo} t_{ij} (R_i - R_j)_\mu c^+_{i\sigma} c_{j\sigma} \qquad \ldots.(16)$$

Also, $j_\mu(t) = e^{iHt} j_\mu e^{-iHt}$ is the Heisenberg representation of j_μ. Eq. (13) can be written in the alternative form in terms of current-current correlation function as:

$$\sigma_{\mu\nu}(\omega) = \frac{1}{2V}\int_{-\infty}^{\infty} e^{i\omega t} d\tau \int_0^{\beta} \langle j_\mu(0)\, j_\nu(\tau + i\lambda)\rangle d\lambda \qquad \ldots.(17)$$

The dc conductivity formula from above equation can be obtained as

$$\sigma_{dc} = \lim_{\omega \to 0} \sigma_{\mu\nu}(\omega) \qquad \ldots.(18)$$

For suitable Hamiltonian one can calculate current-current correlation and hence conductivity for a many body interacting system. In the present thesis, we have attempted a calculation of c-axis conductivity using a extended tight binding Hubbard model having the contribution of the third dimensional inter unit cell resonant tunneling for bilayered cuprates in normal state.

In the next section we have presented the detailed theoretical calculation related to present investigation employing the above Green's function equation of motion approach.

THEORETICAL FORMULATION

Chapter 4

THEORETICAL FORMULATION

4.1 Influence of three site interaction on electronic spectra (Within $t-t'-t_\perp-J-J_3$ model):

We model the doped bilayer cuprates like Bi-2212 having two CuO_2 planes per unit cell as described in introduction in detail. In order to mimic the observed electronic states, the various extended hopping energies within CuO_2 plane and between the two CuO_2 planes within the unit cell alongwith long range three site exchange (J_3) term has been included. The Hamiltonian for our model is described as:

$$H = H_{t-t'-t_\perp} + H_{J-J_3} \qquad \text{....(1)}$$

where,

$$H_{t-t'-t_\perp} = -t\sum_{rij\sigma} c^{+}_{ri\sigma}c_{rj\sigma} - t'\sum_{rij'\sigma} c^{+}_{ri\sigma}c_{rj'\sigma} + \sum_{\substack{ij\sigma \\ r\neq s}} t_\perp c^{+}_{ri\sigma}c_{sj\sigma} + U'\sum_{ri\sigma} n_{ri\sigma}n_{ri-\sigma} \qquad \text{....(2a)}$$

$$H_{J-J_3} = \frac{J}{2}\sum_{r\langle ij\rangle}\left(\overset{\circ}{S}_{ri}.\overset{\circ}{S}_{rj} - \frac{1}{4}n_{ri}n_{rj}\right) - \frac{J_3}{4}\sum_{ri\delta'\neq\delta\sigma}\left(c^{+}_{ri+\delta\sigma}n_{ri-\sigma}c_{ri+\delta'\sigma} + c^{+}_{ri+\delta\sigma}c^{+}_{ri-\sigma}c_{ri+\delta'-\sigma}c_{ri\sigma}\right) \qquad \text{...(2b)}$$

Where, r=1, s=2 (r=2, s=1) for bilayer system. The first term in the kinetic part of the Hamiltonian shown in equation (2a), is the planar electronic kinetic energy that includes the contribution of the next nearest neighbor

(t') and the third term in (2a) represents the momentum dependent interlayer coupling, $\varepsilon_{\perp k} = -\frac{t_\perp}{4}(\cos k_x a - \cos k_y a)^2$ as suggested by electronic band structure calculations [Chakravarty et al. (1993)] and recent ARPES measurements [Norman et al (2003), Feng et al. (2001 & 2002)] also. The additional Coulomb energy (U') is the fictitious Coulomb interaction involved in kinetic part only. The term U' is introduced in order to put double occupancy constraints as we are not using projection operator formalism to project out doubly occupied sites. The interaction part of Hamiltonian shown in equation (2b) contains nearest neighbor exchange energy (J) contribution alongwith three site exchange interaction term (J_3).

In order to solve the extended Hamiltonian as shown in equations (1) to (2b), and to obtain the expressions of electronic spectral function $A(k,\omega)$ and density of states, we follow the approach developed by Pathak et al. (2005). In this approach, the kinetic part (2a) of the Hamiltonian will be treated using Green's functions within Hubbard-I approximation [Maska (1993, 1997)]. On the other hand the exchange part (2b) is treated within mean-field approximation separately. Treating the first part of the Hamiltonian $H_{t-t'-t_\perp}$ within the Hubbard self-energy approximation [Shin et al. (2000)], one gets the Green's function as:

$$G_{rr}^{\sigma}(k,\omega) = \frac{1}{\left[\omega - \varepsilon_k - \varepsilon_k' - \frac{\varepsilon_{k\perp}^2}{\omega - \varepsilon_k} - \sum_r^{\sigma}(k,\omega) - \mu\right]} \qquad \ldots\ldots(3)$$

Here, k is momentum and ω the energy of a hole, ε_k is the energy originating from the hopping term t, ε'_k is originating from the t' and, $\varepsilon_{k\perp}$ is arising from hopping between the CuO_2 planes. Explicitly:

$$\varepsilon_k = -2t(\cos k_x a + \cos k_y a) \qquad \ldots.(4)$$

$$\varepsilon'_k = -4t'(\cos k_x a \cos k_y a), \text{ and} \qquad \ldots.(5)$$

$$\varepsilon_{k\perp} = -\frac{t_\perp}{4}(\cos k_x a - \cos k_y a)^2 \qquad \ldots.(6)$$

Here, the k dependence of $\varepsilon_{k\perp}$ has been taken as suggested by Chakravarty et al. (1993). $\sum_r^\sigma(k,\omega)$ is the Hubbard-self-energy calculated under the strong Coulomb correlation limit (i.e. the limit $U' \to \infty$) to singly occupied sites only. From (3), the one electron renormalized energies will be given by:

$$\varepsilon_k \to \tilde{\varepsilon}_{rk}^\sigma(\omega) = \varepsilon'_k + \varepsilon_k + \frac{\varepsilon_{k\perp}^{\ 2}}{\omega - \varepsilon_k} + \sum_r^\sigma(k,\omega) \qquad \ldots.(7)$$

The form of the self-energy within the Hubbard-I approximation where the life time effects are neglected [Shin et al. (2000), Ajay et al. (1999)] is given below

$$\sum_r^\sigma(\omega) = \frac{U' n_{r\text{-}\sigma}\omega}{\omega - U'(1 - n_{r\text{-}\sigma})} \qquad \ldots.(8)$$

In High T_c cuprates at low doping, carriers move in a planar antiferromagnetically ordered background. As the hole concentration increases the long range AFM order starts weakening. However, short-range AFM correlation persists at even higher hole doping levels [Nazarenko et al. (1996), Pan et al. (2000), Dai et al. (1999)]. In order to consider the effect

of local antiferromagnetic order it is assumed that self energy for $\uparrow$ spin is just equal to that of $\downarrow$ spin i.e.

$$\Sigma_r^{\uparrow}(\omega) = \Sigma_r^{\downarrow}(\omega) = \Sigma(\omega)$$

and in the limit $U' \to \infty$, self-energy (now spin independent) is given by;

$$\Sigma(\omega) = -\frac{n_H \omega}{(2 - n_H)} \qquad \text{....(9)}$$

Here, we have used $n_{r\uparrow} = n_{r\downarrow}$ and $n_H = n_{r\uparrow} + n_{r\downarrow}$ and $n_H = 1 - n$, hole concentration.

The two sublattice approach has been adopted to take into account the short range antiferromagnetic order in doped system [Pathak et al. (2005)]. For a square lattice, the lattice is divided into two sublattices A and B such that nearest neighbour of sublattice A (say spin up) belongs to sublattice B (say spin down) and vice -versa. Within the two sublattice approach the sublattice operators in the momentum space can be defined as:

$$c_{ri\sigma} = \frac{1}{\sqrt{N}} \sum_{rk} a_{rk\sigma} e^{ik.R_i} \qquad \text{for } i \in A$$

$$c_{ri\sigma} = \frac{1}{\sqrt{N}} \sum_{rk} b_{rk\sigma} e^{ik.R_i} \qquad \text{for } i \in B \qquad \text{....(10)}$$

Using the above transformations, the kinetic part of the Hamiltonian (2a) can now be rewritten in momentum space in the following form:

$$H^{kin}(\omega) = \sum_{rk\sigma} \tilde{\varepsilon}_k(\omega)\left(a^+_{rk\sigma} b_{rk\sigma} + b^+_{rk\sigma} a_{rk\sigma}\right) + \sum_{rk\sigma} \varepsilon'_k(\omega)\left(a^+_{rk\sigma} a_{rk\sigma} + b^+_{rk\sigma} b_{rk\sigma}\right) \qquad \text{....(11)}$$

and, $$\tilde{\varepsilon}_k(\omega) = \varepsilon_k + \frac{\varepsilon_{k\perp}^2}{\omega - \varepsilon_k} - \frac{2}{2 - n_H}\omega - \mu \quad \text{....(12)}$$

In equation (11), the first term originates from the nearest neighbour hopping matrix, while the second term corresponds to the second nearest neighbour hopping.

The second term in the Hamiltonian (1) attributed to the exchange interaction (equation (2b)) has been treated within the mean-field approximation. It is written as:

$$H^{int}_{J-J_3} = -\frac{J}{2}\sum_{\langle ij\rangle r}[\tilde{n}_{ri\downarrow}c^+_{rj\uparrow}c_{rj\uparrow} + \tilde{n}_{ri\uparrow}c^+_{rj\downarrow}c_{rj\downarrow}] - \frac{J_3}{2}\sum_{rijj'}[c^+_{rj\uparrow}\tilde{n}_{ri\downarrow}c_{rj'\uparrow} + c^+_{rj\uparrow}c^+_{ri\downarrow}c_{rj'\downarrow}c_{ri\uparrow}] \quad \text{....(13)}$$

where, the following parameter has been used

$$\tilde{n}_{ri} = \langle c^+_{ri\uparrow}c_{ri\uparrow} + c^+_{ri\downarrow}c_{ri\downarrow}\rangle \quad \text{....(14)}$$

and we have not taken into account the spin density and hence the AFM ordering at this stage in order to avoid complexity. In the two sublattices, we write:

$$\tilde{n}_{ri\sigma} = n_{rA\sigma} \qquad i \in A \text{, and}$$

$$\tilde{n}_{ri\sigma} = n_{rB\sigma} \qquad i \in B$$

After performing Fourier transformation the Hamiltonian (13) can be written in the form;

$$H^{int}_{J\text{-}J_3} = -\frac{J}{2}Z\sum_{rk\sigma}[n_{rA\text{-}\sigma}b^+_{rk\sigma}b_{rk\sigma} + n_{rB\text{-}\sigma}a^+_{rk\sigma}a_{rk\sigma}]$$
$$-\frac{J_3}{4}Z^2\sum_{rkk'\sigma}[b^+_{rk\sigma}n_{rA\text{-}\sigma}a_{rk'\sigma} + b^+_{rk\sigma}a^+_{rk-\sigma}a_{rk'-\sigma}a_{rk\sigma}] \quad \text{....(15)}$$

where for square lattice the coordination number Z is equal to 4.

Finally, combining the equations (11) and (15) (kinetic and exchange part of the model) the effective Hamiltonian of our model can be written as:

$$\tilde{H}(\omega)=\sum_{rk\sigma}\tilde{\varepsilon}_k(\omega)\left(a^+_{rk\sigma}b_{rk\sigma}+b^+_{rk\sigma}a_{rk\sigma}\right)+\sum_{rk\sigma}\{\varepsilon'_k-\frac{J}{2}Z\langle n_{rB-\sigma}\rangle\}a^+_{rk\sigma}a_{rk\sigma}$$
$$+\sum_{rk\sigma}\{\varepsilon'_k-\frac{J}{2}Z\langle n_{rA-\sigma}\rangle\}b^+_{rk\sigma}b_{rk\sigma}-\frac{J_3}{4}Z^2\sum_{rkk'\sigma}[b^+_{rk\sigma}\langle n_{rA-\sigma}\rangle a_{rk'\sigma}+b^+_{rk\sigma}a^+_{rk-\sigma}\,a_{rk'-\sigma}\,a_{rk\sigma}] \quad \text{.....(16)}$$

The kinetic part and the exchange part of the Hamiltonian (16) are not calculated on the same footing. The kinetic part is solved within the Hubbard self-energy approach under the consideration of fictitious Coulomb interaction $U'\to\infty$ to avoid doubly occupied sites. The appearance of U' is limited to kinetic part only, and is not involved in the exchange part. As we are interested in optimal doped regimes where J_3 is significant and of the order of kinetic energy, so H_J has been treated within the mean-field approximation.

To study the spectral function, one sets up equations of motion for Green's function $G^{aa}_{\sigma}(k,\omega)=\langle\langle a_{rk\sigma};a^+_{rk\sigma}\rangle\rangle$ using the linearized effective Hamiltonian (16). One follow the procedure described in our earlier works [Pathak et al. (2005), Ajay et al. (1999)], and finally arrive at the following Green's function:

$$G^{aa}_{\sigma}(k,\omega)=\frac{1}{2\pi}\frac{\left(\omega-\varepsilon'_k+J\langle n_H\rangle\right)}{\left[\left(\omega-\varepsilon'_k+J\langle n_H\rangle\right)^2-\left(\tilde{\varepsilon}_k(\omega)(\tilde{\varepsilon}_k(\omega)-4J_3\langle n_H\rangle)\right)\right]} \quad \text{....(17)}$$

Keeping only the first order contribution of three site term (J_3) in the propagator and using simple algebra, the equation (17) is written into a tractable form as:

$$G_{\sigma}^{aa}(k,\omega)=\frac{1}{2\pi}\left[\frac{\left(\omega-\varepsilon_k^{'}+J\langle n_H\rangle\right)}{\left(\omega-\varepsilon_k^{'}+J\langle n_H\rangle\right)^2-\left\{\tilde{\varepsilon}_k(\omega)-2J_3\langle n_H\rangle\right\}^2}\right] \qquad .....(18)$$

The above equation (18) can be manipulated in the following form:

$$G_{\sigma}^{aa}(k,\omega)=\frac{1}{2\pi}\left[\frac{A'}{(\omega-\alpha)}+\frac{B'}{(\omega-\beta)}+\frac{C'}{(\omega-\gamma)}+\frac{D'}{(\omega-\delta)}\right]$$

where α,β,γ and δ are four quasi-particle energy branches corresponding to poles of the Green's function (18) and

$$A'=1-B'-C'-D'$$

$$B'=\frac{1}{(\beta-\alpha)}\left\{\delta+\beta+\gamma-2\varepsilon_k-\varepsilon_k'+J\langle n_H\rangle-C'(\gamma-\alpha)-D'(\delta-\alpha)\right\}$$

$$C'=\frac{F-D'(\delta-\alpha)(\beta-\delta)}{(\gamma-\alpha)(\beta-\gamma)}$$

$$D'=\frac{G-F\delta}{(\delta-\alpha)(\beta-\delta)(\gamma-\delta)}$$

$$F=-J\langle n_H\rangle(\delta+\gamma-2\varepsilon_k)-\varepsilon_k^2-2\varepsilon_k\varepsilon_k'+(2\varepsilon_k+\varepsilon_k'-\delta)(\delta-\alpha)-\gamma^2$$

$$G=J\langle n_H\rangle(\varepsilon_k^2-\delta\gamma)+(2\varepsilon_k+\varepsilon_k')\delta\delta-\varepsilon'\varepsilon_k^2-\delta^2\gamma-\delta\gamma^2$$

where,

$$\alpha,\beta=\frac{1}{2(1-v)}\left\{(-b-v\varepsilon_k)\pm\sqrt{(b+v\varepsilon_k)^2+4(1-v)(\varepsilon_k^2+b\varepsilon_k-\varepsilon_{k\perp}^2)}\right\}$$

$$\gamma,\delta=\frac{1}{2(1+v)}\left\{(-d+\varepsilon_k+v\varepsilon_k)\pm\sqrt{(d-\varepsilon_k-v\varepsilon_k)^2+4(1+v)(d\varepsilon_k+\varepsilon_{k\perp}^2)}\right\}$$

$$b = -\varepsilon_k' + J\langle n_H \rangle - 2J_3\langle n_H \rangle$$

$$d = -\varepsilon_k' - \varepsilon_k + J\langle n_H \rangle + 2J_3\langle n_H \rangle$$

$$v = \frac{2}{2 - \langle n_H \rangle}$$

One can calculate spectral function $A(k,\omega)$ by using the relationship:

$$A(k,\omega) = -\frac{1}{\pi} \mathrm{Im}\left[G_\sigma^{aa}(k,\omega)\right] \qquad \ldots.(19)$$

where Im stands for imaginary part of Green's function. Using equation (18) and (19) the expression for planar electronic spectral function can be written in the following form:

$$A(k,\omega) = \left[\frac{A'\Gamma}{\Gamma^2 + (\omega - \alpha)^2} + \frac{B'\Gamma}{\Gamma^2 + (\omega - \beta)^2} + \frac{C'\Gamma}{\Gamma^2 + (\omega - \gamma)^2} + \frac{D'\Gamma}{\Gamma^2 + (\omega - \delta)^2} \right] \qquad \ldots.(20)$$

Wherein to fit the line shape of the ARPES experimental results one needs to solve δ-functions involved in the above theoretical expressions of spectral function $A(k,\omega)$. The δ-function can be approximated by a broadened quasiparticle peak. For this purpose, the Lorentzian type of broadening has been considered as:

$$\delta(\omega - \tilde{\varepsilon}_k) \cong \frac{1}{\pi} \underset{\Gamma \to 0}{\mathrm{Lim}} \frac{\Gamma}{(\omega - \tilde{\varepsilon}_k)^2 + \Gamma^2} \qquad \ldots.(21)$$

The essential point of the above Lorentizan fitting is inspired by the form of $A(k,\omega)$ observed in ARPES measurements. The broadening factor Γ is taken to be independent of k and ω, following the numerical calculation of Leung et. al. (1997). These authors have also determined Γ by fitting the

calculated spectral function $A(k,\omega)$ to ARPES measurements. The spectral function can be calculated from equation (20) at different points (k_x, k_y) of the Brillouin zone as a function of three site exchange interaction term and interlayer coupling as well as other parameters of the model Hamiltonian.

From the above expression (20) of spectral function $A(k,\omega)$, one can calculate the DOS for bilayer cuprates in normal state at zero temperature by using the formula:

$$N(\omega) = \frac{a^2}{4\pi^2} \int_{-\frac{\pi}{a}}^{\frac{\pi}{a}} \int_{-\frac{\pi}{a}}^{\frac{\pi}{a}} A(k,\omega)\, dk_x dk_y \qquad \ldots.(22)$$

From above equations (20) and (22), one can analyze the influence of J_3 and $t_\perp$ on $A(k,\omega)$ and DOS of bilayer cuprates using numerical computation.

4.1.1 Results and Discussion

The expressions of spectral function $A(k,\omega)$ (equation (20)) and density of states (DOS) given by equation (22) are obtained within $t - t' - t_\perp - J - J_3$ model for doped bilayer cuprates as a function of the parameters of model Hamiltonian. The numerical computation of theoretically calculated $A(k,\omega)$ has been performed, especially at $(\pi,0)$ point of the Brillouin zone, where bilayer splitting is observed to be maximum. During the numerical computation the range of various parameters have been taken from existing band structure calculations and the prediction made by recent ARPES measurements [Damacelli et al. (2003), Feng et al.

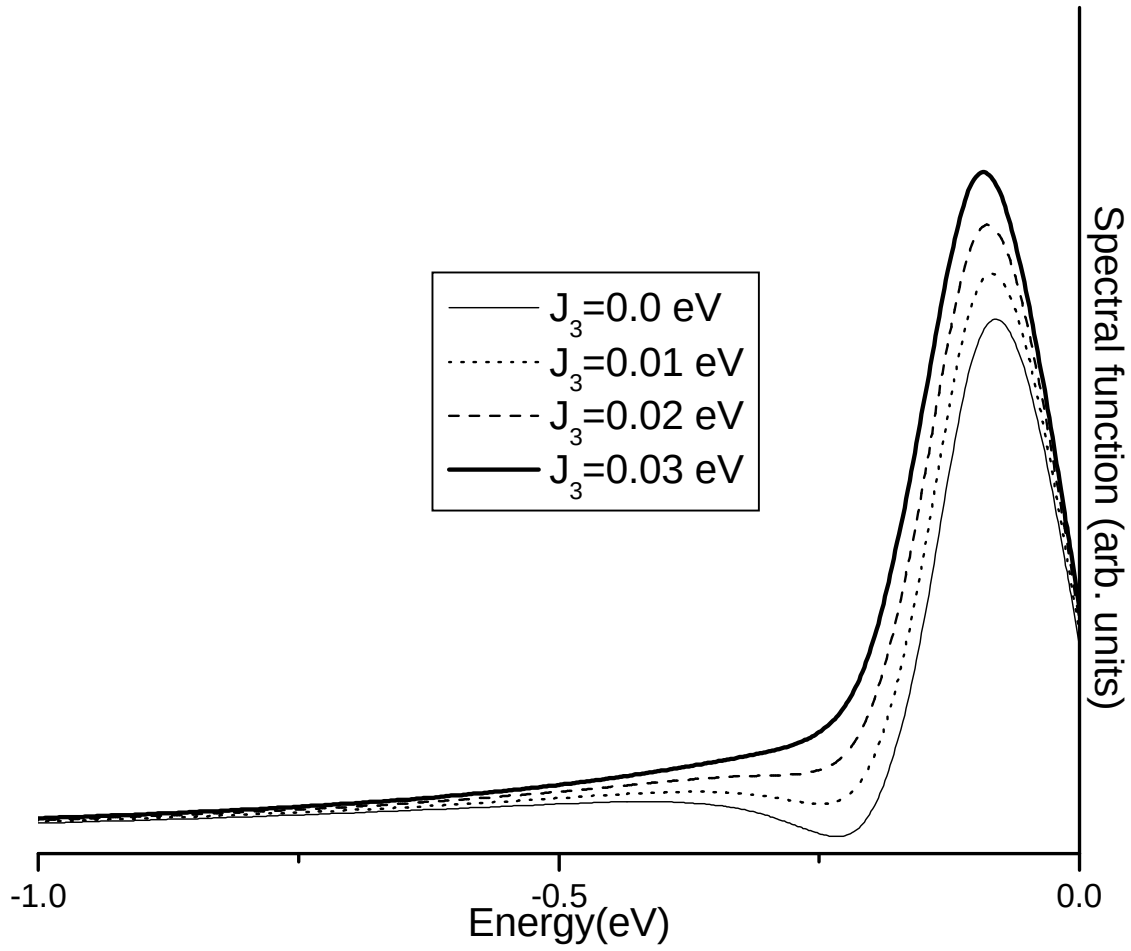

Figure (1). Spectral function $A(k,\omega)$ versus energy at ($k_x=\pi$, $k_y=0$, t=0.15eV, t' =-0.0375eV, $t_\perp$ =0.14eV, Γ =0.1eV, n_H =0.25, J=0.1eV) for different values of J_3 (0.0, 0.01, 0.02 and 0.03eV)

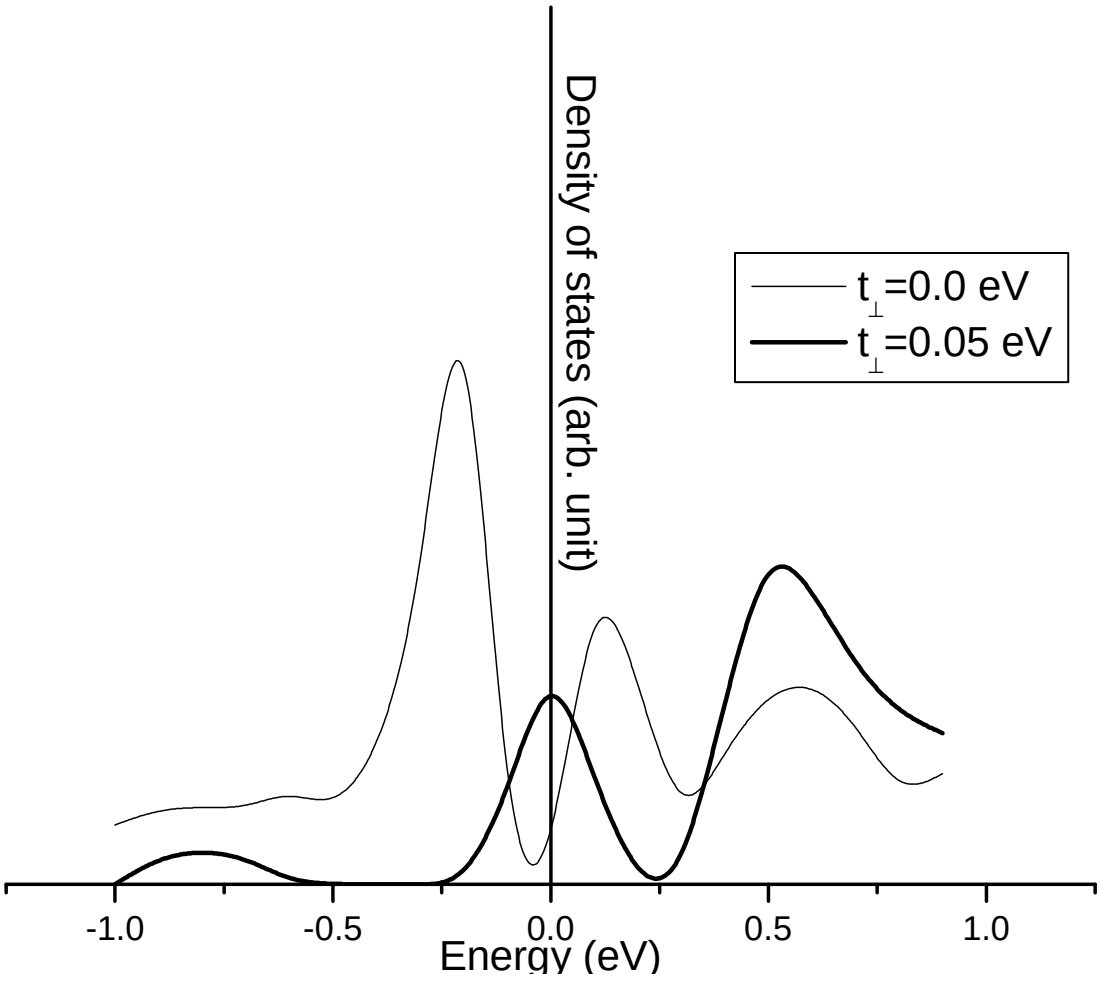

Figure (2). Density of states (DOS) versus energy at (t =0.15eV, t′=-0.0375eV, J_3=0.0eV, Γ=0.1eV, n_H=0.25, J=0.1eV) for different values of $t_\perp$(0.0eV and 0.05eV).

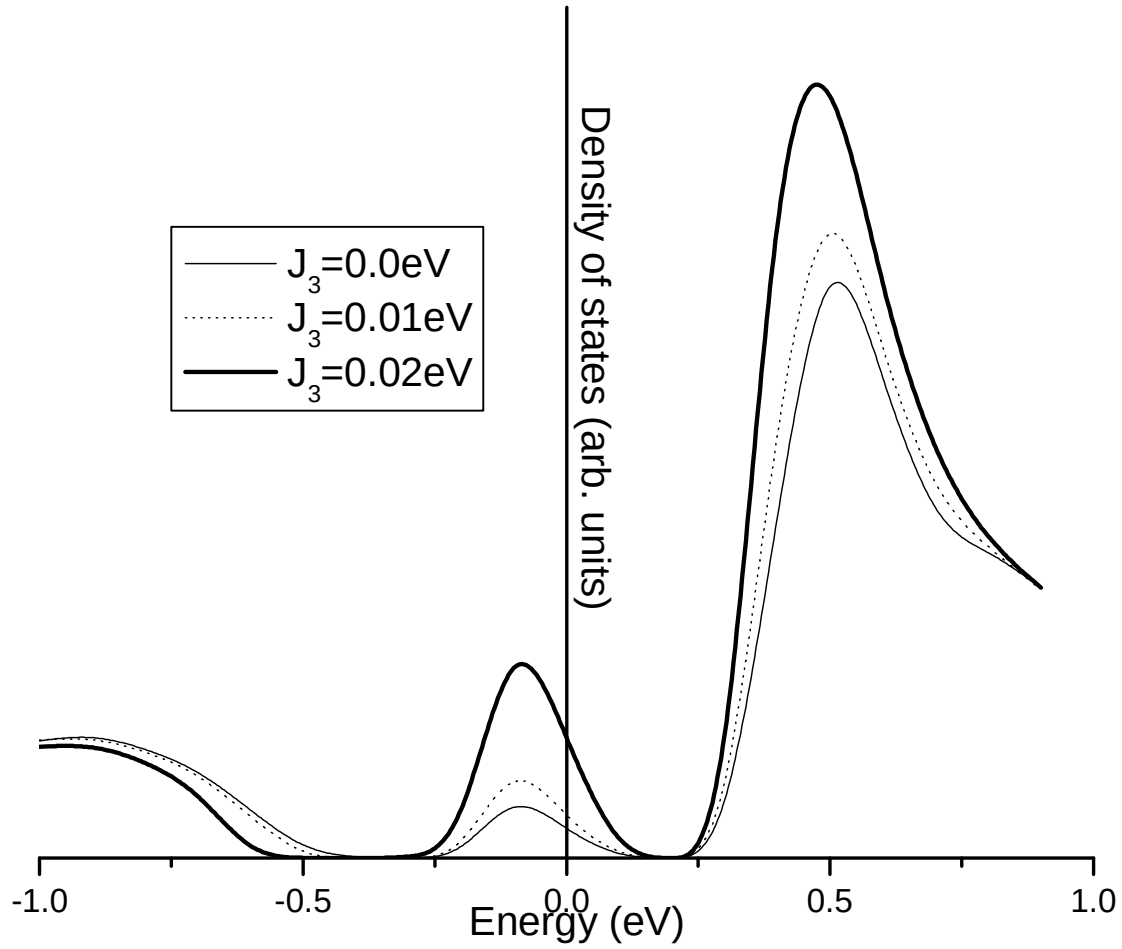

Figure (3). Density of states (DOS) versus energy at (t =0.15eV, t′=-0.0375eV, $t_{\perp}$ =0.14eV, Γ=0.1eV, n_H =0.25, J=0.1eV) for different values of J_3 (0.0, 0.01 and 0.02eV).

(2001 & 2002), Chaung et al. (2001)]. In figure (1), the variation of spectral function $A(k,\omega)$ as a function of energy (ω) is presented especially at (π,0) point of the Brillouin zone for different values of three site exchange interaction term (J_3 =0.0, 0.01, 0.02 and 0.03 eV) and finite coupling between the plane ($t_\perp$ =0.14 eV) keeping all other parameter fixed (t =0.15eV, t'=-0.0375eV, n_H =0.25, J =0.1eV, Γ =0.1eV). One can observe in figure (1) that the spectral function shows up bilayer splitting in the optimal doped regime in the absence of J_3. This observation is in qualitative agreement with the photoemission measurements in bilayer cuprates $Bi_2Sr_2CaCu_2O_{8+x}$ having two CuO_2 planes per unit cell [Feng et al. (2002), Chaung et al. (2001)]. Further, one can observe in figure (1) that on increasing J_3 (0.01 to 0.03 eV) the bilayer splitting gets reduced and there is an evolution of spectral peak as the spectral function reveals a sharp peak close to Fermi level. Hence, the spectral function is affected by the three site exchange term (J_3) and the actual effect of J_3 is more of like exchange kinetic energy [Koltenbah et al. (1997)] term and leads to reduction in bilayer splitting as well as redistribution of spectral weight close to Fermi level.

In figure (2), the variation of the density of state (DOS) versus energy (ω) is plotted in the absence of interlayer coupling parameter ($t_\perp$ = 0.0 eV), as well as in the presence of $t_\perp$ (=0.05 eV) in optimally doped cuprates, keeping all other parameters fixed. The variation of DOS in the presence of interlayer coupling ($t_\perp$) shows a finite DOS at Fermi level and there is an

evolution of third peak structure at Fermi level which is in agreement with recent analysis of DOS attempted by various workers [Prelovesek et al. (2002), Pathak et al. (2005)].

To analyze the role of J_3 on DOS in figure (3), the variation of DOS with energy for different values of three site exchange interaction (J_3) in optimal doped regime have been presented keeping all other parameters fixed (t =0.15eV, t' =-0.0375eV, $t_\perp$ =0.14eV, n_H =0.25, J =0.1eV, Γ =0.1eV). One can point out from figure 3 that on increasing J_3, DOS at Fermi level get enhanced. Further on increasing J_3, the DOS evolves with three peak structure with a prominent peak above the Fermi level.

Finally, the spectral function $A(k,\omega)$ and density of states (DOS) for the $t-t'-t_\perp-J-J_3$ model within two sublattice approach and Hubbard self-energy approximation employing the Green's function equations of motion technique for doped bilayer cuprates is obtained. The interlayer coupling ($t_\perp$) splits the spectral function. The bilayer splitting is found to be reduced on increasing three site exchange interaction (J_3) in doped cuprates. The results obtained for DOS indicate that the J_3 term enhances the DOS at the Fermi level. It is also pointed out that in optimal doped bilayer cuprates in normal state, the J_3 term plays a role in renormalizing the spectral weight close to Fermi level. It will be interesting to analyze the role of three site exchange interaction on the other physical properties and superconducting

state of doped high T_c cuprates as J_3 term involves the nearest neighbor site correlations in optimal doped regime and can influence the electronic spectra in superconducting state. This work will be taken up in near future.

4.2 Influence of the third dimensional coupling on the electronic spectra (Within extended bilayered Hubbard model)

In order to analyze the electronic spectral function of doped cuprates having two CuO_2 layers in a unit cell (like in the case of $Bi_2Sr_2CaCu_2O_{8+x}$, and $YBa_2Cu_3O_{7-x}$) in normal state in the light of existing ARPES measurements one has to require to take into account the various hopping energies alongwith strong electronic correlations that exists within the CuO_2 planes. As described in the introduction in detail, the Hubbard model with various matrix elements within and between the CuO_2 planes is believed to be a good starting point to study the electronic states of cuprates. For the system like Bi-2212 and Y-123 which have two Cu-O planes per unit cell, we proposed a model Hamiltonian that incorporates the intra cell coupling, inter cell resonant tunneling alongwith strong Coulomb interaction that exist in cuprates. The detail mechanism of resonance tunneling is depicted in figure (1) for Bi-2212 and Y-123 systems.

The model Hamiltonian for cuprates with two Cu-O planes per unit cell which incorporates third dimensional inter cell resonant tunneling is given as:

$H = H_{intracell} + H_{intercell}$,

Here,

$H_{intracell} =$

$$\sum_{m=1,2}\left[\sum_{k,\sigma}\varepsilon_{rk}c^{+}_{mrk\sigma}c_{mrk\sigma} + U\sum_{k,k',q,r}c^{+}_{mrk+q\uparrow}c_{mrk'\uparrow}c^{+}_{mrk'-q\downarrow}c_{mrk\downarrow} + \sum_{r\neq s,k,\sigma}\varepsilon_{k\perp}\left(c^{+}_{mrk\sigma}c_{msk\sigma} + c^{+}_{msk\sigma}c_{mrk\sigma}\right)\right] \quad 1(a)$$

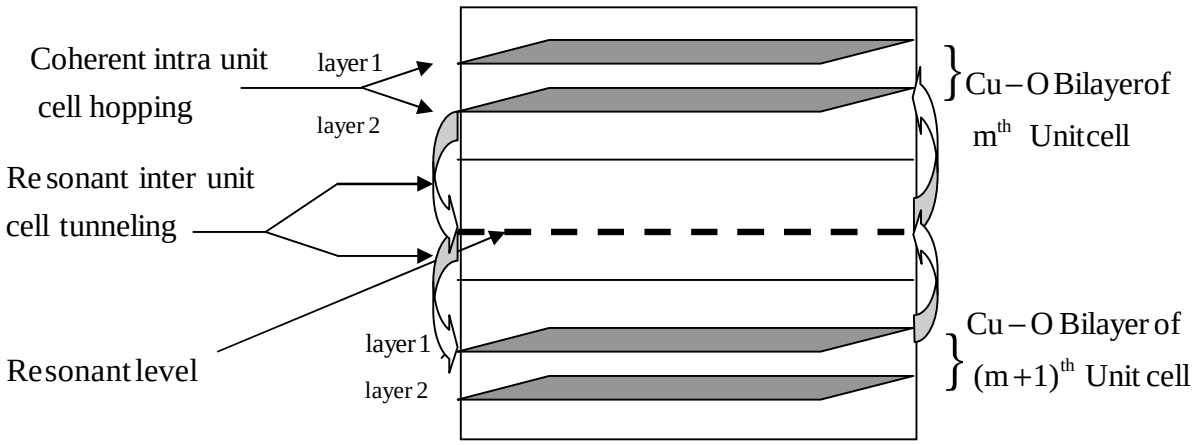

Figure (1). Schematic presentation of intra cell coupling and inter unit cell resonant tunneling in bilayer cuprates (Bi-2212 and Y-123))

$$H_{intercell} = \varepsilon_0 \sum_{l} b_l^{+} b_l + \sum_{m,r,s,k,\sigma,l} T_{rs}(m, m+1)\left[\left(c^{+}_{mrk\sigma} b_l + b_l^{+} c_{m+1sk\sigma}\right) + \left(c^{+}_{m+1sk\sigma} b_l + b_l^{+} c_{mrk\sigma}\right)\right] \quad ..1(b)$$

Where, m is unit cell indices and r, s are layer indices within a unit cell (where r=1, s=2 and vice-versa). $c^{+}_{mrk\sigma}(c_{mrk\sigma})$ are creation (annihilation) operator for the holes of m^{th} unit cell, r^{th} Cu-O plane with wave vector k and spin σ .The 1^{st} term in 1(a) is kinetic energy of charge carrier (holes) within the Cu-O plane. The kinetic energy ε_{rk} also includes the chemical potential of coupled bilayer system and therefore, initially we have taken Fermi energy E_F=0 for our calculations. The 2^{nd} term in 1 (a) is the on site Coulomb energy at $Cu3d^9$ site and in cuprates this energy is quiet large (in the range 5 to 10 eV) as compared to hopping energy. The 3^{rd} term in 1(a) is the single particle coupling between the bilayers within the unit cell and we have assumed momentum dependent of the form: $\varepsilon_{k\perp} = -\frac{t_\perp}{4}(\cos k_x a - \cos k_y a)^2$ as suggested by band structure calculation [Chakravarty et al. (1993)] and ARPES measurements [Feng et al. (2001), Feng et al. (2002), Bansil et al. (2005), Markiewicz et al. (2005)].

The 1^{st} term in 1(b) represents the energy of the resonant level due to oxygen deficient BiO chain which lies mid way between the two Cu-O planes lying in adjoining unit cells (figure (1)). The 2^{nd} term in 1(b) represents the single particle resonant tunneling from lower layer (say r^{th} layer) of m^{th} unit cell to upper layer (say s^{th} layer) of adjacent $(m+1)^{th}$ unit cell and vice-versa. The parameter T_{rs} (m,m+1) represent the inter unit cell resonant tunneling matrix element for the case when tunneling probability between two Cu-O

planes in different unit cells is of the order of unity [Abrikosov (1999)]. During the theoretical calculation $T_{rs}(m,m+1)$ is taken as T_{12} for the case of nearest CuO planes in adjacent unit cells (Fig 1).

To obtain an expression for planar single particle spectral function A(k, ω), we need to calculate the corresponding Green's function $G_{11}(k,\omega) = \langle\langle c_{11k\sigma} | c^{+}_{11k\sigma} \rangle\rangle$. The Green's function equation of motion approach is employed [Lal et al. (1998), Ajay et al. (2002)] to derive set of coupled equations in different limiting case.

(a) Equations of motion in the absence of electron correlations (i.e. $U \to 0$ limit):

To find the Green's function $G_{11}(k,\omega)$ for the Hamiltonian given by (1) in the absence of Coulomb energy term (i.e. U=0), the following set of five coupled Green's function equations are obtained exactly and without any decoupling approximation:

$$(\omega - \varepsilon_k)\langle\langle c_{11k\sigma} | c^{+}_{11k\sigma} \rangle\rangle = \frac{1}{2\pi} + \varepsilon_{k\perp}\langle\langle c_{12k\sigma} | c^{+}_{11k\sigma} \rangle\rangle + T_{12}\langle\langle b_l | c^{+}_{11k\sigma} \rangle\rangle \quad \ldots(2)$$

$$(\omega - \varepsilon_k)\langle\langle c_{12k\sigma} | c^{+}_{11k\sigma} \rangle\rangle = \varepsilon_{k\perp}\langle\langle c_{11k\sigma} | c^{+}_{11k\sigma} \rangle\rangle, \quad \ldots(3)$$

$$(\omega - \varepsilon_0)\langle\langle b_l | c^{+}_{11k\sigma} \rangle\rangle = T_{12}\left(\langle\langle c_{22k\sigma} | c^{+}_{11k\sigma} \rangle\rangle + \langle\langle c_{11k\sigma} | c^{+}_{11k\sigma} \rangle\rangle\right) \quad \ldots(4)$$

$$(\omega - \varepsilon_k)\langle\langle c_{22k\sigma} | c^{+}_{11k\sigma} \rangle\rangle = \varepsilon_{k\perp}\langle\langle c_{21k\sigma} | c^{+}_{11k\sigma} \rangle\rangle + T_{12}\langle\langle b_l | c^{+}_{11k\sigma} \rangle\rangle \quad \ldots.(5)$$

and

$$(\omega - \varepsilon_k)\langle\langle c_{21k\sigma} | c^{+}_{11k\sigma} \rangle\rangle = \varepsilon_{k\perp}\langle\langle c_{22k\sigma} | c^{+}_{11k\sigma} \rangle\rangle \quad \ldots.(6)$$

After solving the above set of coupled equations, one can obtain the expression of the propagator:

$$G_{11}(k,\omega) = \left\langle\left\langle c_{11k\sigma} \middle| c^{+}_{11k\sigma} \right\rangle\right\rangle$$
$$= \frac{1}{2\pi}(\omega-\varepsilon_k)\times\left[\frac{(\omega-\varepsilon_0)\left\{(\omega-\varepsilon_k)^2-\varepsilon_{k\perp}{}^2\right\}-T_{12}{}^2(\omega-\varepsilon_k)}{\left\{(\omega-\varepsilon_k)^2-\varepsilon_{k\perp}{}^2\right\}\left[(\omega-\varepsilon_0)\left\{(\omega-\varepsilon_k)^2-\varepsilon_{k\perp}{}^2\right\}-2T_{12}{}^2(\omega-\varepsilon_k)\right]}\right] \quad \ldots.(7)$$

If, in the above expression of $G_{11}(k,\omega)$, the resonant tunneling is taken as zero (T_{12}=0), we obtain the propagator for bilayer system having intra cell coupling only, and equation (7) reduced to the following:

$$G_{11}(k,\omega) = \frac{1}{2\pi}\left[\frac{\omega-\varepsilon_k}{(\omega-\varepsilon_k)^2-\varepsilon_{k\perp}^2}\right] \quad \ldots.(8)$$

One can check from above equation (8) that there are two quasiparticle energy branches (i.e. $\omega_{1,2} = \varepsilon_k \pm \varepsilon_{k\perp}$): a manifestation of intrabilayer coupling between two CuO_2 planes within the unit cell.

(b) The Green's function equations of motion in the presence of Coulomb interaction:

In the presence of finite Coulomb correlations in the above Hamiltonian (1), we solve the Hamiltonian and obtain the following set of coupled equations:

$$(\omega-\varepsilon_k)\left\langle\left\langle c_{11k\sigma} \middle| c^{+}_{11k\sigma} \right\rangle\right\rangle = \frac{1}{2\pi} + \sum_{k_1'q} U\left\langle\left\langle c_{11k_1'\sigma}c^{+}_{11k_1'-q-\sigma}c_{11k-q-\sigma} \middle| c^{+}_{11k\sigma} \right\rangle\right\rangle$$
$$+\varepsilon_{k\perp}\left\langle\left\langle c_{12k\sigma} \middle| c^{+}_{11k\sigma} \right\rangle\right\rangle + T_{12}\left\langle\left\langle b_1 \middle| c^{+}_{11k\sigma} \right\rangle\right\rangle \quad \ldots(9)$$

$$(\omega-\varepsilon_k)\left\langle\left\langle c_{12k\sigma} \middle| c^{+}_{11k\sigma} \right\rangle\right\rangle = \varepsilon_{k\perp}\left\langle\left\langle c_{11k\sigma} \middle| c^{+}_{11k\sigma} \right\rangle\right\rangle + \sum_{k_1'q} U\left\langle\left\langle c_{12k_1'\sigma}c^{+}_{12k'-q_1\sigma}c_{12k-q-\sigma} \middle| c^{+}_{11k\sigma} \right\rangle\right\rangle \quad \ldots(10)$$

$$(\omega-\varepsilon_0)\left\langle\left\langle b_1 \middle| c^{+}_{11k\sigma} \right\rangle\right\rangle = T_{12}\left(\left\langle\left\langle c_{22k\sigma} \middle| c^{+}_{11k\sigma} \right\rangle\right\rangle + \left\langle\left\langle c_{11k\sigma} \middle| c^{+}_{11k\sigma} \right\rangle\right\rangle\right) \quad \ldots(11)$$

$$(\omega-\varepsilon_k)\langle\langle c_{22k\sigma}\,|\,c^{+}_{11k\sigma}\rangle\rangle=\varepsilon_{k\perp}\langle\langle c_{21k\sigma}\,|\,c^{+}_{11k\sigma}\rangle\rangle+\sum_{k_1'q}U\langle\langle c_{22k_1'\sigma}c^{+}_{22k_1'-q-\sigma}c_{22k-q-\sigma}\,|\,c^{+}_{11k\sigma}\rangle\rangle+T_{12}\langle\langle b_l\,|\,c^{+}_{11k\sigma}\rangle\rangle$$

...(12)

and

$$(\omega-\varepsilon_k)\langle\langle c_{21k\sigma}\,|\,c^{+}_{11k\sigma}\rangle\rangle=\varepsilon_{k\perp}\langle\langle c_{22k\sigma}\,|\,c^{+}_{11k\sigma}\rangle\rangle+\sum_{k_1'q}U\langle\langle c_{21k_1'\sigma}c^{+}_{21k_1'-q-\sigma}c_{21k-q-\sigma}\,|\,c^{+}_{11k\sigma}\rangle\rangle \quad \ldots (13)$$

The above set of five coupled equations contains hierarchy of higher order Green's functions due to the introduction of electron correlation effects. These higher order equations are decoupled in the spirit of Hartree Fock approximation at first stage and finally, one gets the following set of coupled equations:

$$(\omega-\tilde{\varepsilon}_k)\langle\langle c_{11k\sigma}\,|\,c^{+}_{11k\sigma}\rangle\rangle=\frac{1}{2\pi}+\varepsilon_{k\perp}\langle\langle c_{12k\sigma}\,|\,c^{+}_{11k\sigma}\rangle\rangle+T_{12}\langle\langle b_l\,|\,c^{+}_{11k\sigma}\rangle\rangle \quad \ldots.(14)$$

$$(\omega-\tilde{\varepsilon}_k)\langle\langle c_{12k\sigma}\,|\,c^{+}_{11k\sigma}\rangle\rangle=\varepsilon_{k\perp}\langle\langle c_{11k\sigma}\,|\,c^{+}_{11k\sigma}\rangle\rangle, \quad \ldots(15)$$

$$(\omega-\varepsilon_0)\langle\langle b_1\,|\,c^{+}_{11k\sigma}\rangle\rangle=T_{12}\left(\langle\langle c_{22k\sigma}\,|\,c^{+}_{11k\sigma}\rangle\rangle+\langle\langle c_{11k\sigma}\,|\,c^{+}_{11k\sigma}\rangle\rangle\right) \quad \ldots(16)$$

$$(\omega-\tilde{\varepsilon}_k)\langle\langle c_{22k\sigma}\,|\,c^{+}_{11k\sigma}\rangle\rangle=\varepsilon_{k\perp}\langle\langle c_{21k\sigma}\,|\,c^{+}_{11k\sigma}\rangle\rangle+T_{12}\langle\langle b_l\,|\,c^{+}_{11k\sigma}\rangle\rangle \quad \ldots.(17)$$

and

$$(\omega-\tilde{\varepsilon}_k)\langle\langle c_{21k\sigma}\,|\,c^{+}_{11k\sigma}\rangle\rangle=\varepsilon_{k\perp}\langle\langle c_{22k\sigma}\,|\,c^{+}_{11k\sigma}\rangle\rangle \quad \ldots(18)$$

where $\tilde{\varepsilon}_k=\varepsilon_k+U\langle n_{-\sigma}\rangle$ and $\langle n_{-\sigma}\rangle=\sum_k\langle c_{11k\text{-}\sigma}\,|\,c^{+}_{11k\text{-}\sigma}\rangle=\sum_k\langle c_{22k\text{-}\sigma}\,|\,c^{+}_{22k\text{-}\sigma}\rangle$ and we have assumed the uniform distribution of charge carriers in different layers (i.e. $n_{1\text{-}\sigma}=n_{2\text{-}\sigma}=n_{-\sigma}$) and a paramagnetic situation without having AFM correlations.

Solving equations (14-18), one obtaines the Green's function:

$$G_{11}(k,\omega)=\frac{1}{2\pi}(\omega-\tilde{\varepsilon}_k)\times\left[\frac{(\omega-\varepsilon_0)\left\{(\omega-\tilde{\varepsilon}_k)^2-\varepsilon_{k\perp}{}^2\right\}-T_{12}{}^2(\omega-\tilde{\varepsilon}_k)}{\left\{(\omega-\tilde{\varepsilon}_k)^2-\varepsilon_{k\perp}{}^2\right\}\left[(\omega-\varepsilon_0)\left\{(\omega-\tilde{\varepsilon}_k)^2-\varepsilon_{k\perp}{}^2\right\}-2T_{12}{}^2(\omega-\tilde{\varepsilon}_k)\right]}\right] \quad \ldots.(19)$$

On comparing equation (19) and (7), one can point out that the only difference in these equations lies in the fact that quasiparticle energy ε_k is replaced by $\tilde{\varepsilon}_k=\varepsilon_k+U\langle n_{-\sigma}\rangle$ in equation (7), a result applicable for weakly correlated systems. The high T_c cuprates possesses strong electronic correlation and to take care of these calculations, one need to develop a decoupling scheme for the higher order Green's functions as described below.

(c) The decoupling of higher order Green's functions:

In order to take into account the electronic correlation effects that exist in cuprates, the equations of motion of higher order Green's functions appearing in equations (9, 10, 12 & 13) can be rewritten and the decoupling in higher order Green's functions in these equations of motion is made at second stage. During the decoupling of higher order Green's function, it is also assumed that the system is paramagnetic. This makes the equations tractable and avoids complications. With these approximations and simplification the higher order Green's functions that exist in equation (9), (10), (12) & (13) can now be written as:

$$\begin{aligned}(\omega-\varepsilon_{k_1'})\left\langle\left\langle c_{11k_1'\sigma}c^{+}_{11k_1'\text{-}q\text{-}\sigma}c_{11k-q-\sigma}\,\middle|\,c^{+}_{11k\sigma}\right\rangle\right\rangle &= \frac{\delta_{k_1'k}}{2\pi}\left\langle c^{+}_{11k_1'\text{-}q\text{-}\sigma}c_{11k-q-\sigma}\right\rangle+\varepsilon_{k_1'\perp}\left\langle\left\langle c^{+}_{11k_1'-q-\sigma}c_{11k-q-\sigma}c_{12k_1'\sigma}\,\middle|\,c^{+}_{11k\sigma}\right\rangle\right\rangle\\ &\quad+T_{12}\left\langle\left\langle c^{+}_{11k_1'\ q\ \sigma}c_{11k\ q\ \sigma}b_l\,\middle|\,c^{+}_{11k\sigma}\right\rangle\right\rangle\\ &\quad-\sum_{k_1'q}U\left\langle\left\langle c^{+}_{11k_1'-q-\sigma}c_{11k_1'-q-\sigma}c_{11k_1'\sigma}c^{+}_{11k_1'-q-\sigma}c_{11k-q-\sigma}\,\middle|\,c^{+}_{11k\sigma}\right\rangle\right\rangle\end{aligned} \quad \ldots(20)$$

$$(\omega-\varepsilon_{k_1'})\langle\langle c_{12k_1'\sigma}c^{+}_{12k_1'-q-\sigma}c_{12k-q-\sigma}\,|\,c^{+}_{11k\sigma}\rangle\rangle=\varepsilon_{k_1'\perp}\langle\langle c^{+}_{12k_1'-q-\sigma}c_{12k-q-\sigma}c_{11k_1'\sigma}\,|\,c^{+}_{11k\sigma}\rangle\rangle$$
$$-\sum_{k_1'q}U\langle\langle c^{+}_{12k_1'-q-\sigma}c_{12k_1'-q-\sigma}c_{12k_1'\sigma}c^{+}_{12k_1'-q-\sigma}c_{12k-q-\sigma}\,|\,c^{+}_{11k\sigma}\rangle\rangle$$

...(21)

$$(\omega-\varepsilon_{k_1'})\langle\langle c_{22k_1'\sigma}c^{+}_{22k_1'-q-\sigma}c_{22k-q-\sigma}\,|\,c^{+}_{11k\sigma}\rangle\rangle=\varepsilon_{k_1'\perp}\langle\langle c^{+}_{22k_1'-q-\sigma}c_{22k-q-\sigma}c_{21k_1'\sigma}\,|\,c^{+}_{11k\sigma}\rangle\rangle$$
$$+T_{12}\langle\langle c^{+}_{22k_1'-q-\sigma}c_{22k-q-\sigma}b_l\,|\,c^{+}_{11k\sigma}\rangle\rangle$$
$$+U\sum_{k_1'q}\langle\langle c^{+}_{22k_1'-q-\sigma}c_{22k_1'-q-\sigma}c_{22k_1'\sigma}c^{+}_{22k_1'-q-\sigma}c_{22k-q-\sigma}\,|\,c^{+}_{11k\sigma}\rangle\rangle$$

...(22)

and

$$(\omega-\varepsilon_{k_1'})\langle\langle c_{21k_1'\sigma}c^{+}_{21k_1'-q-\sigma}c_{21k-q-\sigma}\,|\,c^{+}_{11k\sigma}\rangle\rangle=\varepsilon_{k_1'\perp}\langle\langle c^{+}_{21k_1'-q-\sigma}c_{21k-q-\sigma}c_{22k_1'\sigma}\,|\,c^{+}_{11k\sigma}\rangle\rangle$$
$$-U\sum_{k_1'q}\langle\langle c^{+}_{21k_1'-q-\sigma}c_{21k_1'-q-\sigma}c_{21k_1'\sigma}c^{+}_{21k_1'-q-\sigma}c_{21k-q-\sigma}\,|\,c^{+}_{11k\sigma}\rangle\rangle$$

...(23)

Substituting above equations (20-23), after truncating the hierarchy of still higher order Green's function within the Hartree Fock approximation, the finally obtained set of five coupled equations of Green's functions are as follows:

$G_{11}(k,\omega)=\langle\langle c_{11k\sigma}\,|\,c^{+}_{11k\sigma}\rangle\rangle$, $G_{12}(k,\omega)=\langle\langle c_{12k\sigma}\,|\,c^{+}_{11k\sigma}\rangle\rangle$, $G_{b1}(k,\omega)=\langle\langle b_1\,|\,c^{+}_{11k\sigma}\rangle\rangle$,

$G_{22}(k,\omega)=\langle\langle c_{22k\sigma}\,|\,c^{+}_{11k\sigma}\rangle\rangle$, and $G_{21}(k,\omega)=\langle\langle c_{21k\sigma}\,|\,c^{+}_{11k\sigma}\rangle\rangle$ as follows:

$$(\omega-\varepsilon_k)G_{11}(k,\omega)=\frac{1}{2\pi}\left[1+\sum_{k_1'}U\frac{\langle n_{k-\sigma}\rangle}{((\omega-\varepsilon_{k_1'})+U\langle n_{-\sigma}\rangle)}\right]+\varepsilon_{k\perp}\left[1+\sum_{k_1'}U\frac{\langle n_{k-\sigma}\rangle}{((\omega-\varepsilon_{k_1'})+U\langle n_{-\sigma}\rangle)}\right]G_{12}$$
$$+T_{12}\left[1+\sum_{k_1'}U\frac{\langle n_{k-\sigma}\rangle}{((\omega-\varepsilon_{k_1'})+U\langle n_{-\sigma}\rangle)}\right]G_{bl}(k,\omega)\qquad\text{...(24)}$$

$$(\omega-\varepsilon_0)G_{b1}(k,\omega)=T_{12}G_{22}+T_{12}G_{11}\qquad\text{...(25)}$$

$$(\omega-\varepsilon_k)G_{12}(k,\omega)=\varepsilon_{k\perp}\left[1+\sum_{k_1'}U\frac{\langle n_{k-\sigma}\rangle}{(\omega-\varepsilon_{k_1'})+U\langle n_{-\sigma}\rangle}\right]G_{11} \qquad \ldots(26)$$

$$(\omega-\varepsilon_k)G_{22}(k,\omega)=\varepsilon_{k\perp}\left[1+\sum_{k_1'}U\frac{\langle n_{k-\sigma}\rangle}{(\omega-\varepsilon_{k_1'})+U\langle n_{-\sigma}\rangle}\right]G_{21}+T_{12}\left[1+\sum_{k_1'}U\frac{\langle n_{k-\sigma}\rangle}{(\omega-\varepsilon_{k_1'})+U\langle n_{-\sigma}\rangle}\right]G_{b1}$$

$\ldots(27)$

$$(\omega-\varepsilon_k)G_{21}(k,\omega)=\varepsilon_{k1}\left[1+\sum_{k_1'}U\frac{\langle n_{k-\sigma}\rangle}{(\omega-\varepsilon_{k_1'})+U\langle n_{-\sigma}\rangle}\right]G_{22} \qquad \ldots(28)$$

In arriving at above five coupled equations (24 to 28) it is assumed that the charge carriers in Cu-O planes are equally distributed and also used a paramagnetic situation (i.e. carriers with up spin are equal to carriers with down spin). Solving the above coupled equations, one derives the Green's functions $G_{11}(k,\omega)$ using:

$$\left[(\omega-\varepsilon_k)-\frac{\varepsilon_{k\perp}{}^2}{(\omega-\varepsilon_k)}(1+F_{k\omega})^2-\frac{T_{12}{}^2}{(\omega-\varepsilon_0)}(1+F_{k\omega})\right]G_{11}=\frac{1}{2\pi}(1+F_{k\omega})+\frac{T_{12}{}^2}{(\omega-\varepsilon_0)}(1+F_{k\omega})G_{22}$$

$\ldots.(29)$

and

$$\left[(\omega-\varepsilon_k)-\frac{\varepsilon_{k\perp}{}^2}{(\omega-\varepsilon_k)}(1+F_{k\omega})^2-\frac{T_{12}{}^2}{(\omega-\varepsilon_0)}(1+F_{k\omega})\right]G_{22}=\frac{T_{12}{}^2}{(\omega-\varepsilon_0)}(1+F_{k\omega})G_{11} \qquad \ldots(30)$$

where $F_{k\omega}=\sum_{k_1'}U\frac{\langle n_{k-\sigma}\rangle}{(\omega-\varepsilon_{k_1'})+U\langle n_{-\sigma}\rangle}$

Solving above equation (29) and (30) we obtain:

$$G_{11}(k,\omega)=\frac{1}{2\pi}(\omega-\varepsilon_k)(1+F_{k\omega})\times$$
$$\left[\frac{(\omega-\varepsilon_k)^2(\omega-\varepsilon_0)-\varepsilon_{k\perp}{}^2(\omega-\varepsilon_0)(1+F_{k\omega})^2-T_{12}{}^2(\omega-\varepsilon_k)(1+F_{k\omega})}{\{(\omega-\varepsilon_k)^2-\varepsilon_{k\perp}{}^2(1+F_{k\omega})^2\}\{(\omega-\varepsilon_k)^2(\omega-\varepsilon_0)-\varepsilon_{k\perp}{}^2(\omega-\varepsilon_0)(1+F_{k\omega})^2-2T_{12}{}^2(\omega-\varepsilon_k)(1+F_{k\omega})\}}\right]$$

...(31)

It is important to note that in the limit of $U\to 0$ i.e. without electronic correlations, the above propagator $G_{11}(k,\omega)$ reproduces the results obtained in equation (7) and indicate the consistency of the approximation used. On simplification one can rewrite the above equation as:

$$G_{11}(k,\omega)=\frac{1}{2\pi}(\omega-\varepsilon_k)(1+F_{k\omega})\left\{\frac{\omega^3+A\omega^2+B\omega+C}{\omega^5+D\omega^4+E\omega^3+F\omega^2+G\omega+H}\right\} \quad ...(32)$$

Where,

$A=-(\varepsilon_0+2\varepsilon_k)$

$B=2\varepsilon_k\varepsilon_0+\varepsilon_k{}^2-\varepsilon_{k\perp}{}^2(1+F_{k\omega})^2-T_{12}{}^2(1+F_{k\omega})$

$C=-\{\varepsilon_k{}^2\varepsilon_0-\varepsilon_{k\perp}{}^2\varepsilon_0(1+F_{k\omega})^2-\varepsilon_k T_{12}{}^2(1+F_{k\omega})\}$

$D=-(\varepsilon_0+4\varepsilon_k)$

$E=4\varepsilon_k\varepsilon_0+6\varepsilon_k{}^2-2\varepsilon_{k\perp}{}^2(1+F_{k\omega})^2-2T_{12}{}^2(1+F_{k\omega})$

$F=-\{6\varepsilon_k{}^2\varepsilon_0+4\varepsilon_k{}^3-4\varepsilon_k\varepsilon_{k\perp}{}^2(1+F_{k\omega})^2-2\varepsilon_0\varepsilon_{k\perp}{}^2(1+F_{k\omega})^2-6\varepsilon_k T_{12}{}^2(1+F_{k\omega})\}$

$G=\{4\varepsilon_k{}^3\varepsilon_0-2\varepsilon_k{}^2\varepsilon_{k\perp}{}^2(1+F_{k\omega})^2+\varepsilon_k{}^4-4\varepsilon_k\varepsilon_0\varepsilon_{k\perp}{}^2(1+F_{k\omega})^2-6\varepsilon_k{}^2T_{12}{}^2(1+F_{k\omega})+\varepsilon_{k\perp}{}^4(1+F_{k\omega})^4+2T_{12}{}^2\varepsilon_{k\perp}{}^2(1+F_{k\omega})^3\}$

and

$H=-\{\varepsilon_k{}^4\varepsilon_0-2\varepsilon_k{}^2\varepsilon_0\varepsilon_{k\perp}{}^2(1+F_{k\omega})^2-2\varepsilon_k{}^3T_{k12}{}^2(1+F_{k\omega})+\varepsilon_{k\perp}{}^4\varepsilon_0(1+F_{k\omega})^4+2\varepsilon_{k\perp}{}^2(1+F_{k\omega})^3\varepsilon_k T_{12}{}^2\}$

Using simple algebra above equation (32) can be rearranged as:

$$G_{11}(k,\omega) = \frac{1}{2\pi}\sum_{i=1}^{5}\frac{A_i}{(\omega - \alpha_i)} \qquad \ldots(33)$$

Where, $\alpha_1 \ldots\ldots \alpha_5$ are the five quasi-particle energies corresponding to five poles of Green's function which have been computed numerically, also:

$$A_5 = \frac{(na - jb)(gd - hb) - (nd - pb)(ga - fb)}{(ne - qb)(gd - hb) - (nd - pb)(ge - ib)},$$

$$A_4 = \frac{(ga - fb)(ne - qb) - (ge - ib)(na - jb)}{(ne - qb)(gd - hb) - (nd - pb)(ge - ib)},$$

$$A_3 = \frac{1}{b}(a - dA_4 - eA_5),$$

$$A_2 = \frac{1}{(\alpha_2 - \alpha_1)}\left[\begin{array}{l}(\alpha_4 + \alpha_5 + \alpha_2 + \alpha_3 + A - \varepsilon_k)(1 + F_{k\omega}) - (\alpha_3 - \alpha_1)A_3 - \\ (\alpha_4 - \alpha_1)A_4 - (\alpha_5 - \alpha_1)A_5\end{array}\right],$$

and

$$A_1 = (1 + F_{k\omega}) - A_2 - A_3 - A_4 - A_5,$$

Here,

$$a = (\alpha_2 - \alpha_1)\left[\begin{array}{l}B - \varepsilon_k A + \alpha_3^2 + \alpha_4^2 + \alpha_5^2 + \alpha_3\alpha_4 + \alpha_3\alpha_5 + \alpha_4\alpha_5 \\ -(\varepsilon_0 + 3\varepsilon_k)(\alpha_3 + \alpha_4 + \alpha_5)\end{array}\right](1 + F_{k\omega})$$

$$b = \alpha_1^{\,2}(\alpha_3 - \alpha_2) + \alpha_2^{\,2}(\alpha_1 - \alpha_3) + \alpha_3^{\,2}(\alpha_2 - \alpha_1)$$

$$d = \alpha_1^{\,2}(\alpha_4 - \alpha_2) + \alpha_2^{\,2}(\alpha_1 - \alpha_4) + \alpha_4^{\,2}(\alpha_2 - \alpha_1)$$

$$e = \alpha_1^{\,2}(\alpha_5 - \alpha_2) + \alpha_2^{\,2}(\alpha_1 - \alpha_5) + \alpha_5^{\,2}(\alpha_2 - \alpha_1)$$

$$f = (1 + F_{k\omega})(\alpha_2 - \alpha_1)\left[\begin{array}{l}C - \varepsilon_k B - \alpha_4^2(\alpha_3 + \alpha_5) - \alpha_5^2(\alpha_3 + \alpha_4) - \alpha_3^2(\alpha_4 + \alpha_5) \\ -(A - \varepsilon_k)(\alpha_3\alpha_4 + \alpha_3\alpha_5 + \alpha_4\alpha_5) - 2\alpha_3\alpha_4\alpha_5\end{array}\right]$$

g= $\alpha_1^2(\alpha_2\alpha_4+\alpha_2\alpha_5-\alpha_3\alpha_4-\alpha_3\alpha_5)+\alpha_2^2(\alpha_3\alpha_4+\alpha_3\alpha_5-\alpha_1\alpha_4-\alpha_1\alpha_5)$
$+\alpha_3^2(\alpha_1\alpha_4+\alpha_1\alpha_5-\alpha_2\alpha_4-\alpha_2\alpha_5)$

h= $\alpha_1^2(\alpha_2\alpha_3+\alpha_2\alpha_5-\alpha_4\alpha_5-\alpha_3\alpha_4)+\alpha_2^2(\alpha_4\alpha_5+\alpha_3\alpha_4-\alpha_1\alpha_3-\alpha_1\alpha_5)$
$+\alpha_4^2(\alpha_1\alpha_5+\alpha_1\alpha_3-\alpha_1\alpha_5-\alpha_2\alpha_3)$

i= $\alpha_1^2(\alpha_2\alpha_3+\alpha_2\alpha_4-\alpha_4\alpha_5-\alpha_3\alpha_5)+\alpha_2^2(\alpha_4\alpha_5+\alpha_3\alpha_4-\alpha_1\alpha_3-\alpha_1\alpha_4)$
$+\alpha_5^2(\alpha_1\alpha_4+\alpha_1\alpha_3-\alpha_2\alpha_4-\alpha_2\alpha_3)$

j= $(1+F_{k\omega})(\alpha_2-\alpha_1)\left[\varepsilon_k C-\alpha_3^2\alpha_4\alpha_5-\alpha_3\alpha_4^2\alpha_5-\alpha_3\alpha_4\alpha_5^2+(\varepsilon_0+3\varepsilon_k)\alpha_3\alpha_4\alpha_5\right]$

n= $\alpha_4\alpha_5\left[\alpha_1^2(\alpha_2-\alpha_3)+\alpha_2^2(\alpha_3-\alpha_1)+\alpha_3^2(\alpha_1-\alpha_2)\right]$

p= $\alpha_3\alpha_5\left[\alpha_1^2(\alpha_2-\alpha_4)+\alpha_2^2(\alpha_4-\alpha_1)+\alpha_4^2(\alpha_1-\alpha_2)\right]$

and

q= $\alpha_3\alpha_4\left[\alpha_1^2(\alpha_2-\alpha_5)+\alpha_2^2(\alpha_5-\alpha_1)+\alpha_5^2(\alpha_1-\alpha_2)\right]$

The planar single particle spectral function $A(k,\omega)$ can be calculated from the above Green's function $G_{11}(k,\omega)$ numerically by using the relationship :

$$A(k,\omega)=-\frac{1}{\pi}\mathrm{Im}G_{11}(k,\omega), \qquad \ldots(34)$$

Where Im stands for imaginary part of Green's function. Using equation (33) and (34) the expression for planar electronic spectral function can be written in the following form:

$$A(k,\omega)=\frac{1}{\pi}\sum_{i=1}^{5}\frac{\Gamma A_i}{\Gamma^2+(\omega-\alpha_i)^2} \qquad \ldots(35)$$

To fit the line shape of the photoemission experimental results, we need to solve δ-functions involved in the spectral function (equation (35)). The

calculation of A(k, ω) would give a broadening of the quasiparticle peak. A Lorentizian type of broadening is used as given below:

$$\delta(\omega - \tilde{\varepsilon}_k) \cong \frac{1}{\pi} \operatorname{Lim}_{\Gamma \to 0} \frac{\Gamma}{(\omega - \tilde{\varepsilon}_k)^2 + \Gamma^2} \qquad \ldots(36)$$

The phenomenological broadening parameter Γ is taken to be independent of k and ω [Leung et al. (1997)]. The parameter Γ takes care of quasi-particle scattering rate. The line shape of the peak in the ARPES spectral function A(k, ω) can be analyzed using equation (35) numerically.

4.2.1 Results and Discussion

The spectral function A(k, ω) is measured by angle resolved photoemission spectroscopy. The measured A(k, ω) can be numerically analyzed using equations (7), (19), (35) and (36). Initially the A(k, ω) is numerically computed in the absence of electronic correlations using equations (7) and (19). The A(k, ω) is analyzed especially at $(\pi,0)$ points of the Brillouin zone, where the splitting in the ARPES spectra of Bi2212 is found to be maximum in normal state and a lot of experimental data is available. These calculations would be relevant to bilayer cuprates, Bi-2212, because the range of various intra and inter cell parameters used in the present analysis have been taken from recent electronic band structure calculations [Chakravarty (1993 & 1999)] and works on electronic spectra of Bi2212 cuprates [Feng et al. (2001), Feng et al. (2002), Bansil et al. (2005), Markiewicz et al. (2005)].

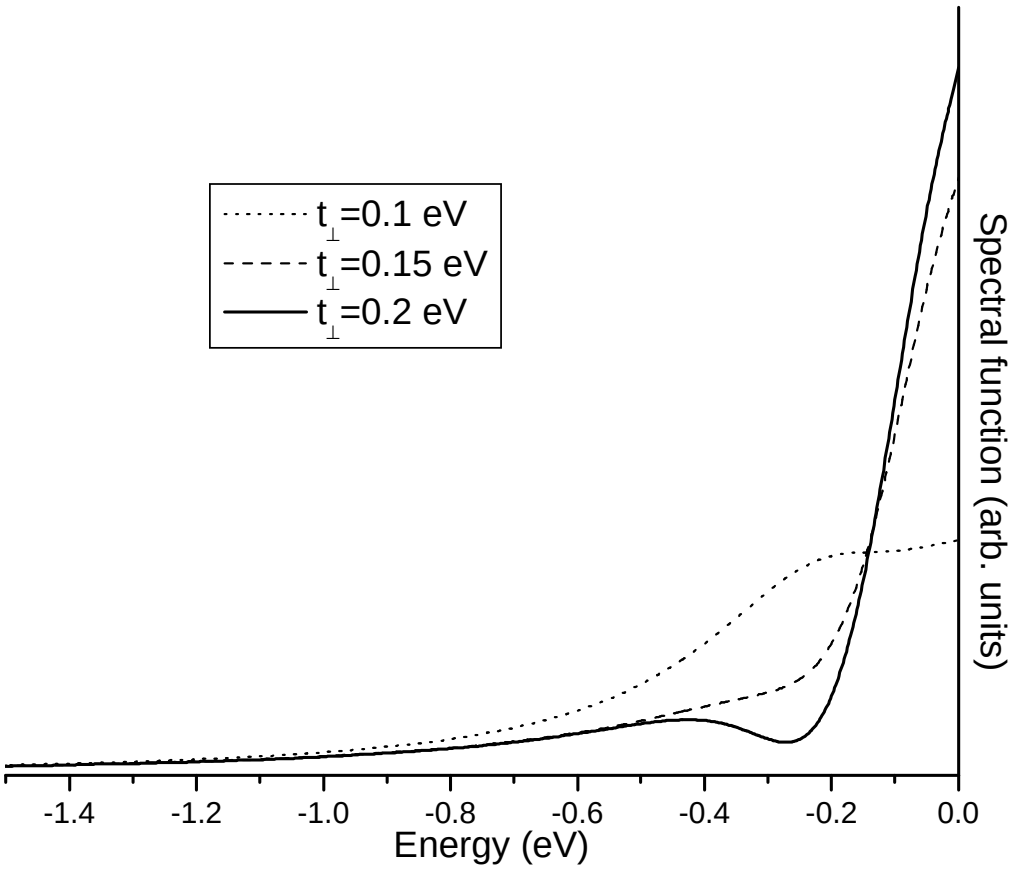

Figure (2). Spectral function versus energy at (π,0) point of the Brillouin zone keeping t=0.4 eV, T_{12}=0.1 eV, U=0.0 eV, n=0.2, Γ=0.25 eV, and ε_0=0.05 eV

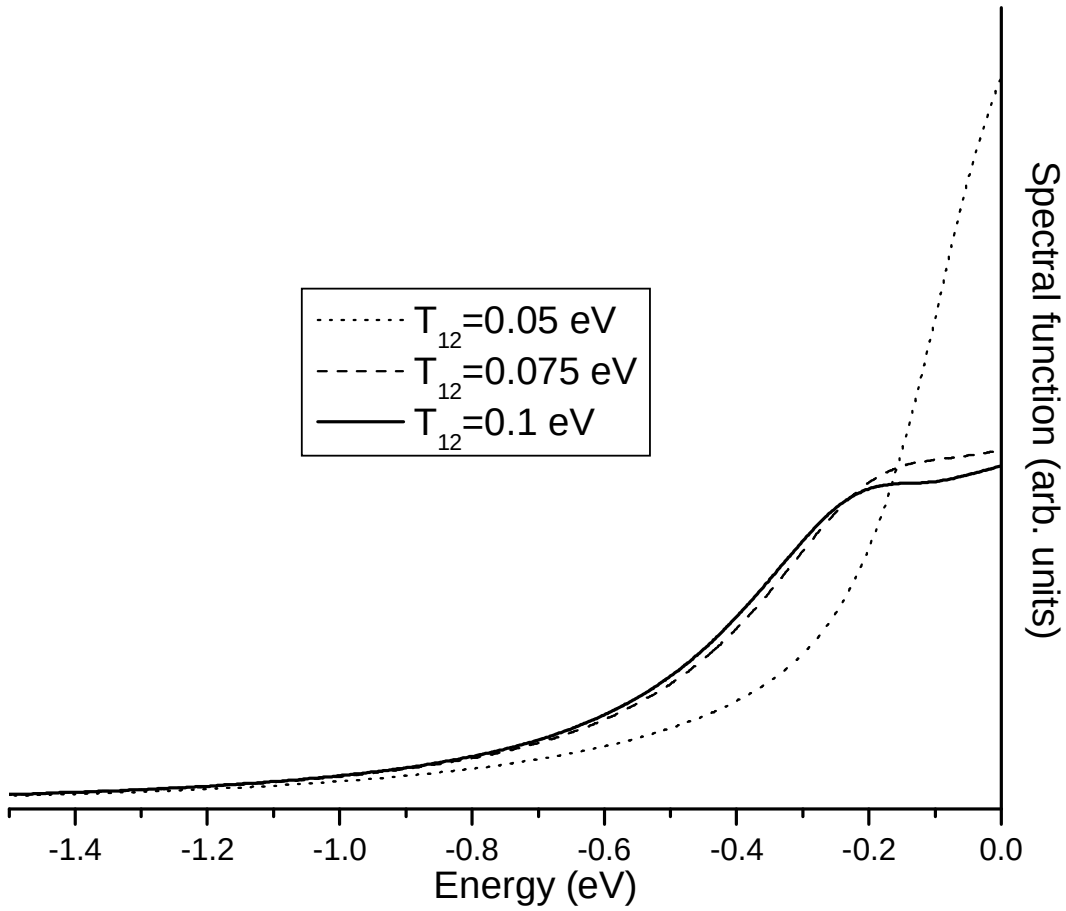

Figure (3). Spectral function versus energy at $(\pi,0)$ point of the Brillouin zone keeping t=0.4 eV, $t_{\perp}$=0.1 eV, U=0.0 eV, n=0.2, Γ=0.25 eV, and ε_0=0.05 eV

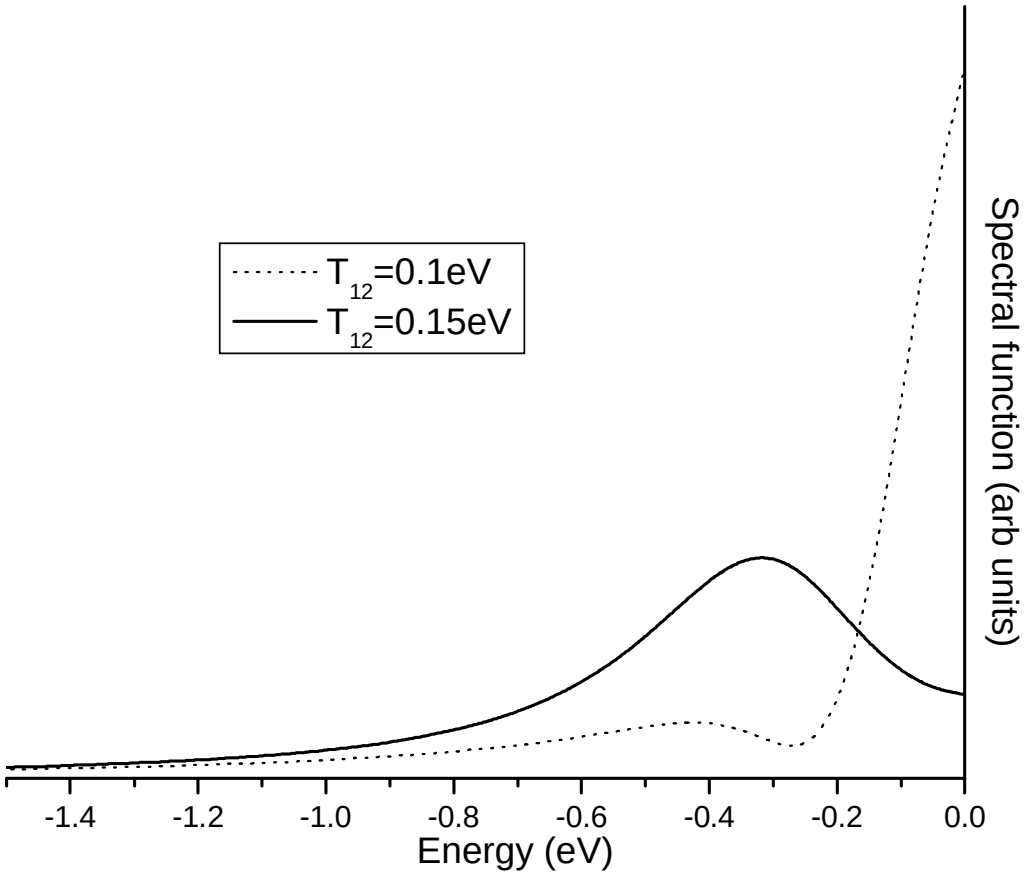

Figure (4). Spectral function versus energy at $(\pi,0)$ point of the Brillouin zone keeping t=0.4 eV, $t_{\perp}$=0.2 eV, U=0.0 eV, n=0.2, Γ=0.25 eV, and ε_0=0.05 eV.

In figure (2), one can observe the spectral function $A(k,\omega)$ against energy (ω) for different intra cell coupling strength in optimal doped regime of Bi-2212 in the normal state using equation (19) (in the presence of inter cell resonant tunneling (T_{12}=0.1 eV) and for the case U=0.0 eV). The variation of $A(k,\omega)$ versus band energy (ω) at $(\pi,0)$ point of Brillouin zone shows a splitting in the spectral function in the presence of intra cell coupling between the planes ($t_{\perp}$=0.2 eV). Such a bilayer splitting in Bi-2212 at $(\pi,0)$ point is also observed in recent ARPES measurements [Feng et al. (2002), Chaung et al. (2001) and Kordyuk et al. (2002)]. On introducing the inter unit cell resonant tunneling (T_{12}=0.05eV, 0.075eV and 0.1eV and keeping $t_{\perp}$=0.1 eV), one can point out a broadening in the spectral function (figure (3)). Also, the bilayer splitting in the spectral function disappeared due to broadening in the spectra on increasing inter cell resonant tunneling term (T_{12}=0.1 eV to 0.15 eV) (figure (4)). Such broadening in the normal state spectra has also been predicted by simulated ARPES line shapes in Bi-2212 bilayer systems as manifestation of third dimensional inter unit cell coupling [Bansil et al. (2005), Markiewicz et al. (2005)]. On comparing figure (2) and figure (4) one can observe that intra cell coupling ($t_{\perp}$) leads the bilayer splitting in the spectral function, while inter unit cell resonant tunneling (T_{12}) suppresses the bilayer splitting and induces broadening in the spectral peak close to Fermi level.

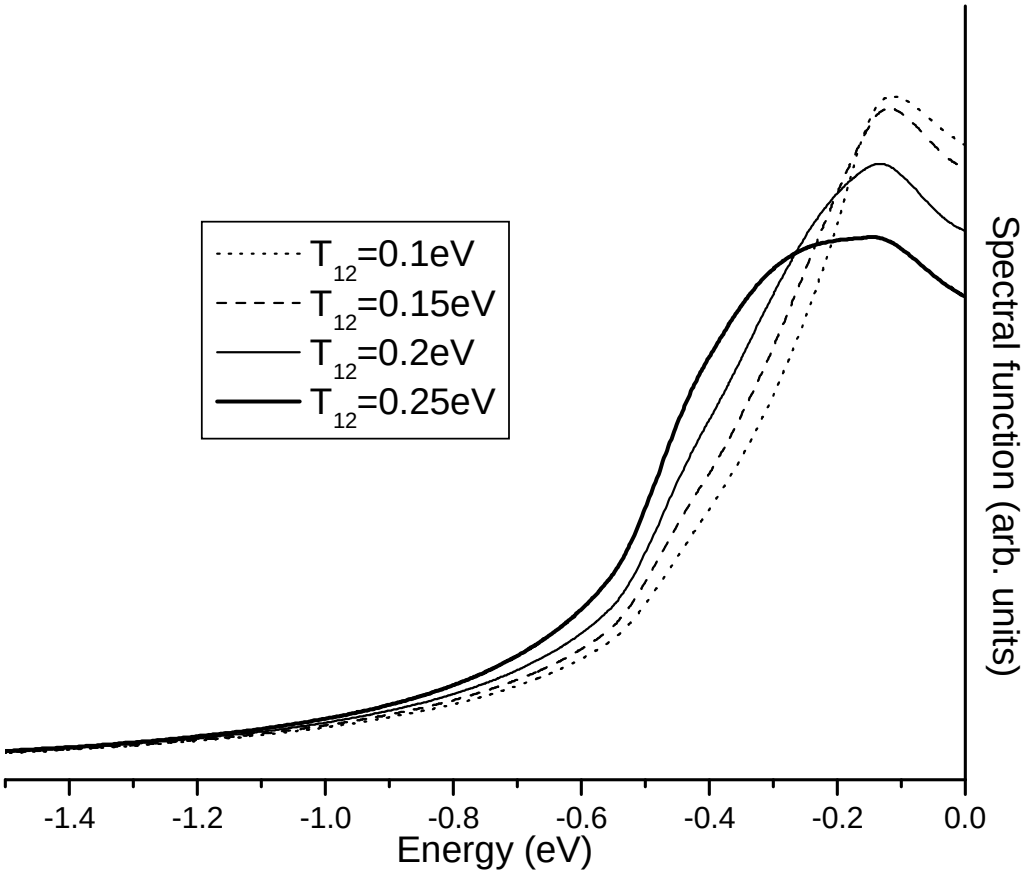

Figure (5). Spectral function versus energy at $(\pi,0)$ point of the Brillouin zone keeping t=0.4 eV, $t_{\perp}$=0.2 eV, U=3.0 eV, n=0.2, Γ=0.25 eV, and ε_0=0.05 eV.

One can also analyze the influence of inter cell resonant tunneling term (T_{12}) on the spectral function at $(\pi,0)$ point in the presence of Coulomb correlation (U), keeping other parameters fixed, and using Green's function equation (31). In figure (5), the spectral function versus energy for different values of inter cell resonant tunneling term (T_{12}=0.1eV to 0.25eV) in the presence of Coulomb correlation (i.e. U=3eV) have been plotted. It is pointed out from the figure 5 that in the presence of both the electronic correlations, and inter cell resonant tunneling (T_{12}) the broadening in spectra [Norman et al. (2003), Damacelli et al. (2003), Feng et al. (2001), Feng et al. (2002)] is more as compared in the absence of Coulomb correlations (figure (3) and (4)).

Finally, it is concluded that the intra unit cell coupling is responsible for bilayer splitting of electronic spectra, while the inter unit cell resonant tunneling leads to broadening in the spectral features especially at $(\pi,0)$ point of optimally doped bilayer (Bi-2212) cuprates and in good correspondence with recent ARPES measurements [Bansil et al. (2005)]. The electron correlations also play an important role in determining the shape of spectral function. It is pointed out that the presence of finite electron correlations, the inter unit cell resonant tunneling (T_{12}) suppresses the bilayer splitting in the spectral function due to broadening in the spectral features close to Fermi level in optimal doped bilayer cuprates. As the electronic states close to Fermi level determines the electronic transport, therefore, it will be interesting to analyze the influence of third dimensional resonant tunneling on the

transport behaviour along third dimension (i.e. c-axis). In the next subsection, we have developed theoretical formulation in this direction.

4.3 Out-of-plane (c-axis) conductivity for bilayer cuprates (Within extended Hubbard model and Kubo formalism)

In the present section we use the single particle, temperature dependent Green's function formalism to calculate the c-axis electrical conductivity up to order t^2 (t being the nearest neighbor hopping energy) at various carrier concentration and temperature using Kubo formula within extended Hubbard model including third dimensional inter unit cell resonant tunneling.

As a first step of the calculation, we derive the required Green's function and hence chemical potential as a function of doping for the model Hamiltonian by employing Green's function equations of motion approach. The second section is devoted to the calculation of conductivity within Kubo formalism using extended Hubbard model.

4.3.1 Calculation of Green's function and chemical potential

As describe in the introduction the crystal structure of high T_c cuprates contains stakes of CuO_2 planes. The bilayer cuprates (Bi-2212 and Y-123) contains two Cu-O planes per unit cell and the coupling between these Cu-O planes governs the electronic and spectral behaviour of these systems. To analyze the effect of coupling between the Cu-O planes of adjacent unit cell on the c-axis electronic transport, we have incorporated a third dimensional (c-axis) inter unit cell resonant tunneling term (T_{12}) in the Hubbard model. However, keeping in view that two CuO_2 planes within the

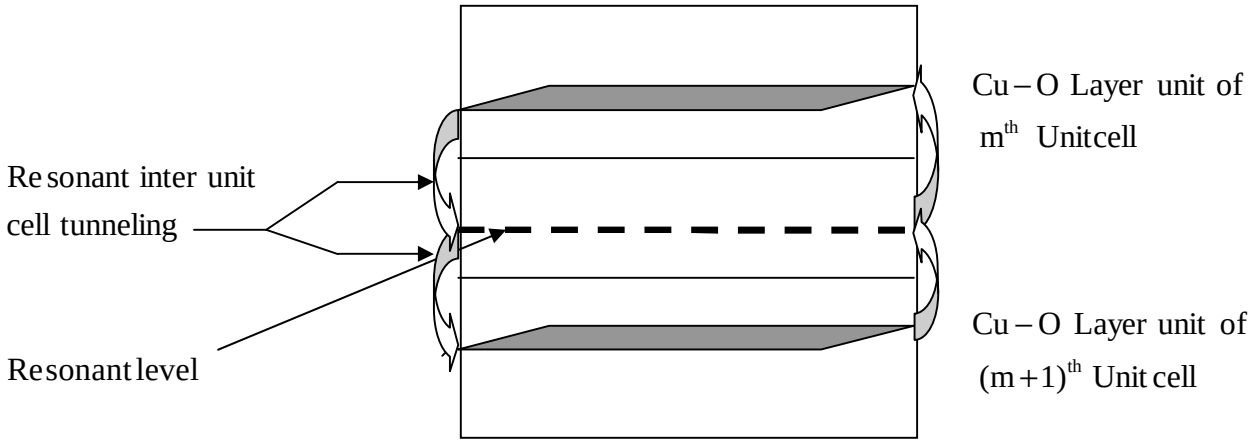

Figure (1). Schematic presentation of inter unit cell resonant tunneling between two Cu-O unit (Bi-2212 and Y-123))

unit cell are separated by small distance (~3 $\overset{o}{A}$) as compared to distance between CuO_2 plane in adjacent unit cells, the two Cu-O planes within the unit cell are taken as a single unit. The mechanism of inter unit cell resonant tunneling as schematically depicted in figure (1) for Bi-2212 and Y-123 systems having two Cu-O plane as a single unit per unit cell and explained in detail in previous section. The extended Hubbard Hamiltonian for cuprates including third dimensional inter cell resonant tunneling term (T_{12}) can be given as:

$$H = \sum_{m,i,j,\sigma} t_{ij} c^{+}_{m,i,\sigma} c_{m,j,\sigma} + U \sum_{m,i} n_{m,i,\sigma} n_{m,i,-\sigma} + \varepsilon_0 \sum_{l} b^{+}_{l} b_{l} + \sum_{m,i,l,\sigma} T_{m,m+1} \left[\left(c^{+}_{m,i,\sigma} b_{l} + b^{+}_{l} c_{m+1,i,\sigma} \right) + \text{h.c.} \right] \quad \text{.....(1)}$$

Where, m is unit cell indices, $c^{+}_{mi\sigma}(c_{mi\sigma})$ are creation (annihilation) operator for the holes of m^{th} unit cell, i^{th} site and spin σ. The 1^{st} term in equation (1) is kinetic energy of charge carrier (holes) within the Cu-O plane. The 2^{nd} term in (1) is the on site Coulomb energy at $Cu3d^9$ site and in cuprates this energy is quiet large (in the range 5 to 8 eV) as compared to hopping energy. The 3^{rd} term in (1) represents the energy of the resonant level due to oxygen deficient BiO chains which lies mid way between the two Cu-O planes lying in adjoining unit cells. The last term in 1(b) represents the single particle resonant tunneling from the layer of m^{th} unit cell to the adjacent $(m+1)^{th}$ unit cell and vice-versa. The parameter $T_{m,m+1}$ represent the inter unit cell resonant tunneling matrix element for the case when tunneling probability between two Cu-O planes in different unit cells is of the order of unity [Abrikosov (1997)]. During the theoretical calculation

$T_{m,m+1}$ is taken as T_{12} for the case of nearest CuO planes in adjacent unit cells (figure (1)).

To calculate the expression of chemical potential as a function of doping and temperature, we need the expression for relevant Green's function $G_{11}(k,\omega)=\langle\langle c_{1i\sigma}\,|\,c^{+}_{1j\sigma}\rangle\rangle$ [Ajay (1999), Lal et al. (1998), Ajay et al. (2002)] and following set of coupled equations are derived assuming uniform distribution of charge carriers in different unit of CuO_2 layers (i.e. $n_{1\sigma}=n_{2\sigma}=n_{\sigma}$) as a paramagnetic situation:

$$(\omega-T_0)\langle\langle c_{1i\sigma}\,|\,c^{+}_{1j\sigma}\rangle\rangle=\frac{\delta_{ij}}{2\pi}+U\langle\langle n_{i-\sigma}c_{1i\sigma}\,|\,c^{+}_{1j\sigma}\rangle\rangle+T_{12}\langle\langle b_l\,|\,c^{+}_{1j\sigma}\rangle\rangle \qquad .....(2)$$

$$(\omega-\varepsilon_0)\langle\langle b_l\,|\,c^{+}_{1j\sigma}\rangle\rangle=T_{12}\langle\langle c_{2i\sigma}\,|\,c^{+}_{1j\sigma}\rangle\rangle+T_{12}\langle\langle c_{1i\sigma}\,|\,c^{+}_{1j\sigma}\rangle\rangle \qquad .....(3)$$

$$(\omega-T_0-U)\langle\langle n_{1i-\sigma}c_{1i\sigma}\,|\,c^{+}_{1j\sigma}\rangle\rangle=\frac{\delta_{ij}}{2\pi}n_{i-\sigma}+T_{12}\langle n_{i-\sigma}\rangle\langle\langle b_l\,|\,c^{+}_{1j\sigma}\rangle\rangle \qquad .....(4)$$

$$(\omega-T_0)\langle\langle c_{2i\sigma}\,|\,c^{+}_{1j\sigma}\rangle\rangle=U\langle\langle n_{i-\sigma}c_{2i\sigma}\,|\,c^{+}_{1j\sigma}\rangle\rangle+T_{12}\langle\langle b_l\,|\,c^{+}_{1j\sigma}\rangle\rangle \qquad .....(5)$$

$$(\omega-T_0-U)\langle\langle n_{2i-\sigma}c_{2i\sigma}\,|\,c^{+}_{1j\sigma}\rangle\rangle=T_{12}\langle n_{i-\sigma}\rangle\langle\langle b_l\,|\,c^{+}_{1j\sigma}\rangle\rangle \qquad .....(6)$$

Solving above equations (2-6), one obtains the desirable Green's function having the following form:

$$G_{11}(k,\omega)=\frac{\delta_{ij}}{2\pi}\times\left[\frac{\{\omega-T_0-U(1-n_{i-\sigma})\}\{(\omega-\varepsilon_0)(\omega-T_0)(\omega-T_0-U)-T_{12}^2(\omega-T_0-U(1-n_{i-\sigma})\}}{(\omega-T_0-U)(\omega-T_0)\{(\omega-\varepsilon_0)(\omega-T_0)(\omega-T_0-U)-2T_{12}^2(\omega-T_0+U(1-n_{i-\sigma})\}}\right] \qquad .....(7)$$

The above equation (7) is written into a tractable form keeping in mind large energy scales of U using simple algebra:

$$G_{11}(k,\omega)=\frac{1}{2\pi}\times\left[\frac{\{\omega-T_0-Un_H\}\{(\omega-\varepsilon_0)(\omega-T_0)-T_{12}^2 n_H\}}{(\omega-T_0)(\omega-T_0-U)\{(\omega-\varepsilon_0)(\omega-T_0)-2T_{12}^2 n_H\}}\right] \quad \text{.....(8)}$$

Where, $n_H=1-\langle n_{i-\sigma}\rangle$ (Hole concentration per site) and we have used a dispersionless in-plane band with energy T_0.

The above equation (9) can be manipulated in the following form:

$$G_{11}(k,\omega)=\frac{1}{2\pi}\times\left[\frac{A}{(\omega-\alpha)}+\frac{B}{(\omega-\beta)}+\frac{C}{(\omega-\gamma)}+\frac{D}{(\omega-\delta)}\right] \quad \text{.....(9)}$$

where α,β,γ and δ are four quasi-particle energy branches corresponding to poles of the Green's function (8) and

$$A=1-B-C-D$$

$$B=\frac{1}{(\beta-\alpha)}\{\delta+\beta+\gamma-\varepsilon_0-2T_0-Un_H-C(\gamma-\alpha)-D(\delta-\alpha)\}$$

$$C=\frac{F-D(\delta-\alpha)(\beta-\delta)}{(\gamma-\alpha)(\beta-\gamma)}$$

$$D=\frac{G-F\delta}{(\delta-\alpha)(\beta-\delta)(\gamma-\delta)}$$

$$F=\delta\beta+\delta\gamma+\beta\gamma-2\varepsilon_0T_0-(\varepsilon_0+T_0)Un_H-T_0^2+T_{12}^2n_H-(\delta+\beta+\gamma-\varepsilon_0-2T_0-Un_H)(\delta+\gamma)$$
$$G=\beta\gamma\delta-(T_0+Un_H)(\varepsilon_0T_0-T_{12}^2n_H)-\delta\gamma(\delta+\beta+\gamma-\varepsilon_0-2T_0-Un_H)$$

where,

$\alpha=T_0$,

$\beta=T_0+U$,

$$\gamma=\frac{1}{2}\left[(\varepsilon_0+T_0)+\sqrt{(\varepsilon_0+T_0)^2+8T_{12}^2n_H}\right]$$

$$\delta=\frac{1}{2}\left[(\varepsilon_0+T_0)-\sqrt{(\varepsilon_0+T_0)^2+8T_{12}^2n_H}\right]$$

Equation (9) can be rewritten in terms of Chemical potential as

$$G_{11}(k,\omega)=\frac{1}{2\pi}\times\left[\frac{A}{(\omega+\mu-\alpha)}+\frac{B}{(\omega+\mu-\beta)}+\frac{C}{(\omega+\mu-\gamma)}+\frac{D}{(\omega+\mu-\delta)}\right] \quad \text{.....(10)}$$

From this equation, we immediately get the electronic density of states (DOS) using the relationship:

$$\rho(\omega)=\frac{2i}{N}\lim_{\eta\to 0^{+}}\sum_{j}\left[G_{jj}(\omega-\mu+i\eta)-G_{jj}(\omega-\mu-i\eta)\right] \quad \text{.....(11)}$$

Using the above Green's function $G_{11}(k,\omega)=\left\langle\left\langle c_{1i\sigma}\middle|c^{+}_{1j\sigma}\right\rangle\right\rangle$, the expression for DOS can be given as

$$\rho(\omega)=A\delta(\omega-\alpha)+B\delta(\omega-\beta)+C\delta(\omega-\gamma)+D\delta(\omega-\delta)\ , \quad \text{.....(12)}$$

where δ -function involved in the above equations are solved using relationship between δ -function and Lorentizian function as

$$\delta(\omega-x)\cong\frac{1}{\pi}\lim_{\eta\to 0}\frac{\eta}{(\omega-x)^{2}+\eta^{2}}.$$

The chemical potential (μ) can be calculated from above equation (12) using the relation between carrier concentration (n_H) and DOS as:

$$n_H=\int d\omega\,\rho(\omega)\frac{1}{e^{\beta(\omega-\mu)}+1} \text{ and } n_H=1-\langle n\rangle. \quad \text{.....(13)}$$

From equation (12) and (13), one can calculate the value of chemical potential μ numerically for given carrier concentration and temperature (T).

4.3.2 Calculation of the c-axis conductivity within Kubo formalism

The high T_c cuprates have highly anisotropic electronic transport behaviour in both the superconducting as well as normal state. The anisotropy in the electronic transport behaviour in the normal state is the display of anisotropic crystal structure. To address the electronic transport in normal state specially along the out-of-plane (i.e. c-axis), one requires to understand the electronic structure of these materials around the Fermi level. As pointed out in the introduction, so far a systematic study of anisotropy in transport behaviour as a function of doping and temperature is still lacking. In the present section, we have analyzed the influence of out-of-plane inter unit cell resonant tunneling on the electronic spectra within the framework of tight binding Hubbard model. It will be interesting to study the c-axis electronic transport as a function of inter unit cell resonant tunneling, carrier concentration and temperature in normal state in doped bilayer cuprates. To analyze the c-axis conductivity, we follow the Kubo formula given as:

$$\sigma_{\mu\nu}(\omega) = \frac{i}{V}\lim_{\eta\to 0^+}\int_0^\infty \langle [J_\mu(t), \chi_\nu]\rangle e^{-i\omega t-\eta t}dt \qquad \text{.....(14)}$$

Where, J_μ is μ component of the current operator and χ_ν is the ν component of the electric polarization operator. In Wannier basis, we have

$$\breve{\chi} = e\sum_{i\sigma} R_i n_{i\sigma} \quad \text{and,} \qquad \text{.....(15)}$$

$$J_\mu = \frac{d}{dt}\chi_\mu = -ie\sum_{ij\sigma} t_{ij}(R_i - R_j)_\mu c^+_{i\sigma} c_{j\sigma} \quad \text{..... (16)}$$

and $J_\mu(t) = e^{iHt} J_\mu(0) e^{-iHt}$ is the Heisenberg representation of current correlation function. Here, R_i is the component of the lattice-site position vectors parallel to the external field. Equation (14) can be written in alternative form as:

$$\sigma_{\mu\nu}(\omega) = \frac{1}{2V}\int_{-\infty}^{\infty} d\tau\, e^{i\omega\tau} \int_0^\beta \langle [J_\mu(0) j_\nu(\tau + i\lambda)]\rangle d\lambda \quad \text{.....(17)}$$

Using equation (17), we define the dissipative part of electrical conductivity along c-axis ($\sigma_c(\omega)$) as:

$$\sigma_c(\omega) = \frac{e^2}{2V}\sum_{ij\sigma\sigma' kl} (\overset{\circ}{R}_{1i} - \overset{\circ}{R}_{2j})(\overset{\circ}{R}_{2k} - \overset{\circ}{R}_{1l}) t_{1ij} t_{2kl} \int_{-\infty}^{\infty} d\tau e^{i\omega\tau} \times \int_0^\beta d\lambda \langle c^+_{1i\sigma} c_{1j\sigma} e^{iH(\tau+i\lambda)} c^+_{2k\sigma'} c_{2l\sigma'} e^{-iH(\tau+i\lambda)}\rangle$$

.....(18)

To solve above equation, one have to calculate the expectation value of $\langle c^+_{1i\sigma} c_{1j\sigma} e^{iH(\tau+i\lambda)} c^+_{2k\sigma'} c_{2l\sigma'} e^{-iH(\tau+i\lambda)}\rangle$ for which the two particle real time, temperature dependent Green's function is required and supposed to be a difficult task. Here, we are interested in an approximate analysis of the c-axis conductivity within above Kubo formalism to the order t^2 because all contributions of order greater than t^2 to the conductivity comes from the calculation of equation (18). Hence, single particle imaginary time Green's function will be relevant for this purpose [Rodrigues (1979), Mahan (1990)] to make the solution tractable. To obtain the contribution of order t^2 we must calculate equation $\langle c^+_{1i\sigma} c_{1j\sigma} e^{iH(\tau+i\lambda)} c^+_{2k\sigma'} c_{2l\sigma'} e^{-iH(\tau+i\lambda)}\rangle$ in zero order in t. This

can be done by substitution t=0 in model Hamiltonian (i.e. $H \to U\sum_{mi} n_{mi\uparrow} n_{mi\downarrow}$, where m=1,2)

In equation (18), one can rewrite $\sum_{\sigma\sigma'} \langle c^{+}_{1i\sigma} c_{1j\sigma} e^{iH(\tau+i\lambda)} c^{+}_{2k\sigma'} c_{2l\sigma'} e^{-iH(\tau+i\lambda)} \rangle$ in a tractable form as:

$$\sum_{\sigma\sigma'} \langle c^{+}_{1i\sigma} c_{1j\sigma} e^{iH(\tau+i\lambda)} c^{+}_{2k\sigma'} c_{2l\sigma'} e^{-iH(\tau+i\lambda)} \rangle$$

$$= \sum_{\sigma\sigma'} \langle c^{+}_{1i\sigma} c_{1j\sigma} (c^{+}_{2k\sigma'} c_{2l\sigma'} - i(\tau + i\lambda)[c^{+}_{2k\sigma'} c_{2l\sigma'}, H] + ...) \rangle \qquad .....(19)$$

The right hand side of the above expression is solved up to first order contribution of U and the commutation relation $[c^{+}_{2k\sigma'} c_{2l\sigma'}, H]$ appearing in above equation is given as follows

$$[c^{+}_{2k\sigma'} c_{2l\sigma'}, H] = c^{+}_{2k\sigma'} [c_{2l\sigma'}, H] - [c^{+}_{2k\sigma'}, H] c_{2l\sigma'}$$
$$= U c^{+}_{2k\sigma'} \delta_{\sigma\sigma'} c_{2l\sigma} n_{2l\downarrow} + U \delta_{\sigma\sigma'} c^{+}_{2k\sigma} n_{2k\downarrow} c_{2l\sigma'} .$$

Using above results equation (19) is now reduce to the following form

$$\sum_{\sigma\sigma'} \langle c^{+}_{1i\sigma} c_{1j\sigma} e^{iH(\tau+i\lambda)} c^{+}_{2k\sigma'} c_{2l\sigma'} e^{-iH(\tau+i\lambda)} \rangle = \langle c^{+}_{1i\sigma} c_{2l\sigma} c_{1j\sigma} c^{+}_{2k\sigma} e^{iU(\tau+i\lambda)(n_{2k-\sigma} - n_{2l-\sigma})} \rangle \qquad ...(20)$$

With the help of equation (20), equation (18) may be expressed as

$$\sigma_c(\omega) = \frac{e^2}{2V} \sum_{ijkl} (\overset{\circ}{R}_i - \overset{\circ}{R}_j)(\overset{\circ}{R}_k - \overset{\circ}{R}_l) t_{ij} t_{kl} \int_{-\infty}^{\infty} d\tau e^{i\omega\tau} \times \int_0^{\beta} d\lambda \langle c^{+}_{1i\sigma} c_{2l\sigma} c_{1j\sigma} c^{+}_{2k\sigma} e^{iU(\tau+i\lambda)(n_{2k-\sigma} - n_{2l-\sigma})} \rangle$$

and a simple algebraic manipulation reproduces:

$$\sigma_c(\omega) = -\frac{e^2}{2V} c^2 T_0^2 g\eta \int_{-\infty}^{\infty} d\tau e^{i\omega\tau} \times \int_0^{\beta} d\lambda \langle c^{+}_{1l\sigma} c_{2l\sigma} c_{1k\sigma} c^{+}_{2k\sigma} e^{iU(\tau+i\lambda)(n_{2k-\sigma} - n_{2l-\sigma})} \rangle \qquad .....(21)$$

where, c is the out of plane lattice parameter, g is the number of nearest neighbors and η is the number density (η=N/V). The thermal average in equation (21) within our approach reduces to:

$$\langle c^{+}_{1l\sigma} c_{2l\sigma} (-c^{+}_{2k\sigma} c_{1k\sigma}) e^{iU(\tau+i\lambda)(n_{2k-\sigma}-n_{2l-\sigma})} \rangle = \langle e^{iU(\tau+i\lambda)(n_{2k-\sigma})} (-c^{+}_{2k\sigma} c_{1k\sigma}) \rangle \langle e^{-iU(\tau+i\lambda)(n_{2l-\sigma})} c^{+}_{1l\sigma} c_{2l\sigma} \rangle$$

where, one can further obtains

$$\langle e^{iU(\tau+i\lambda)(n_{2k-\sigma})} (-c^{+}_{2k\sigma} c_{1l\sigma}) \rangle = -\langle c^{+}_{2k\sigma} c_{1k\sigma} \rangle + \langle n_{2k-\sigma} c^{+}_{2k\sigma} c_{1k\sigma} \rangle (1 - e^{U(\tau+i\lambda)})$$

$$\langle e^{iU(\tau+i\lambda)(n_{2l-\sigma})} c^{+}_{1l\sigma} c_{2l\sigma} \rangle = \langle c^{+}_{1l\sigma} c_{2l\sigma} \rangle - \langle n_{2l-\sigma} c^{+}_{1l\sigma} c_{2l\sigma} \rangle (1 - e^{-U(\tau+i\lambda)})$$

Using above results in equation (21), we finally obtain

$$\sigma_c(\omega) = -\sigma_0 \int_{-\infty}^{\infty} d\tau e^{i\omega\tau} \times \int_0^{\beta} d\lambda [-\langle c^{+}_{2k\sigma} c_{1k\sigma} \rangle + \langle n_{2k-\sigma} c^{+}_{2k\sigma} c_{1k\sigma} \rangle (1 - e^{U(\tau+i\lambda)})] \times [\langle c^{+}_{1l\sigma} c_{2l\sigma} \rangle - \langle n_{2l-\sigma} c^{+}_{1l\sigma} c_{2l\sigma} \rangle (1 - e^{-U(\tau+i\lambda)})] \quad \text{.....(22)}$$

Where, $\sigma_0 = e^2 c^2 T_0^2 g\eta$, e=electric charge, T_0=in-plane energy, g=number of nearest neighbors. Within mean field approach equation (22) can be rewritten in the following form:

$$\sigma_c(\omega) = \sigma_0 \int_{-\infty}^{\infty} d\tau e^{i\omega\tau} \times \int_0^{\beta} d\lambda [\langle c^{+}_{2k\sigma} c_{1k\sigma} \rangle \langle c^{+}_{1l\sigma} c_{2l\sigma} \rangle [1 - \langle n_{2k-\sigma} \rangle (1 - e^{U(\tau+i\lambda)})][1 - \langle n_{2l-\sigma} \rangle (1 - e^{-U(\tau+i\lambda)})] \quad \text{.....(23)}$$

To obtain an expression for the dc conductivity along c-axis, one can use the limit $\omega \to 0$ in equation (23) as:

$$\sigma_c = \lim_{\omega \to 0} \sigma_c(\omega) \quad \text{.....(24)}$$

In order to analyze c-axis conductivity as a function of temperature, carrier concentration and various parameters of the model Hamiltonian given by equation (23), one needs to find correlations of the type $\langle c^{+}_{2i\sigma} c_{1i\sigma} \rangle$

for symmetrical bilayer cuprate system. The expression for correlation function ($\langle c^{+}_{2i\sigma} c_{1i\sigma} \rangle$)can be obtained from corresponding propagator i.e. Green's function $G_{12}(k,\omega) = \langle\langle c_{1i\sigma} | c^{+}_{2j\sigma} \rangle\rangle$ within the Hamiltonian given by equation (1) and employing Green's function equations of motion technique. Assuming uniform distribution of charge carriers in different layers (i.e. $n_{1\sigma} = n_{2\sigma} = n_{\sigma}$) and a paramagnetic situation. The following set of five coupled Green's function equations are finally obtained:

$$(\omega - T_0)\langle\langle c_{1i\sigma} | c^{+}_{2j\sigma} \rangle\rangle = U\langle\langle n_{i-\sigma} c_{1i\sigma} | c^{+}_{2j\sigma} \rangle\rangle + T_{12}\langle\langle b_l | c^{+}_{1j\sigma} \rangle\rangle \quad \text{....(25)}$$

$$(\omega - \varepsilon_0)\langle\langle b_l | c^{+}_{1j\sigma} \rangle\rangle = T_{12}\langle\langle c_{2i\sigma} | c^{+}_{2j\sigma} \rangle\rangle + T_{12}\langle\langle c_{1i\sigma} | c^{+}_{2j\sigma} \rangle\rangle \quad \text{.....(26)}$$

$$(\omega - T_0 - U)\langle\langle n_{1i-\sigma} c_{1i\sigma} | c^{+}_{2j\sigma} \rangle\rangle = T_{12}\langle n_{i-\sigma}\rangle\langle\langle b_l | c^{+}_{2j\sigma} \rangle\rangle \quad \text{.....(27)}$$

$$(\omega - T_0)\langle\langle c_{2i\sigma} | c^{+}_{1j\sigma} \rangle\rangle = \frac{\delta_{ij}}{2\pi} + U\langle\langle n_{i-\sigma} c_{2i\sigma} | c^{+}_{2j\sigma} \rangle\rangle + T_{12}\langle\langle b_l | c^{+}_{2j\sigma} \rangle\rangle \quad \text{.....(28)}$$

and

$$(\omega - T_0 - U)\langle\langle n_{2i-\sigma} c_{2i\sigma} | c^{+}_{1j\sigma} \rangle\rangle = \frac{\delta_{ij}}{2\pi} n_{i-\sigma} + T_{12}\langle n_{i-\sigma}\rangle\langle\langle b_l | c^{+}_{2j\sigma} \rangle\rangle \quad \text{.....(29)}$$

Solving equations (25-29), one obtains the desirable Green's function:

$$G_{12}(k,\omega) = \frac{\delta_{ij}}{2\pi} \times \left[\frac{\{\omega - T_0 + Un_H\}^2 T_{12}^2}{(\omega - T_0 - U)(\omega - T_0)\{(\omega - \varepsilon_0)(\omega - T_0)(\omega - T_0 - U) - 2T_{12}^2(\omega - T_0 + Un_H)\}} \right]$$

where $n_H = 1 - \langle n_{i-\sigma}\rangle$ is the carrier concentration (holes)

The above equation can be written in the following form:

$$G_{12}(k,\omega) = \frac{1}{2\pi} \times \left[\frac{I}{(\omega - \alpha_1)} + \frac{J}{(\omega - \beta_1)} + \frac{K}{(\omega - \gamma_1)} + \frac{L}{(\omega - \delta_1)} + \frac{M}{(\omega - \xi_1)} \right] \quad \text{.....(30)}$$

where $\alpha_1, \beta_1, \gamma_1, \delta_1$ and ξ_1 are five quasi-particle energy branches corresponding to five poles of the above Green's function equation (30) and also

$$I = -J - K - L - M$$

$$J = \frac{1}{(\beta_1 - \alpha_1)}\{-K(\gamma(-\alpha_1) - L(\delta_1 - \alpha_1) - M(\xi_1 - \alpha_1)\}$$

$$K = \frac{a_1 - d_1 L - e_1 M}{b_1}$$

$$L = \frac{(b_1 f_1 - g_1 a_1)(b_1 q_1 - n_1 e_1) - (b_1 j_1 - n_1 a_1)(i_1 b_1 - g_1 e_1)}{(b_1 h_1 - g_1 d_1)(b_1 q_1 - n_1 e_1) - (b_1 p_1 - n_1 d_1)(i_1 b_1 - g_1 e_1)}$$

$$M = \frac{(b_1 j_1 - n_1 a_1)(b_1 h_1 - g_1 d_1) - (b_1 f_1 - g_1 a_1)(b_1 p_1 - n_1 d_1)}{(b_1 h_1 - g_1 d_1)(b_1 q_1 - n_1 e_1) - (i_1 b_1 - g_1 e_1)(b_1 p_1 - n_1 d_1)}$$

$$b_1 = (\gamma_1 - \alpha_1)(\beta_1 - \gamma_1)$$

$$d_1 = (\delta_1 - \alpha_1)(\beta_1 - \delta_1)$$

$$e_1 = (\xi_1 - \alpha_1)(\beta_1 - \xi_1)$$

$$a_1 = -T_{12}^2$$

$$g_1 = (\gamma_1 - \alpha_1)(\beta_1 - \gamma_1)(\delta_1 + \xi_1)$$

$$h_1 = (\delta_1 - \alpha_1)(\beta_1 - \delta_1)(\xi_1 + \gamma_1)$$

$$i_1 = (\xi_1 - \alpha_1)(\beta_1 - \xi_1)(\delta_1 + \gamma_1)$$

$$f_1 = -2(T_0 + Un_H)T_{12}^2$$

$$n_1 = \delta_1 \xi_1 (\beta_1 - \gamma_1)(\gamma_1 - \alpha_1)$$

$$p_1 = \gamma_1 \xi_1 (\beta_1 - \delta_1)(\delta_1 - \alpha_1)$$

$$q_1 = \gamma_1 \delta_1 (\beta_1 - \xi_1)(\xi_1 - \alpha_1)$$

$$j_1 = -(T_0 + Un_H)^2 T_{12}^2$$

The corresponding correlation can be obtained using Green's function G_{12} given by equation (30) using the standard relation

$$\langle B(t')\ A(t)\rangle = i \lim_{\xi \to 0} \int_{-\infty}^{\infty} \frac{\left[\langle\langle A, B\rangle\rangle_{\omega + i\xi} - \langle\langle A, B\rangle\rangle_{\omega - i\xi} \right]}{\{e^{\beta\omega} + 1\}} e^{i\omega(t-t')} d\omega . \qquad \text{.....(31)}$$

Using the above relation and equation (30), correlation function ($\langle c_{1l\sigma}^{+} c_{2l\sigma} \rangle$) is obtained as:

$$\langle c_{2j\sigma}^{+}, c_{1j\sigma} \rangle = \frac{1}{2\pi} \times \left[\frac{I}{e^{\beta(\alpha_1 - \mu)} + 1} + \frac{J}{e^{\beta(\beta_1 - \mu)} + 1} + \frac{K}{e^{\beta(\gamma_1 - \mu)} + 1} + \frac{L}{e^{\beta(\delta_1 - \mu)} + 1} + \frac{M}{e^{\beta(\xi_1 - \mu)} + 1} \right] \qquad \text{...(32)}$$

Using equations (24) and (32), one can analyze numerically the out-of-plane (c-axis) conductivity as a function of temperature, carrier concentration and third dimensional inter unit cell resonant tunneling in bilayer cuprates in normal state.

4.3.3 Results and Discussion

We have obtained the expression of the renormalized out-of-plane (c-axis) conductivity $\left(\tilde{\sigma}_c = \sigma_c / \sigma_0 \right)$ in normal state of doped bilayer cuprates like Bi-2212 and Y-123. It is pointed out from equation (24) that $\tilde{\sigma}_c$ depends on third dimensional intercell resonant tunnelling, carrier concentration and Coulomb correlations. In order to compare our calculated c-axis conductivity with available experimental and theoretical results we have performed numerical computation using equation (24) and (32).

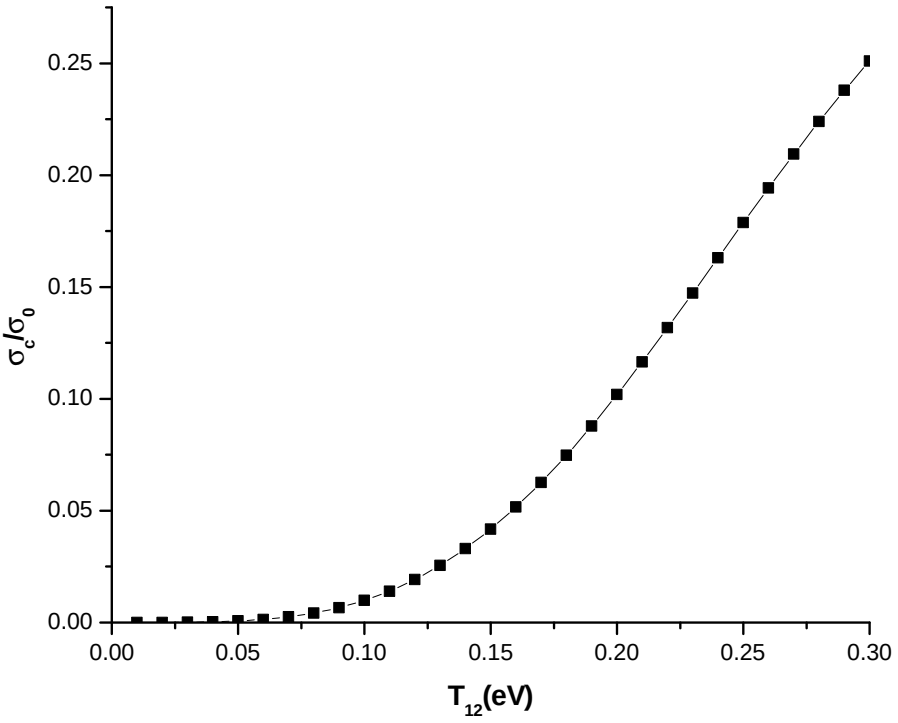

Figure (2) Renormalized c-axis conductivity verses inter unit cell tunnelling (T_{12}) at finite temperature (T=300K) keeping other parameters (T_0=0.3eV, U=3.0eV, n=0.2, ε_0 =0.01eV) constant.

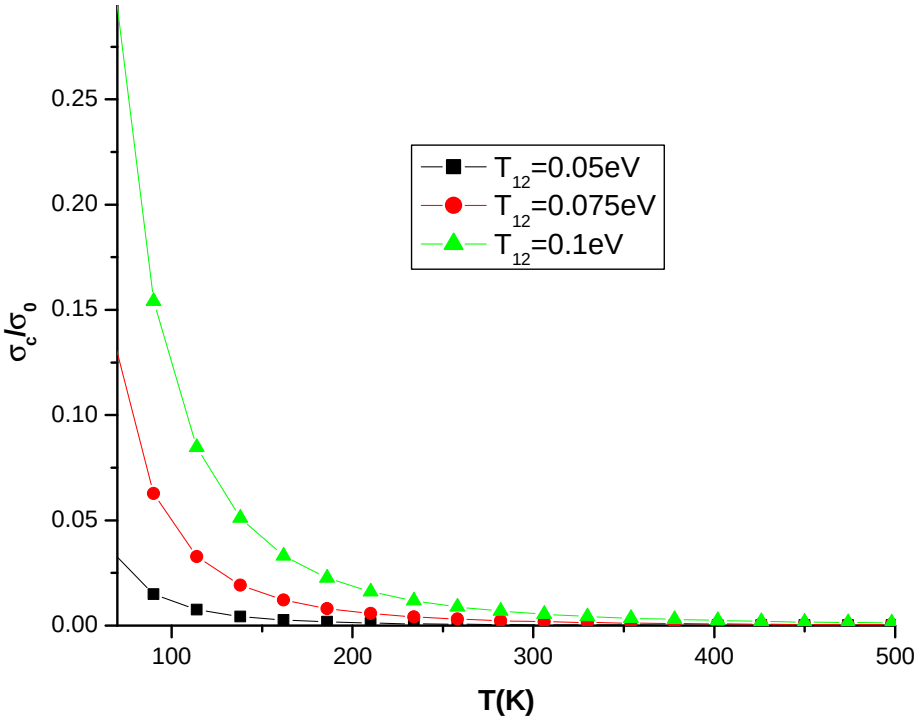

Figure (3) Renormalized c-axis conductivity verses temperature for different values of inter unit cell tunnelling (T_{12}=0.05, 0.075, 0.1 eV) keeping other parameters (T_0=0.3eV, U=3.0eV, n=0.2, ε_0 =0.01eV) constant.

In figure (2) we have presented the variation of renormalized c-axis conductivity ($\tilde{\sigma}_c$) as a functions of out-of-plane inter unit cell resonant tunneling (T_{12}) at room temperature (T=300^{0}K) keeping other parameters (t=0.3eV, U=3.0eV, n=0.2 and ε_0=0.01eV) fixed. One can point from figure (2) that the renormalized c-axis conductivity ($\tilde{\sigma}_c$) increases with the out-of-plane inter unit cell resonant tunneling (T_{12}). However, the increment in $\tilde{\sigma}_c$ is very small for low values of T_{12}. In order to analyze the influence of inter unit cell resonant tunneling (T_{12}) on $\tilde{\sigma}_c$ in figure (3), we have shown the variation of $\tilde{\sigma}_c$ with temperature for given values of T_{12} (=0.05eV, 0.075eV and 0.1eV). It is clear from figure (3) that $\tilde{\sigma}_c$ shows an exponential decrement with temperature (T) which is in qualitative agreement with the experimental observations. Further, on increasing the out-of-plane inter unit cell resonant tunneling (T_{12}), one can infer from figure (3) that there is an increment in $\tilde{\sigma}_c$. This increment in $\tilde{\sigma}_c$ is found to be large at low temperature and in tune with the recent theoretical analysis of c-axis transport [Wu et al. (1998) and Turlakov et al. (2001)].

In figure (4), we have shown the variation of $\tilde{\sigma}_c$ with temperature (T) as a function of different values of Coulomb energy (U=1.0eV, 3.0eV and 4.0eV) keeping other parameters fixed (t=0.3eV, T_{12}=0.1eV, n=0.2 and ε_0=0.01eV). It is important to note from figure (4) that on increasing the Coulomb energy, the conductivity along c-axis decreases for higher in-plane Coulomb interaction. The influence of Coulomb correlation on $\tilde{\sigma}_c$ is prominent at

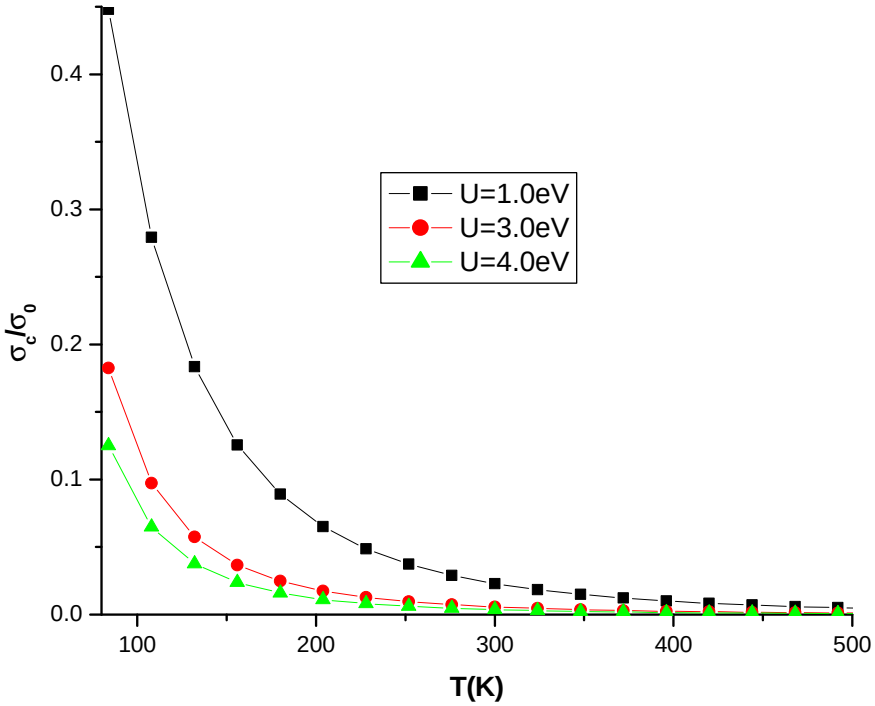

Figure (4) Renormalized c-axis conductivity verses temperature for different values of Coulomb energy (U=1.0, 3.0, 4.0 eV) keeping other parameters (T_0=0.3eV, T_{12}=0.1eV, n=0.2, ε_0 =0.01eV) constant.

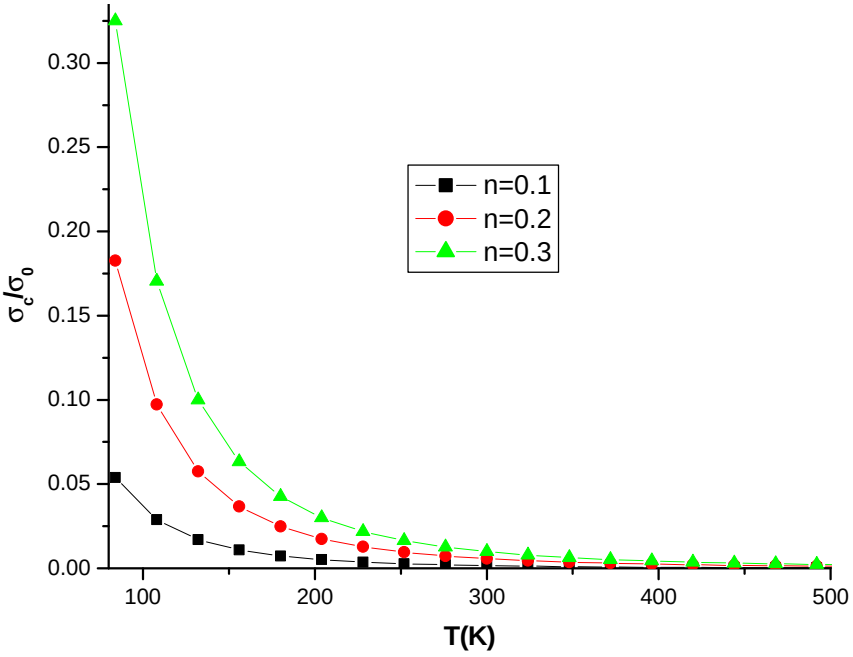

Figure (5) Renormalized c-axis conductivity verses temperature for different values of carrier concentration (n=0.1, 0.3, 0.4) keeping other parameters (T_0=0.3eV, U=3.0eV, T_{12}=0.1eV, ε_0 =0.01eV) constant.

temperatures below room temperature (T=300^{0}K). Although, the trend of variation of $\tilde{\sigma}_c$ with T exhibit an exponential decay in $\tilde{\sigma}_c$.

To analyze the effect of carrier concentration (doping) on the c-axis conductivity ($\tilde{\sigma}_c$), we have presented (figure (5)) the variation of $\tilde{\sigma}_c$ versus temperature (T) for different values of carrier concentrations (n=0.1, 0.2 and 0.3) keeping other parameters (t=0.3eV, T_{12}=0.1eV, U=3.0eV and ε_0=0.01eV) fixed. It is evident from figure (5) that $\tilde{\sigma}_c$ increases with carrier concentration as expected [Nakamura and Uchida (1993), Giura et al. (2003)].

In conclusion, employing Kubo formalism using single particle Green's function technique within the extended Hubbard model which necessarily includes the out-of-plane inter unit cell resonant tunneling (T_{12}) applicable for Bi-2212 and Y-123, we have numerically calculated the renormalized c-axis conductivity $\tilde{\sigma}_c$ as a function of temperature, carrier concentration, Coulomb energy and out-of-plane inter unit cell resonant tunneling (T_{12}). It is pointed out that the out-of-plane inter unit cell resonant tunneling (T_{12}) as well as doping increases the c-axis conductivity while the in-plane Coulomb correlation suppresses the conductivity along c-axis.

Although the present theoretical analysis of c-axis conductivity within Kubo formulation is based on approximate treatment of Coulomb correlations without taking care of higher order term and employing single particle Green's functions, but still the features of c-axis transport as a function of temperature (T), out-of-plane inter unit cell resonant tunneling (T_{12}), Coulomb energy as well as carrier (hole) concentration are close to

experimental results at least qualitatively. Therefore, present analysis of c-axis transport provides a guideline for more rigorous treatment of complex in-plane and out-of-plane transport observed in normal state of layered high T_c cuprates.

SUMMARY

Chapter 5

SUMMARY

In the present thesis, we have analyzed the influence of the third dimension coupling on the normal state electronic spectra of bilayer cuprates employing Green's function equations of motion approach within tight binding extended Hubbard model and $t-t'-t_{\perp}-J-J_3$ model, which necessarily includes the three site exchange interaction and the inter unit cell resonant tunneling (T_{12}). The influence of inter unit cell resonant tunneling on the out of plane (c-axis) conductivity has also been analyzed for bilayer cuprates in normal state employing Kubo formula and Green's function technique.

In the section 4.1 the spectral function $A(k,\omega)$ and density of states (DOS) has been obtained for bilayer cuprates within $t-t'-t_{\perp}-J-J_3$ model in normal state. We have used Green's function technique within Hubbard self-energy approximation and employed a two sublattice approach to derive the equations of motion. Using relevant Green's function we have calculated spectral function and DOS of bilayer cuprates. On the basis of numerical computation, we have analyzed the effect of three site exchange interaction term (J_3) and interlayer coupling within the unit cell on the electronic spectral function and DOS of bilayer cuprates. We have concluded that within Hubbard self energy approximation and the two sublattice approach one can find a splitting of electronic spectral function due to interlayer

coupling ($t_\perp$) at (π ,0) point of the Brillouin zone. It is also predicted that the increment in three site exchange interaction reduces the splitting in the spectra and there is a evolution of spectral peak close to Fermi level. Hence, the spectral function is affected by the three site exchange term (J_3). The results on DOS indicated that on increasing J_3, DOS at Fermi level get enhanced. Finally, it is concluded that in normal state in optimal doped bilayer cuprates the J_3 term plays an important role in renormalizing the spectral weight close to Fermi level and can also plays a role in the superconducting state.

In the section 4.2, we have used the concept of the 'resonant tunneling' (Bohm (1951); Abrikosov (1997,1999)) in bilayer cuprates. The inter cell resonant tunneling term has been incorporated alongwith the intra cell coupling in the Hubbard Hamiltonian to study the electronic spectra in normal state in bilayer cuprates like Bi-2212. Using the model Hamiltonian, we have calculated the spectral function making decoupling approximation at different stages in the Green's function equations of motion. We have also performed numerical computation to analyze spectral function for bilayer cuprates as a function of various parameters of model Hamiltonian. In conclusion, within the extended Hubbard model, we find a splitting of normal state electronic spectral function for finite coupling between the CuO_2 planes ($t_\perp$) at (π ,0) point of the Brillouin zones in the absence of Coulomb correlation in optimally doped regimes. On introducing the inter unit cell resonant tunneling (T_{12}), we find a broadening in the spectral function close

to Fermi surface and the bilayer splitting in the spectral function disappeared due to broadening in the spectra on increasing inter cell resonant tunneling. These results are found to be in qualitative agreement with recent ARPES predictions in Bi-2212 bilayer systems as manifestation of third dimensional inter unit cell coupling [Bansil et al. (2005), Markiewicz et al. (2005)].

The Coulomb correlation (U) also plays an important role in the broadening of spectral function away from the Fermi level. It is found that the broadening in electronic spectra is more in the presence of both the Coulomb energy (U) as well as the inter unit cell resonant tunneling. Finally, it is concluded that the inter unit cell resonant tunneling (T_{12}) suppresses the bilayer splitting in the spectral function due to broadening in the spectral features close to Fermi level in optimal doped bilayer cuprates and contribute to the electronic spectra in normal state.

In the section 4.3 we have extended the above study by analyzing the influence of third dimension on the out-of-plane (c-axis) electrical conductivity in bilayer cuprates (Bi-2212) within Kubo formula employing single particle temperature dependent Green's function formalism [Rodrigues (1979), Mahan (1990)] in the light of extended Hubbard model including inter unit cell resonant tunneling term (T_{12}). On the basis of numerical computation we have analyzed the out-of-plane conductivity as a function of temperature (T), inter cell resonant tunneling (T_{12}), Coulomb energy (U) and carrier concentration (n). Finally, it is concluded that the out-of-plane conductivity decreases exponentially with temperature in bilayer cuprates in

normal state which in tune with recent analysis [Nakamura et al. (1993), Wu et al. (1998) and Turlakov et al. (2001)]. It is also predicted that the inter cell resonant tunneling (T_{12}) increases the c-axis conductivity and coulomb correlations suppresses the c-axis conductivity in doped bilayered cuprates in normal state.

LITERATURE CITED

LITERATURE CITED

Abrikosov, A. A. (1997), Phys. Rev. B 55, 11735

Abrikosov, A. A. (1999), Physica C 317, 154

Ajay (1999), Physica C 316, 267

Ajay; Lal, R. and Joshi, S. K. (1999), Physica C 325, 201

Ajay; Pratap, A.; Joshi, S. K. (2002), Physica C 371, 139

Alexandrov, A. S. (1988), Phys. Rev. B 38, 925

Alexandrov, A. S. and Mott, N. F. (1994), Rep. Prog. Phys. 57, 1197

Alexandrov, A. S.; Kabanov, V. V. and Mott N. F. (1996), Phys Rev. Lett. 77, 4796

Allen, P. B.; Pickett, W. E. and Krakauer, H. (1988), Phys. Rev. B 37, 7482

Anderson, P. W. (1987), Science 235, 1196

Anderson, P. W. (1997), The theory of superconductivity in high T_c cuprates, Priceton University press, Priceton

Anderson, P. W. and Zou, Z. (1988), Phys. Rev. Lett. 60, 132

Anderson, P. W.; Ramakrishnan, T. V.; Strong, S. and Clarke, D. G. (1996), Phys Rev. Lett.77, 4241

Ando, Y.; Boebinger, G. S.; Passner, A.; Kimura, T. and Kishio, K. (1995), Phys. Rev. Lett. 75, 4662

Atkinson W. A.; Wu, W.C. and Corbette, J.P. (1998), JPCS 59, 1791

Auerbach, A. and Arovas, D. P. (1988), Phys. Rev. Lett. 61, 617

Bansil, A.; Lindroos, M.; Sahrakorpi, S. and Markiewicz, R. S. (2005), Phys. Rev. B 71, 012503

Bardeen, J.; Cooper, L. N. and Schrieffer, J .R. (1957), Phys. Rev. 106, 162

Bednorz, J. G. and Muller K. A. (1986), Z. Phys. B 64, 189

Bohm, D. (1951), Quantum Theory, Prentice Hall, New York

Chakravarty, S.; Lee, H. Y. and Abraham, E. (1999), Phys. Rev. Lett. 82, 2366

Chakravarty, S.; Sudbo, A; Anderson, P.W.; and Strong, S.; (1993) Science 261, 337

Chu, C. W.; Hor, P. H.; Meng, R. L.; Gao, L.; Huang, Z. J.; Wang, Y. Q. (1987), Phys. Lett. 58, 405

Chuang, Y. D.; Gromko, A. D.; Fedorov, A.; Dessau, D.S.; Aiura, Y.; Oka, K.; Ando, Y.; Eisaki, H. and Uchida, S. I. (2001), arXiv : cond-mat/0102386

Chuang, Y. D.; Gromko, A. D.; Fedorov, A. V.; Aiura, Y.; Oka, K.; Ando, Y.; Lindroos, M.; Markieweiz R. S.; Bansil, A. and Dessau D. S. (2004), Phys. Rev. B, 69, 094515

Chuang, Y. D.; Gromko, A. D.; Fedorov, A.; Aiura, Y.; Oka, K.; Ando, Y.; Eisaki, H.; Uchida, S. I. and Dessau, D. S. (2001), Phys. Rev. Lett. 87, 117002

Chuang, Y. D.; Gromko, A. D.; Fedorov, A. V.; Aiura, Y.; Oka, K.; Ando, Y. and Dessau, D.S. (2001), arXiv: cond-mat/0107002 v2

Clarke, D. G.; Strong, S. P. and Anderson, P. W. (1995), Phys Rev. Lett. 74, 4499

Cooper, S. L.; Nyhus, P.; Reznik, D.; Klein, M.V.; Lee, W. C.; Ginzberg D. M.; Veal, B. W.; Paulikas, A. P. and Dabrovski, B. (1993), Phys Rev. Lett. 70, 1533

Cooper, S. L.; Reznik, D.; Kotz, A.; Karlow, M. A.; Liu R.; Klein M. V.; Lee, W. C.; Giapintzakis J. and Ginzberg, D. M. (1993), Phys. Rev. B 47, 8233

Dagotto, E. (1994), Rev. Mod. Phys. 66, 1196

Dai, P.; Mook, A.; Hayden, S. M.; Apple, G.; Perring, T. G.; Hunt, R. D. and Dogan, F. (1999), Science 284, 1344

Damacelli, A.; Hussain, Z.; and Shen, Z. X. (2003), Rev. Mod. Phys. 75 473

Dessau, D. S.; Wells, B. O.; Shen, Z. X.; Spicer, W. E.; Arko, A. J.; List, R. S.; Mitzi, D. B. and Kapitulnik, A. (1991), Phys. Rev. Lett. 66, 2160

Devereaux, T.P. (2003), Phys. Rev. B 68, 094503

Feng, D. L.; Armitage, N. P.; Lu, D. H.; Damacelli, A.; Hu, J. P.; Bogdanov, P.; Lanzara, A.; Ronning, F., Shen, K. M.; Eisaki H.; Kim C., Shen Z. X. (2001), Phys. Rev. Lett., 86, 5550

Feng, D. L.; Damascelli, A.; Shen, K. M.; Motoyama, N.; Lu, D. H.; Eisaki, H.; Shimizu, K.; Shimoyama, J. I.; Kishio, K.; Kaneko, N.; Greven, M.; Gu, G. D.; Zhou, X. J.; Kim, C.; Ronning, F.; Armitage, N. P. and Shen, Z. X. (2002), Phys. Rev. Lett. 88, 107001

Feng, D. L.; Eisaki, H.; Shen, K. M.; Damascelli, A.; Kim, C.; Lu, D. H.; Shimizu, K.; Shimoyama, J. I.; Kishio, K.; Motoyama, N.; Kaneko, N.; Greven, M. and Gu, G. D. (2002), International Journal of Modern Physics B, Vol 16, 1691

Frohlich, H. (1950), Phys. Rev. 79, 845

Fujita, T.; Takahashi, H. and Mori, N. (1996), Phys. Rev. B 54, 10061

Ginzberg, V. L. (1964), Zh.Eksp Teor. Fiz. 47, 2318, (Sov. Phys. JETP 20, 1549 (1965))

Giura, M.; Fastampa, R.; Sarti, S. and Silva, E. (2003), Phys. Rev. B 68, 134505

Giura, M.; Fastampa, R.; Sarti, S.; Pompeo, N. and Silva, E. (2007), Physica C 460, 831

Govind and Joshi, S. K. (2003), Physica C 398, 13

Gros, C.; Joynt, R.; and Rice, T. M. (1987), Phys. Rev. B 36, 381

Ho, A.F. and Schofield, A.J. (2005), Phys. Rev. B 71, 045101

Hofmann, U.; Keller, J. and Kulic, M. (1990), Z. Phys. B 81, 25

How, X. H.; Zhu, W. J.; Li, J. Q.; LI, J. W.; Xing, J. W.; Wu, F.; Huang, Y. Z. and Zhao, Z. X. (1994), Phys. Rev. B 50, 496

Hubbard, J. (1963), Proc. R. Soc. London, Ser. A 276, 238

Hubbard, J. (1964), Proc. Roy. Sci. A 281, 401.

Inoue, M. and Takemori, T. (1987), Solid State Common. 63, 201

Iye Y. (1992) D.M. Ginsberg (Ed.) Physical properties of high temperature superconductors III, Ch. 4, World Scientfic, Singapore

Jaklic,J. and Prelovsek (1997), Phys. Rev. B, 55, R7307

Kamanski, A.; Rosenkranz, S.; Fretwell, H. M.; Li, Z. Z.; Raffy, H.; Randeria, M.; Norman, M. R. and Campuzano, J. C. (2003), Phys. Rev. Lett. 90, 207003

Kendziora, C.; Martin, M. C.; Haartye, A.; Mihaly, L. and Forros, L. (1993), Phys. Rev. B 48, 3531

Kim, M. S.; Choi J. H. and Lee S. I. (2001), Phys. Rev. B, 63, 092507

Kishore, R. and Granato, E. (1990), J.Phys: condens matter 2, 5633

Kishore, R. (1987), Phys. Rev. B 35, 6854

Koltenbah, B. E. C. and Joynt, R. (1997), Rep. Prog. Phys. 60, 23

Kordyuk, A. A.; Borisenko, S. V.; Kim, T. K.; Nenkov, K.; Knupfer, M.; Golden, M. S.; Fink, J.; Berger, H.; Follath R. (2002), Phys. Rev. Lett. 89, 077003

Kubo, R. (1957), J. Phys. Soc. Japan 28, 1402

Kumar, N. and Jayannavar, A. M. (1992), Phys. Rev. B 45, 5001

Lal, R.; Ajay; Hota, R. L. and Joshi, S. K. (1998), Phys. Rev. B 57, 6126

Leggett, A. J. (1992), Braz. J. Phys. 22, 129

Leung, P. W.; Wells, B. O. and Gooding R. J.(1997), Phys. Rev. B 56, 6320

Levi, B.G. (1996), Phys. Today 19

Levin, K., Kim J. H., Lu J. P., Si Q. (1991), Physica C 175, 449

Levin, G. A. (2004), Phys. Rev. B 70, 064515

Li, Q. P.; Koltenbah, B. E. C. and Joynt, R. (1993), Phys. Rev. B 48, 437

Little, W. A. (1969), Phys. Rev. A 134, 1416

Little, W. A. (1981), Int. J. Quantum Chem. 15, 545

Littlewood, P. B. and Verma, C. M. (1992), Phys. Rev. B 45, 12636

Liu, M. and Xing, D. Y. (1994), Phys. Rev. B 49, 682

Mahan, G.D. (1990), Many particle physics-2nd ed., Plenum Press, New York

Maier, T.A.; Pruschke, T. and Jarrell, M. (2002) Phys. Rev. B 66, 075102

Markiewicz, R. S.; Sahrakorpi, S.; Lindroos, M.; Lin, H. and Bansil, A. (2005), airXiv: cond- mat/0503064

Maska, M. (1993) Phys. Rev. B 48, 1160

Maska, M. (1997), Phys. Rev. B 55, 3943

Misha, T. and Leggett, A.J. (2001), Phys. Rev. B 63, 064518

Mori, M.; Tohyama, T. and Maekawa, S. (2002), Phys Rev. B 66, 064502

Mori, M.; Tohyama, T. and Maekawa, S. (2003), Physica C 392, 123

Nagaosa, N. (1996), Physica C 263, 54

Nakamura, F; Kodama, S; Sakita, S.; Maeno, Y.; Fujita, T.; Takahashi, H. and Mori, N. (1996), Phys Rev. B 54, 10061

Nakamura, Y. and Uchida, S. (1993), Phys. Rev. B 47, 8369.

Nazarenko, A.; Moreo, A.; Dagotto, E. and Riera, J. (1996), Phys. Rev. B 54, 768.

Neal, H. L. (1996) Solid State Communications, 98, 317

Norman, M. R. and Ding, H. (1998), Phys. Rev. B 57, R11089

Norman, M. R. and Pepin, C. (2003), Rep. Prog. Phys. 66, 1547

Nyhus, P.; Karlow, M. A. and Cooper, S. L. (1994), Phys. Rev. B 50, 13898

Onnes, H. K.(1911), Comm. Phys. Lab Univ. Leiden 119B, 1

Ozyuzer, L.; Zasadzinski, J. F.; Kendziora, C.; Gray, K. E. (2000), Phys. Rev. B 61, 3629

Pan, S. H.; Hudson, E. W.; Gupta, A. K.; Ng, K. W.; Eisaki, H.; Uchida, S. and Davis, J. C. (2000), Phys Rev. Lett. 85, 1536

Pathak, P. K. and Ajay (2006), Physica C 398, 13

Pathak, P. K.; Ajay and Joshi, S. K. (2005), Physica C 423, 127

Pickett W. E. (1989), Rev. Mod. Phys. 61, 433

Pietig, R.; Bulla, R. and Blawid, S. (1999), Phys. Rev. Lett. 82, 4046

Plakida, N. M. and Oudovenko, V. S. (2007), Physica C 460, 993

Pratap, A.; Lal, R.; Govind and Joshi, S.K. (2001), Phys. Rev. B 64, 224512

Prelovsek, P. and Ramsak, A. (2002), Phys. Rev. B 65, 174529

Ramsak, A.; Sega, I. and Prelovsek, P. (1998), Phys Rev. Lett. 81, 3745

Rodrigues, W. A. (1979), Revista Brasileira de Fisica 9, 109

Rojo, A. G. and Levin, K. (1993), Phys. Rev. B 48, 16861

Shin, C. T.; Lee, T. K.; Mau, C. Y. and Chen, Y. C. (2000), Phys. Rev. Lett. 85, 1536

Stasio, M. D.; Muller, K. A. and Pietronero, L. (1990), Phys. Rev. Lett. 64, 2827

Su, G. (1993), J. Phys. A 26, L139.

Tallon, J. C. and Loran, J. W. (2001), Physica C 349, 53

Tamasaku, K.; Ito, T.; Takagi, H. and Uchida, S. (1994), Phys Rev. Lett. 72, 3088

Terasaki, I.; Sato, Y.; Niyamoto, S.; Tajima, S. and Tanka S. (1995), Phys. Rev. B 52, 16246

Tesanovic, Z. (1987), Phys. Rev. B 36, 2364

Timusk, T. and Statt, B. (1999), Rep. Prog. Phys 62, 61

Tokura, Y.; Fujimori, A.; Matsubara, H.; Watabe, H.; Takagi, H.; Uchida, S.; Sakai, M.; Ikeda, H.; Okuda, S. and Tanaka, S; (1989), Phys. Rev. B 39, 9704

Turlakov, M and Leggett, A (2001), Phys. Rev. B 63, 064518

Wang, N. L.; Buschinger, B.; Geibal, C. and Steglich, F. (1996), Phys. Rev. B 54, 7449

Wang, Y. R.; Wu, J. and Franz, M. (1993), Phys. Rev. B 47, 140

Watanabe, T.; Fujii, T. and Matsuda, A. (1997), Phys Rev. Lett. 79, 2113

Weber, W. (1987), Phys Rev. Lett. 58, 1371

Wells, B. O.; Shen, Z. X.; Matsura, A.; King, D.; Kastner, M.; Greven, M. and Birgenaa, R. J. (1995), Phys. Rev. Lett. 74, 964

Winkeler, L.; Sadewasser, S.; Beschoten, B.; Frank H.; Nouvertne, F. and Guntherodt, G. (1996), Physica C 265, 194

Wu, M. K.; Ashburn, J. R.; Torng, C. J.; Hor, P. H.; Meng, R. L.; Goa, L.; Huang, Z. J.; Wang, Y. Q. and Chu, C. W. (1987), Phys. Rev. Lett. 58, 908

Wu, W. C.; Atkinson W. A. and Corbette, J. P. (1998), J. Supercond. 11, 305

Zhang, W.; Zho, L.; Liu, H.; Meng, J.; Dong, X.; Lu, W.; Wen, J. S.; Xu, Z. J.; Gu, G. D.; Sasagawa, T.; Wang, G.; Zhu, Z.; Zhang, H.; Zhou, Y.; Wang, X.; Zhao, Z.; Chen, C.; Xu, Z. and Zhou, X. J. (2007), airXiv:cond- mat.supr-con/0711.1706v1

Zhou, X. J.; Cuk, T.; Devereaux, T.; Nagaosa, N.; and Shen, Z. X. (2006), arXiv:cond-mat/0604284v1

Zoli, M. (1997), Phys. Rev. B 56, 111

Zubarev, D. N. (1960), Sov. Phys. Usp. 3, 302

List of Publications

(A) Papers in refereed Journals:

(1) B.S.Tewari, Ajay and R.Kishore
Influence of three site exchange interaction on the electronic spectra of doped bilayer high T_c cuprates, Accepted in Physica C (2007)

(2) Ajay, B.S.Tewari, Govind and S.K.Joshi
Influence of intra cell coupling and inter cell resonant tunneling on the electronic spectra in bilayer high T_c cuprates, (Communicated to JPCS (2007))

(3) B.S.Tewari, Archana Dhyani and Ajay
Role of inter cell resonant tunneling on the out of plane electric transport behavior in layered cuprates, (Manuscript under preparation)

(B) Contribution in Conferences/Symposia:

(4) Ajay, B.S.Tewari, Govind and S.K.Joshi
Electronic spectra of bilayer high Tc cuprates: role of intra and interunit cell couplings, Presented at International Workshop on the Physics of Mesoscopic and Disordered Materials(MESODIS), held at , Physics Department IIT-Kanpur, Dec. 04-08 (2006)

(5) B.S.Tewari and Ajay
Influence of three site exchange interaction on electronic spectra of layered high T_c cuprates, Presented at 51-th DAE, Solid State Physics Symposium held at Barktullah University, Bhopal, during 26-30 Dec. (2006)

(6) B.S.Tewari, Ajay and S.K.Joshi
Influence of long range hoppings and three site exchange interaction on the electronic spectra of bilayer cuprate Superconductors: presented (poster) at Summer School on “From BCS to Exotic Superconductivity , held at Cargese, France, during July 16 to 28, (2007)

PHYSC 124738
2 January 2008 Disk Used
ARTICLE IN PRESS
No. of Pages 7, Model 5+

Available online at www.sciencedirect.com
ScienceDirect
Physica C xxx (2008) xxx–xxx
PHYSICA C
www.elsevier.com/locate/physc

Influence of three site exchange interaction on the electronic spectra of doped bilayer high T_c cuprates

B.S. Tewari [a], Ajay [a,*], R. Kishore [b]

[a] Department of Physics, G.B.Pant University of Agriculture and Technology, Pantnagar, Uttaranchal 263145, India
[b] Instituto de Pesquisas Espaciais (INPE), CP 515, CEP 12245-970, São José dos Campos, São Paulo, Brazil

Received 29 October 2007; received in revised form 21 November 2007; accepted 5 December 2007

Abstract

The influence of the three site exchange term (J_3) on electronic spectral function $A(k,\omega)$ and density of states (DOS) is analyzed in doped bilayer high T_c cuprates in the normal state. The model Hamiltonian is based on the extended t–J–J_3 model as derived from the Hubbard model under strong coupling limit so that it necessarily includes three site exchange term (J_3). For the bilayer cuprates having two CuO_2 planes in a unit cell, the coupling between the planes ($t_\perp$) is also included. The expressions of $A(k,\omega)$ and DOS are obtained by employing the Green's function equation of motion technique within two sublattice approach and approximations applicable for strongly correlated systems. On the basis of numerical computation, we have found that three site exchange term (J_3) affects the shape of the spectral function $A(k,\omega)$ and the DOS in optimal doped region of bilayer cuprates. The J_3 term suppresses the bilayer splitting in the electronic spectra while enhances the DOS at Fermi level. The results are viewed in terms of recent ARPES measurement in bilayer cuprate in normal state.

PACS: 74.25.Jb; 74.72.Bk; 74.72.Hs

Keywords: Electronic spectra of bilayer cuprates; Extended t–J–J_3 model; Strong electronic correlations; Three site exchange interaction (J_3)

1. Introduction

The crystal structure of high temperature cuprate superconductors is highly anisotropic due to the existence of the stakes of two dimensional CuO_2 planes. In undoped state, these materials are planar antiferromagnetic (AFM) insulators due to a hole in $Cu3d^9$ state. Upon doping (i.e. on introducing holes) up to a certain extent they undergo a phase transition from AFM state to a strange normal state or a superconducting state depending on the temperature. The high T_c cuprate materials are classified into single layer material [$Bi_2Sr_2CuO_{6+x}$ (Bi2201), $La_{2-x}Sr_xCuO_4$ (LSCO)], bilayer [$YBa_2Cu_3O_{7-x}$ (Y123), $Bi_2Sr_2CaCu_2O_{8+x}$ (Bi2212), $HgBa_2CaCu_2O_{6+x}$ (Hg1212)] and trilayer materials [$Bi_2Sr_2Ca_2Cu_3O_{10+x}$ (Bi2223)], on the basis of number of CuO_2 planes in an unit cell.

Recent photoemission studies show a marked difference in the electronic spectra of these different categories of cuprates [1–8]. The angle resolved photoemission studies (ARPES) on bilayer and trilayer compounds show a splitting of spectral function at $(\pi,0)$ point of the Brillouin zone which has not been observed in single layer per unit cell cuprates [3,4]. It emphasizes the role of coupling of the electronic states of neighbors CuO_2 planes in the out of plane direction due to the small separation between these layers. Further, the ARPES results in these cuprate compounds point a maximum splitting in spectral function in a normal state in comparison to superconducting state at the antinodal point of the Brillouin zone. The splitting is also observed in overdoped Bi-2212 samples above T_c but with a much larger splitting energy (~110 meV) [7].

* Corresponding author. Tel.: +91 5944 234115; fax: +91 5944 233473.
E-mail address: ajay_phys@yahoo.co.in (Ajay).

0921-4534/$ - see front matter © 2007 Published by Elsevier B.V.
doi:10.1016/j.physc.2007.12.002

The Hubbard model and its strong coupling version (i.e. t–J model) are good candidates for describing the electronic structure of the high T_c cuprates and since the discovery of high T_c cuprates, a lot of attempt has been made on the Hubbard model, t–J models and their extensions. In fact, there is no single model sofar to describe all the electronic properties of these high T_c cuprate superconductors in normal as well as in superconducting states. Hubbard model is weaker in describing the AFM exchange correlations in underdoped regime. The t–J model can be obtained by projecting out doubly occupied sites from the Hubbard model in strong coupling limit [9,10]. Further at exactly half filling, the t–J model reduces to the Heisenberg model, where spin dynamics is well understood. It is also pointed out that the two dimensional (2D) t–J model is also inadequate for describing the electronic spectra of high temperature cuprates [11–15].

Generally, the three site exchange interaction term (J_3) which arises naturally in the strong coupling version of Hubbard model, i.e. t–J model, has not been given due attention so far in theoretical studies. Though the magnitude of J_3 is of the order δJ, (where δ is the hole density and J is antiferromagnetic exchange interaction). Recently, Li et al. [16] have pointed out on the basis of numerical analysis that the three site exchange term becomes important in the dilute limit (where δ is greater than 0.05). The three site exchange term comprises the coupling of a site with the two distinct nearest neighbor sites.

The depiction of the virtual processes involved in spin–spin exchange term (J term) and the three site exchange term (J_3) are shown in Fig. 1. The virtual process occurs when two spins are on the nearest neighbor site on a square planar lattice. The virtual hopping of one spin onto the site occupied by other spin followed by either spin hopping back to the first site resulting the J term interaction. On the other hand the three site exchange interaction (J_3) arises in dilute limit, when the possibility of finding the other three nearest neighbor sites unoccupied is exactly one. There is equal chance of one of the spin hopping onto any of these vacant neighbor sites when one spin has a virtual hopping onto the site occupied by the other spin [17].

Therefore, in order to analyze the electronic spectra of doped bilayer cuprates, one needs to extend the t–J model by including three site exchange interaction term (J_3). Most of the studies conducted on t–J model are based on numerical approach and amongst them there are very few attempts are analytical. The problem with analytical studies is that one does not know how to handle the competition between the kinetic part and the exchange part on the same footing and as a result of which one relies on approximations. In most of the studies on t–J model the numerical methods like exact diagonalisation for small cluster, quantum Monte Carlo simulation and variational calculations for clusters are used [17–19] where finite size effects are overlooked.

Further, the studies based on the extended t–J model have become important in the view of the recent ARPES

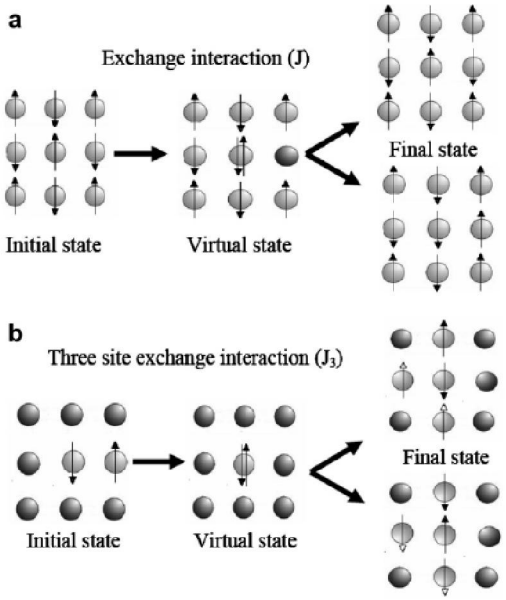

Fig. 1. The schematic presentation of the initial, virtual and final states (a) for spin–spin exchange term (J), (b) for the three site exchange interaction term (J_3) on two dimensional antiferromagnetically ordered cuprate square plane.

measurements. On the basis of exact diagonalization studies of the t–t'–t''–J model, Laung et al. [20] concluded that the next nearest neighbors hopping (t') and the second next nearest neighbors hopping (t'') becomes important in the case of two dimensional AFM insulator like $Sr_2CuO_2Cl_2$. The inclusion of t' and t'' in t–J model makes it more significant to explain not only dispersion relation but also quasi-particle lifetime of the electronic states in cuprates [17–19]. This is the superiority of t–J model over other models proposed to study doped high T_c layered cuprates.

To explain the splitting in ARPES results of bilayer cuprates Chakravarty et al. [21] predicted that the coupling energy between the CuO_2 planes is highly anisotropic with the momentum dependence of the form of $\varepsilon_{\perp k} = -\frac{t_\perp}{4}(\cos k_x a - \cos k_y a)^2$. The form of momentum dependence of interlayer coupling ensures that the maximum bilayer splitting energy will be at $(\pi,0)$ point of the Brillouin zone. The detailed study regarding the role of interlayer coupling on the spectral properties of doped high T_c cuprates has been conducted by Pathak et al. [22]. These authors have concluded that the spectral function shows a splitting at $(\pi,0)$ point in overdoped regimes in tune with recent ARPES results. These authors have not analyzed the influence of three site exchange coupling (J_3) on the electronic spectra of bilayer cuprates.

Therefore, in light of the above facts, the extended t–J model that incorporates, the next nearest neighbor hopping

Please cite this article in press as: B.S. Tewari et al., Physica C (2008), doi:10.1016/j.physc.2007.12.002

(t') and a momentum dependent interlayer coupling term ($t_\perp$) for two CuO_2 planes per unit cell in bilayer cuprate Bi-2212 is used. The three site exchange term (J_3) in the exchange part of the model Hamiltonian as obtained in the strong coupling version of Hubbard model is also included. Therefore, on the basis of the t–t'–$t_\perp$–J–J_3 model we have planned to analyze the spectral function $A(k,\omega)$ and the density of states (DOS).

2. Theoretical formulation

We model the doped bilayer cuprates like Bi-2212 having two CuO_2 planes per unit cell and include various extended hopping energies within CuO_2 plane and between the two CuO_2 planes within the unit cell alongwith long range three site exchange (J_3) term. The Hamiltonian for our model is described as

$$H = H_{t\text{–}t'\text{–}t_\perp} + H_{J\text{–}J_3}, \tag{1}$$

where

$$H_{t\text{–}t'\text{–}t_\perp} = -t\sum_{\vec{n}ij\sigma} c^+_{ri\sigma}c_{rj\sigma} - t'\sum_{\vec{n}ij'\sigma} c^+_{ri\sigma}c_{rj'\sigma} + \sum_{ij\sigma r\neq s} t_\perp c^+_{ri\sigma}c_{sj\sigma} + U'\sum_{ri\sigma} n_{ri\sigma}n_{ri-\sigma}, \tag{2a}$$

$$H_{J\text{–}J_3} = \frac{J}{2}\sum_{r\langle ij\rangle}\left(\vec{S}_{ri}\cdot\vec{S}_{rj} - \frac{1}{4}n_{ri}n_{rj}\right) - \frac{J_3}{4}\sum_{ri\delta\delta'\neq\delta\sigma}\left(c^+_{ri+\delta\sigma}n_{ri-\sigma}c_{ri+\delta'\sigma} + c^+_{ri+\delta\sigma}c^+_{ri-\sigma}c_{ri+\delta'-\sigma}c_{ri\sigma}\right), \tag{2b}$$

where $r = 1$, $s = 2$ ($r = 2$, $s = 1$) for bilayer system. The first term in the kinetic part of the Hamiltonian shown in Eq. (2a), is the planar electronic kinetic energy that includes the contribution of the next nearest neighbor (t') and the third term in (2a) represents the momentum dependent interlayer coupling, $\varepsilon_{\perp k} = -\frac{t_\perp}{4}(\cos k_x a - \cos k_y a)^2$ as suggested by electronic band structure calculation [21] and recent ARPES measurements [3–5] also. The additional Coulomb energy (U') is the fictitious Coulomb interaction involved in kinetic part only. The term U' is introduced in order to put double occupancy constraints as we are not using projection operator formalism to project out doubly occupied sites. The interaction part of Hamiltonian shown in Eq. (2b) contains nearest neighbor exchange energy (J) contribution alongwith three site exchange interaction term (J_3).

In order to solve the extended Hamiltonian as shown in Eqs. 1, 2a, 2b, and to obtain the expression of electronic spectral function $A(k,\omega)$ we follow the approach developed by Pathak et al. [22]. In this approach, kinetic part (2a) of the Hamiltonian will be treated using Green's functions within Hubbard-I approximation [9,10]. On the other hand the exchange part (2b) is treated within mean-field approximation separately. Treating the first part of the Hamiltonian $H_{t\text{–}t'\text{–}t_\perp}$ within the Hubbard self-energy approximation [14], one gets the Green's function as

$$G^\sigma_{rr}(k,\omega) = \frac{1}{\left[\omega - \varepsilon_k - \varepsilon'_k - \frac{\varepsilon^2_{k\perp}}{\omega-\varepsilon_k} - \sum_r^\sigma(k,\omega) - \mu\right]}. \tag{3}$$

Here, k is momentum and ω the energy of a hole, ε_k is the energy originating from the hopping term t, ε'_k is originating from the t' and, $\varepsilon_{k\perp}$ is arising from hopping between the CuO_2 planes. Explicitly

$$\varepsilon_k = -2t(\cos k_x a + \cos k_y a), \tag{4}$$

$$\varepsilon'_k = -4t'(\cos k_x a \cos k_y a), \tag{5}$$

$$\varepsilon_{k\perp} = -\frac{t_\perp}{4}(\cos k_x a - \cos k_y a)^2. \tag{6}$$

Here, the k dependence of $\varepsilon_{k\perp}$ has been taken as suggested by Chakravarty et al. [21]. $\sum_r^\sigma(k,\omega)$ is the Hubbard self-energy calculated under the strong Coulomb correlation limit (i.e. the limit $U' \to \infty$). From (3), the one electron renormalized energies will be given by

$$\varepsilon_k \to \tilde{\varepsilon}^\sigma_{rk}(\omega) = \varepsilon'_k + \varepsilon_k + \frac{\varepsilon^2_{k\perp}}{\omega-\varepsilon_k} + \sum_r^\sigma(k,\omega). \tag{7}$$

The form of the self-energy within the Hubbard-I approximation where the life time effects are neglected [14,23,27] is given below:

$$\sum_r^\sigma(\omega) = \frac{U' n_{r-\sigma}\omega}{\omega - U'(1-n_{r-\sigma})}. \tag{8}$$

In High T_c cuprates at low doping carriers move in a planar antiferromagnetically ordered background. As the hole concentration increases the long range AFM order starts weakening. However short-range AFM correlation persists at even higher hole doping levels [24–26]. In order to consider the effect of local antiferromagnetic order it is assumed

$$\sum_r^\uparrow(\omega) = \sum_r^\downarrow(\omega) = \sum(\omega)$$

and in the limit $U' \to \infty$, self-energy (now spin independent) is given by

$$\sum(\omega) = -\frac{n_H\omega}{(2-n_H)}. \tag{9}$$

Here, we have used $n_{r\uparrow} = n_{r\downarrow}$ and $n_H = n_{r\uparrow} + n_{r\downarrow}$ and $n_H = 1 - n$.

The two sublattice approach has been adopted to take into account the short-range antiferromagnetic order [22,27]. For a square lattice, the lattice is divided into two sublattices A and B such that nearest neighbor of sublattice A (say spin up) belongs to sublattice B (say spin down) and vice-versa. Within the two sublattice approach the sublattice operators in the momentum space can be defined as

Please cite this article in press as: B.S. Tewari et al., Physica C (2008), doi:10.1016/j.physc.2007.12.002

$$c_{ri\sigma} = \frac{1}{\sqrt{N}} \sum_{rk} a_{rk\sigma} e^{ik.R_i} \quad \text{for } i \in A,$$
$$c_{ri\sigma} = \frac{1}{\sqrt{N}} \sum_{rk} b_{rk\sigma} e^{ik.R_i} \quad \text{for } i \in B. \tag{10}$$

Using the above transformations the kinetic part of the Hamiltonian (2a) can now be rewritten in momentum space in the following form:

$$H^{\text{kin}}(\omega) = \sum_{rk\sigma} \tilde{\varepsilon}_k(\omega)(a^+_{rk\sigma} b_{rk\sigma} + b^+_{rk\sigma} a_{rk\sigma}) + \sum_{rk\sigma} \varepsilon'_k(\omega) \times (a^+_{rk\sigma} a_{rk\sigma} + b^+_{rk\sigma} b_{rk\sigma}) \tag{11}$$

and,

$$\tilde{\varepsilon}_k(\omega) = \varepsilon_k + \frac{\varepsilon^2_{k\perp}}{\omega - \varepsilon_k} - \frac{2}{2 - n_{\text{H}}}\omega - \mu. \tag{12}$$

In Eq. (11), the first term originates from the nearest neighbor hopping matrix, while the second term corresponds to the second nearest neighbor hopping.

The second term in the Hamiltonian (1) attributed to the exchange interaction (Eq. (2b)) has been treated within the mean-field approximation. It is written as

$$H^{\text{int}}_{J-J_3} = -\frac{J}{2} \sum_{\langle ij \rangle r} [\tilde{n}_{ri\downarrow} c^+_{rj\uparrow} c_{rj\uparrow} + \tilde{n}_{ri\uparrow} c^+_{rj\downarrow} c_{rj\downarrow}] - \frac{J_3}{2} \times \sum_{rij'} [c^+_{rj\uparrow} \tilde{n}_{ri\downarrow} c_{rj'\uparrow} + c^+_{rj\uparrow} c^+_{ri\downarrow} c_{rj'\downarrow} c_{ri\uparrow}], \tag{13}$$

where, the following parameter has been used

$$\tilde{n}_{ri} = \langle c^+_{ri\uparrow} c_{ri\uparrow} + c^+_{ri\downarrow} c_{ri\downarrow} \rangle \tag{14}$$

and we have not taken into account the spin density and hence the AFM ordering at this stage in order to avoid complexity. In the two sublattices, we write

$$\tilde{n}_{ri\sigma} = n_{rA\sigma} \quad i \in A, \text{ and}$$
$$\tilde{n}_{ri\sigma} = n_{rB\sigma} \quad i \in B.$$

After performing Fourier transformation the Hamiltonian (13) can be written in the form

$$H^{\text{int}}_{J-J_3} = -\frac{J}{2} Z \sum_{rk\sigma} [n_{rA-\sigma} b^+_{rk\sigma} b_{rk\sigma} + n_{rB-\sigma} a^+_{rk\sigma} a_{rk\sigma}] - \frac{J_3}{4} Z^2 \sum_{rkk'\sigma} [b^+_{rk\sigma} n_{rA-\sigma} a_{rk'\sigma} + b^+_{rk\sigma} a^+_{rk-\sigma} a_{rk'-\sigma} a_{rk\sigma}], \tag{15}$$

where for square lattice the coordination number Z is equal to 4.

Finally, combining the Eqs. (11) and (15) (kinetic and exchange part of the model) the effective Hamiltonian of our model can be written as

$$\tilde{H}(\omega) = \sum_{rk\sigma} \tilde{\varepsilon}_k(\omega)(a^+_{rk\sigma} b_{rk\sigma} + b^+_{rk\sigma} a_{rk\sigma}) + \sum_{rk\sigma} \left\{ \varepsilon'_k - \frac{J}{2} Z \langle n_{rB-\sigma} \rangle \right\} a^+_{rk\sigma} a_{rk\sigma} + \sum_{rk\sigma} \left\{ \varepsilon'_k - \frac{J}{2} Z \langle n_{rA-\sigma} \rangle \right\} b^+_{rk\sigma} b_{rk\sigma} - \frac{J_3}{4} Z^2 \times \sum_{rkk'\sigma} [b^+_{rk\sigma} \langle n_{rA-\sigma} \rangle a_{rk'\sigma} + b^+_{rk\sigma} a^+_{rk-\sigma} a_{rk'-\sigma} a_{rk\sigma}]. \tag{16}$$

The kinetic part and the exchange part of the Hamiltonian (16) are not calculated on the same footing. The kinetic part is solved within the Hubbard self-energy approach under the consideration of fictitious Coulomb interaction $U' \to \infty$ to avoid doubly occupied sites. The appearance of U' is limited to kinetic part only, and is not involved in the exchange part. As we are interested in optimal doped regimes where J_3 is significant, so H_J has been treated within the mean-field approximation.

To study the spectral function, one sets up equation of motion for Green's function $G^{aa}_\sigma(k,\omega) = \langle\langle a_{rk\sigma}; a^+_{rk\sigma} \rangle\rangle$ using the linearized effective Hamiltonian (16). One follow the procedure described in our earlier works [22,27], and finally arrive at the following Green's function:

$$G^{aa}_\sigma(k,\omega) = \frac{1}{2\pi} \times \frac{(\omega - \varepsilon'_k + J\langle n_{\text{H}} \rangle)}{[(\omega - \varepsilon'_k + J\langle n_{\text{H}} \rangle)^2 - (\tilde{\varepsilon}_k(\omega)(\tilde{\varepsilon}_k(\omega) - 4J_3\langle n_{\text{H}} \rangle))]}. \tag{17}$$

Keeping only the first order contribution of three site term (J_3) in the propagator and using simple algebra, the Eq. (17) is written into a tractable form as

$$G^{aa}_\sigma(k,\omega) = \frac{1}{2\pi} \left[\frac{(\omega - \varepsilon'_k + J\langle n_{\text{H}} \rangle)}{(\omega - \varepsilon'_k + J\langle n_{\text{H}} \rangle)^2 - \{\tilde{\varepsilon}_k(\omega) - 2J_3\langle n_{\text{H}} \rangle\}^2} \right]. \tag{18}$$

The above Eq. (18) can be manipulated in the following form:

$$G^{aa}_\sigma(k,\omega) = \frac{1}{2\pi} \left[\frac{A'}{(\omega - \alpha)} + \frac{B'}{(\omega - \beta)} + \frac{C'}{(\omega - \gamma)} + \frac{D'}{(\omega - \delta)} \right].$$

where α, β, γ and δ are four quasi-particle energy branches corresponding to poles of the Green's function (18) and

$$A' = 1 - B' - C' - D',$$
$$B' = \frac{1}{(\beta - \alpha)} \{\delta + \beta + \gamma - 2\varepsilon_k - \varepsilon'_k + J\langle n_{\text{H}} \rangle - C'(\gamma - \alpha) - D'(\delta - \alpha)\},$$
$$C' = \frac{F - D'(\delta - \alpha)(\beta - \delta)}{(\gamma - \alpha)(\beta - \gamma)},$$
$$D' = \frac{G - F\delta}{(\delta - \alpha)(\beta - \delta)(\gamma - \delta)},$$

$$F = -J\langle n_H\rangle(\delta+\gamma-2\varepsilon_k) - \varepsilon_k^2 - 2\varepsilon_k\varepsilon_k' + (2\varepsilon_k+\varepsilon_k'-\delta) \times(\delta-\alpha) - \gamma^2,$$

$$G = J\langle n_H\rangle(\varepsilon_k^2-\delta\gamma) + (2\varepsilon_k+\varepsilon_k')\delta\gamma - \varepsilon'\varepsilon_k^2 - \delta^2\gamma - \delta\gamma^2,$$

where

$$\alpha,\beta = \frac{1}{2(1-v)}\left\{(-b-v\varepsilon_k) \pm\sqrt{(b+v\varepsilon_k)^2+4(1-v)(\varepsilon_k^2+b\varepsilon_k-\varepsilon_{k\perp}^2)}\right\},$$

$$\gamma,\delta = \frac{1}{2(1+v)}\left\{(-d+\varepsilon_k+v\varepsilon_k) \pm\sqrt{(d-\varepsilon_k-v\varepsilon_k)^2+4(1+v)(d\varepsilon_k+\varepsilon_{k\perp}^2)}\right\},$$

$$b = -\varepsilon_k' + J\langle n_H\rangle - 2J_3\langle n_H\rangle,$$

$$d = -\varepsilon_k' - \varepsilon_k + J\langle n_H\rangle + 2J_3\langle n_H\rangle,$$

$$v = \frac{2}{2-\langle n_H\rangle}.$$

One can calculate spectral function $A(k,\omega)$ by using the relationship

$$A(k,\omega) = -\frac{1}{\pi}\mathrm{Im}[G_\sigma^{aa}(k,\omega)], \tag{19}$$

where Im stands for imaginary part of Green's function. Using Eqs. (18) and (19) the expression for planar electronic spectral function can be written in the following form:

$$A(k,\omega) = \left[\frac{A'\Gamma}{\Gamma^2+(\omega-\alpha)^2} + \frac{B'\Gamma}{\Gamma^2+(\omega-\beta)^2} + \frac{C'\Gamma}{\Gamma^2+(\omega-\gamma)^2} + \frac{D'\Gamma}{\Gamma^2+(\omega-\delta)^2}\right] \tag{20}$$

Wherein to fit the line shape of the ARPES experimental results one needs to solve δ-functions involved in the above theoretical expressions of spectral function $A(k,\omega)$. The δ-function can be approximated by a broadened quasi-particle peak. For this purpose, the Lorentzian type of broadening has been considered as

$$\delta(\omega-\tilde{\varepsilon}_k) \cong \frac{1}{\pi}\operatorname*{Lim}_{\Gamma\to 0}\frac{\Gamma}{(\omega-\tilde{\varepsilon}_k)^2+\Gamma^2}. \tag{21}$$

The essential point of the above Lorentzian fitting is inspired by the form of $A(k,\omega)$ observed in ARPES measurements. The broadening factor Γ is taken to be independent of k and ω, following the numerical calculation of Leung et al. [20]. These authors have also determined Γ by fitting the calculated spectral function $A(k,\omega)$ to ARPES measurements. The spectral function can be calculated from Eq. (20) at different points (k_x,k_y) of the Brillouin zone as a function of three site exchange interaction term and interlayer coupling as well as other parameters of the model Hamiltonian.

From the above expression (20) of spectral function $A(k,\omega)$, one can calculate the DOS for bilayer cuprates in normal state at zero temperature by using the formula

$$N(\omega) = \frac{a^2}{4\pi^2}\int_{-\frac{\pi}{a}}^{\frac{\pi}{a}}\int_{-\frac{\pi}{a}}^{\frac{\pi}{a}} A(k,\omega)\,\mathrm{d}k_x\,\mathrm{d}k_y. \tag{22}$$

From above Eqs. (20) and (22), one can analyze the influence of J_3 on $A(k,\omega)$ and DOS of bilayer cuprates using numerical computation.

3. Results and discussion

The expressions of spectral function $A(k,\omega)$ (Eq. (20)) and density of states (DOS) given by Eq. (22) are obtained with t–t'–$t_\perp$–J–J_3 model for doped bilayer cuprates as a function of the parameters of model Hamiltonian. The numerical computation of theoretically calculated $A(k,\omega)$ has been performed, especially at $(\pi,0)$ point of the Brillouin zone, where bilayer splitting is observed to be maximum. During the numerical computation the range of various parameters have been taken from existing band structure calculations and the prediction made by recent ARPES measurements [2–8,17,22,27]. In Fig. 2, the variation of spectral function $A(k,\omega)$ as a function of energy (ω) is presented especially at $(\pi,0)$ point of the Brillouin zone for different values of three site exchange interaction term ($J_3 = 0.0$, 0.01, 0.02 and 0.03 eV) and finite coupling between the plane ($t_\perp = 0.14$ eV) keeping all other parameter fixed ($t = 0.15$ eV, $t' = -0.0375$ eV, $n_H = 0.25$, $J = 0.1$ eV, $\Gamma = 0.1$ eV). One can observe in Fig. 2 that the spectral function shows up bilayer splitting in the optimal doped regime in the absence of J_3. This observation is in qualitative agreement with the photoemission measurements in bilayer cuprates $Bi_2Sr_2CaCu_2O_{8+x}$ having two CuO_2 planes per unit cell [6,7]. Further, one can observe in Fig. 2 that on increasing J_3 (0.01–0.03 eV) the bilayer splitting gets reduced and there is an evolution of spectral peak as the spectral function reveals a sharp peak close

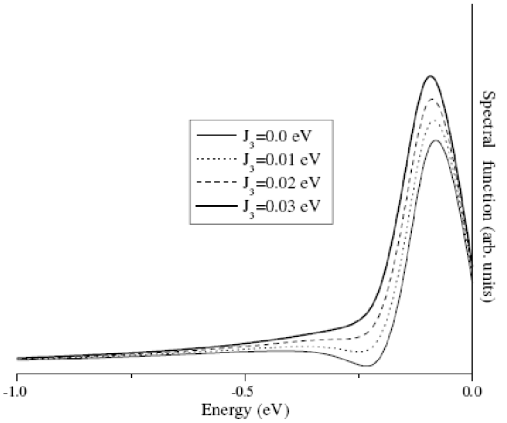

Fig. 2. Spectral function $A(k,\omega)$ versus energy at $(k_x=\pi,\ k_y=0,\ t=0.15$ eV, $t'=-0.0375$ eV, $t_\perp=0.14$ eV, $\Gamma=0.1$ eV, $n_H=0.25$, $J=0.1$ eV) for different values of J_3 (0.0, 0.01, 0.02 and 0.03 eV).

Please cite this article in press as: B.S. Tewari et al., Physica C (2008), doi:10.1016/j.physc.2007.12.002

to Fermi level. Hence, the spectral function is affected by the three site exchange term (J_3) and the actual effect of J_3 is more of like exchange kinetic energy [17] term and leads to reduction in bilayer splitting as well as redistribution of spectral weight close to Fermi level.

In Fig. 3, the variation of the density of state (DOS) versus energy (ω) is plotted in the absence of interlayer coupling parameter ($t_\perp = 0.0$ eV), as well as in the presence of $t_\perp$(=0.05 eV) in optimally doped cuprates, keeping all other parameters fixed. The variation of DOS in the presence of interlayer coupling ($t_\perp$) shows a finite DOS at Fermi level and there is an evolution of third peak structure at Fermi level which is in agreement with recent analysis of DOS attempted by various workers [22,28].

To analyze the role of J_3 on DOS in Fig. 4, the variation of DOS with energy for different values of three site exchange interaction (J_3) in optimal doped regime have been presented keeping all other parameters fixed ($t = 0.15$ eV, $t' = -0.0375$ eV, $t_\perp = 0.14$ eV, $n_H = 0.25$, $J = 0.1$ eV, $\Gamma = 0.1$ eV). One can point out from Fig. 4 that on increasing J_3, DOS at Fermi level get enhanced. Further on increasing J_3, the DOS evolves with three peak structure with a prominent peak above the Fermi level.

Finally, the spectral function $A(k,\omega)$ and density of states (DOS) for the t–t'–$t_\perp$–J–J_3 model within two sublattice approach and Hubbard self-energy approximation employing the Green's function equations of motion technique for doped bilayer cuprates is obtained. The interlayer coupling ($t_\perp$) splits the spectral function. The bilayer splitting is found to be reduced on increasing three site exchange interaction (J_3) in doped cuprates. The results obtained for DOS indicate that the J_3 term enhances the DOS at the Fermi level. It is also pointed out that in optimal doped bilayer cuprates in normal state, the J_3 term plays a role in renormalizing the spectral weight close to Fermi level. It will be interesting to analyze the role of three site exchange interaction on the other physical properties and superconducting state of doped high T_c cuprates as J_3 term involves the nearest neighbor site correlations in optimal doped regime and can influence the electronic spectra in superconducting state.

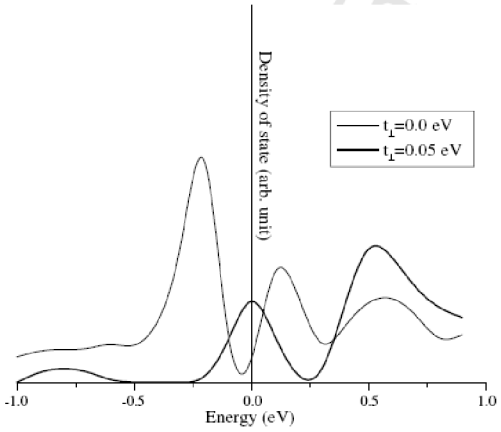

Fig. 3. Density of states (DOS) versus energy at ($t = 0.15$ eV, $t' = -0.0375$ eV, $J_3 = 0.0$ eV, $\Gamma = 0.1$ eV, $n_H = 0.25$, $J = 0.1$ eV) for different values of $t_\perp$ (0.0 eV and 0.05 eV).

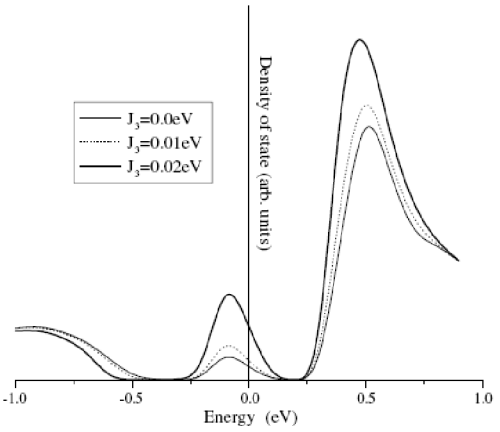

Fig. 4. Density of states (DOS) versus energy at ($t = 0.15$ eV, $t' = -0.0375$ eV, $t_\perp = 0.14$ eV, $\Gamma = 0.1$ eV, $n_H = 0.25$, $J = 0.1$ eV) for different values of J_3 (0.0, 0.01 and 0.02 eV).

Acknowledgements

This work was financially supported by the Department of Science and Technology (DST), New Delhi. Government of India, via Grant No. SP/S-2/M-36/2000. We are thankful to Dr. Prabha Pant, Assistant Professor, Social Science & Humanities, G.B.P.U.A.& T., Pantnagar for her help in editing the manuscript.

References

[1] P.W. Anderson, The Theory of Superconductivity in the High T_c Cuprates, Princeton University press, Princeton, 1997.
[2] A. Damascelli, Z. Hussain, Z.X. Shen, Rev. Mod. Phys. 75 (2003) 473.
[3] M.R. Norman, C. Pepin, Rep. Prog. Phys. 66 (2003) 1547.
[4] D.L. Feng, H. Eisaki, K.M. Shen, A. Damascelli, C. Kim, D.H. Lu, Z-X. Shen, K. Shimizu, J-I. Shimoyama, K. Kishio, N. Motoyama, M. Greven, G.D. Gu, Int. J. Mod. Phys. B 16 (2002) 1691.
[5] D.L. Feng, N.P. Armitage, D.H. Lu, A. Damascelli, J.P. Hu, P. Bogdanov, A. Lanzara, F. Ronning, K.M. Shen, H. Eisaki, C. Kim, Z.-X. Shen, Phys. Rev. Lett. 86 (2001) 5550.
[6] D.L. Feng, A. Damascelli, K.M. Shen, N. Motoyama, D.H. Lu, H. Eisaki, K. Shimizu, J.I. Shimoyama, K. Kishio, N. Kaneko, M. Greven, G.D. Gu, X.J. Zhou, C. Kim, F. Ronning, N.P. Armitage, Z.X. Shen, Phys. Rev. Lett. 88 (2002) 107001.
[7] Y.D. Chauang, A.D. Gromko, A. Fedorov, Y. Aiura, K. Oka, Yoichi Ando, H. Eisaki, S.I. Uchida, D.S. Dessau, Phys. Rev. Lett. 87 (2001) 117002.
[8] A.A. Kordyuk, S.V. Borisenko, T.K. Kim, K. Nenkov, M. Knupfer, M.S. Golden, J. Fink, H. Berger, R. Follath, Phys. Rev. Lett. 89 (2002) 077003.

Please cite this article in press as: B.S. Tewari et al., Physica C (2008), doi:10.1016/j.physc.2007.12.002

[9] M. Maska, Phys. Rev. B 55 (1997) 3943.
[10] M. Maska, Phys. Rev. B 48 (1993) 437.
[11] G. Su, Phys. Rev. B 76 (2005) 092510.
[12] S. Sorella, G.B. Martins, F. Becca, C. Gazza, A. Parola, E. Dagotto, Phys. Rev. Lett. 88 (2002) 117002.
[13] M. Calandra, S. Sorrella, Phys. Rev. B 61 (2000) R11894.
[14] C.T. Shin, T.K. Lee, R. Eder, C.Y. Mau, Y.C. Chen, Phys. Rev. Lett. 85 (2000) 1536.
[15] L.P. Pryadko, S.A. Kivelson, O. Zachar, Phys. Rev. Lett. 92 (2004) 180403.
[16] Q.P. Li, B.E.C. Koltenbah, R. Joynt, Phys. Rev. B 48 (1993) 437.
[17] B.E.C. Koltenbah, R. Joynt, Rep. Prog. Phys. 60 (1997) 23.
[18] E. Degotto, A. Moreo, F. Ortolani, J. Riera, D.J. Scalapino, Phys. Rev. Lett. 67 (1991) 1240.
[19] M. Imada, A. Fujimori, Y. Tokura, Rev. Mod. Phys. 70 (1998) 1039.
[20] P.W. Leung, B.O. Wells, R.J. Gooding, Phys. Rev. B 56 (1997) 6320.
[21] S. Chakravarty, A. Sudbo, P.W. Anderson, S. Strong, Science 261 (1993) 337.
[22] P.K. Pathak, Ajay, S.K. Joshi, Physica C 423 (2005) 127.
[23] Govind, A. Pratap, Ajay, R.S. Tripathi, Physica C 323 (1999) 42.
[24] A. Nazarenko, E. Dagotto, Phys. Rev. B 54 (1996).
[25] S.H. Pan, E.W. Hudson, A.K. Gupta, K.-W. Ng, H. Eisaki, S. Uchida, J.C. Davis, Phys. Rev. Lett. 85 (2000) 1536.
[26] P. Dai, H.A. Mook, S.M. Hayden, G. Apple, T.G. Perring, R.D. Hunt, F. Dogan, Science 284 (1999) 1344.
[27] Ajay, R. Lal, S.K. Joshi, Physica C 325 (1999) 201.
[28] P. Prelovesek, A. Ramsak, Phys. Rev. B 65 (2002) 174529.

VITA

VITA

The author was born on February 8, 1983 at Ranikhet, District Almora in Uttarakhand. He passed his High School in 1997 and Intermediate in 1999 from Government Inter College, Ramnagar District Nainital franchise with U.P. Board, Allahabad. He completed B.Sc. degree from Kumaon University, Nainital in 2002. He obtained Master's degree in Physics from G. B. Pant University of Agriculture & Technology, Pantnagar, Uttarakhand. Thereafter, He admitted for Ph.D. degree with major in Physics and minor in Computer science.

The author was the recipient of University Fellowship, Junior Research Fellowship from Department of Science and Technology, New Delhi and International Travel Fellowship from Institute of Complex and Adaptive Matters running by University of California, Davis.

Bhagya Sindhu Tewari
Ward No.-04, Kaladhunghi
Distt: Nainital
Uttarakhand
Phone no- 09412943667
E-mail: bhagyasindhu@gmail.com

ABSTRACT

Name : Bhagya Sindhu Tewari **Id. No.** : 29674
Degree : Ph.D (Physics) **Department** : Physics
Semester and Year of Admission: I, 2004-2005 **Major** : Physics

Topic: **"INFLUENCE OF THE THIRD DIMENSION ON THE ELECTRONIC SPECTRA AND OUT OF PLANE TRANSPORT BEHAVIOUR IN BILAYERED HIGH T_c CUPRATES IN NORMAL STATE"**

Advisor: Dr. Ajay

In the present thesis, the influence of the three site exchange interaction (J_3) and third dimensional coupling on electronic spectral function $A(k,\omega)$ and density of states (DOS) in doped bilayer high T_c cuprates in the normal state has been investigated. The model Hamiltonian is based on the extended $t-t'-t_\perp$ - $J-J_3$ model as derived from the Hubbard model under strong coupling limit so that it necessarily includes three site exchange term (J_3). For the bilayer cuprates having two CuO_2 planes in a unit cell, the coupling between the planes ($t_\perp$) is also included. The expressions of $A(k,\omega)$ and DOS are obtained by employing the Green's function equations of motion technique within two sublattice approach and approximations applicable for strongly correlated systems. On the basis of numerical computation, we have found that three site exchange term (J_3) affects the shape of the spectral function $A(k,\omega)$ and the DOS in optimal doped region of bilayer cuprates. The J_3 term suppresses the bilayer splitting in the electronic spectra while enhances the DOS at Fermi level. The results are viewed in terms of recent ARPES measurement in bilayer cuprate in normal state. Further, the role of third dimensional inter unit cell resonant tunneling between the copper-oxygen planes on the electronic spectra and out-of-plane transport behaviour in normal state of bilayer high T_c cuprates like $Bi_2Sr_2CaCu_2O_{8+x}$ is also investigated. We have analyzed the spectral function numerically at $(\pi,0)$ point of the Brillouin zone within the Hubbard model having terms representing hopping between the planes within the unit cell and third dimensional resonant tunneling between the planes in two adjoining cells by employing Green's function equation of motion approach making suitable decoupling approximations. It is found that the intra unit cell coupling leads to splitting of spectral peak especially at $(\pi,0)$ point of Brillouin zone, while the inter unit cell resonant tunneling leads to a broadening in the spectral function and suppress the bilayer splitting in the normal state. In the presence of finite electron correlations, the inter unit cell tunneling induce strong broadening in the spectral features. To analyze the effect of third dimensional inter cell resonant tunneling on the out-of-plane (c-axis) electronic conductivity (σ_c), the Hubbard model including resonant tunneling (T_{12}) between the planes in two adjoining cells is used. The expression for out-of-plane (c-axis) conductivity is calculated within Kubo formula using single particle Green's function by employing Green's function equations of motion technique within meanfield approximation. On the basis of numerical computation, it is pointed out that the out-of-plane conductivity increases exponentially with the increment in inter cell resonant tunneling (T_{12}). The effect of T_{12} on σ_c is found to be prominent at low temperatures as compared to temperatures above room temperature (~300^{0}K). Also, the Coulomb correlations (U) suppress the out-of-plane conductivity (σ_c) with temperature, while on increasing carrier concentration the σ_c increases. These theoretical results are viewed in terms of existing c-axis transport measurements.

(Ajay) (Bhagya Sindhu Tewari)

Advisor Author